

A Computationally Efficient Approach to Fully Bayesian Benchmarking

Taylor Okonek¹ and Jon Wakefield^{1,2}

¹*Department of Biostatistics, University of Washington, 3980 15th Ave NE, Box 351617, Seattle, WA 98195, USA. Email: tokonek@uw.edu*

²*Department of Statistics, University of Washington, Padelford Hall, NE Stevens Way, Seattle, WA 98195, USA. Email: jonno@uw.edu*

Abstract

In small area estimation, it is often necessary to resort to model-based methods in order to produce estimates in areas with little or no data. In many settings, we require that some aggregate of small area estimates agree with a national level estimate that may be considered more reliable, for internal consistency purposes. The process of enforcing this agreement is referred to as benchmarking, and while methods currently exist to perform benchmarking in many settings, few are ideal for applications with non-normal outcomes and many are computationally inefficient. Fully Bayesian benchmarking is a theoretically appealing approach insofar as we can obtain posterior distributions conditional on a benchmarking constraint. However, existing implementations are often computationally prohibitive. In this paper, we summarize existing benchmarking methods and their shortcomings in the setting of small area estimation with binary outcomes, and propose an approach in which an unbenchmarked method that produces samples can be combined with a rejection sampler to produce fully Bayesian benchmarked estimates in a computationally efficient way. To illustrate our approach, we provide comparisons of various benchmarking methods in applications to HIV prevalence and under-5 mortality estimation. Code implementing our methodology is available in the R package **simultBench**.

Key words: Small area estimation; unit-level model; under-5 mortality; HIV prevalence.

1 Introduction

In small area estimation, model-based methods are often used when estimates at small levels of aggregation are required (Rao and Molina 2015). While direct estimates are considered best practice when sufficient data are available, they cannot be computed when no data is available in a region, and confidence intervals for areas with little data are often too wide to be of practical use. Model-based methods that incorporate spatial smoothing allow for estimates in all small areas to be produced with little to no data, introducing some bias into the estimates in exchange for tighter interval estimates. Area-level models, such as the popular Fay-Herriot model (Fay and Herriot 1979), consider data at the level of the small area, whereas unit-level models consider data at the level of the individual or cluster (Battese et al. 1988). When area-level sample sizes are particularly small, unit-level models may be more desirable. For a review of unit-level models, see Chapter 7 of Rao and Molina (2015).

It is often required that small area estimates agree with estimates at a higher level of aggregation. For example, subnational estimates may be required to aggregate to a national level estimate. These higher level estimates are referred to as benchmarks, and are frequently considered more reliable than small area estimates since more data is available to inform them, or they are direct (weighted) estimates and therefore less dependent on model assumptions. Benchmarks may be from the same data source that was used to produce small area estimates or from an outside source, referred to as internal benchmarking and external benchmarking, respectively (Bell et al. 2013).

There are many existing benchmarking methods that are justifiable in various theoretical ways. One framework that is particularly appealing is treating benchmarking as a constraint problem, where estimates at smaller areas are constrained to agree with estimates at a higher level of aggregation. Existing methods differ in the ways in which constraints have been incorporated into a modelling framework. Certain approaches follow a two-step procedure: estimates and uncertainty are first obtained from a model that is agnostic to the benchmarking constraint and are then adjusted to satisfy the benchmarking constraint. Other benchmarking approaches incorporate the benchmarking constraint into the data likelihood—referred to as an augmented model in Bell et al. (2013), Berg and Fuller (2018), and Stefan and Hidiroglou (2021)—and thus produce automatically benchmarked estimates. Others propose benchmarking approaches that produce benchmarked posterior distributions for small area estimates, making uncertainty quantification straightforward. Following Zhang and Bryant (2020), we refer to such approaches as fully Bayesian benchmarking approaches. Different approaches are more or less appealing than others—depending on context—with regards to obtaining measures of uncertainty, computational tractability, and the way in which the benchmarking constraint is enforced.

The estimation of under-5 mortality rates (U5MR) at a subnational level motivates our desire for benchmark-

ing. The UN Inter-agency Group for Child Mortality Estimation (IGME) produces annual, national level estimates of U5MR for all countries using a Bayesian B-spline bias-reduction (B3) method (Alkema and New 2014). Various data are used to produce B3 estimates, including vital registration, census, and household surveys, and many of these sources cannot be used for producing subnational estimates because geographic information is lacking, or the data type is not amenable to incorporate into a small area model. Subnational estimates of U5MR are of interest in addition to national level estimates, in accordance with the Sustainable Development Goals (<https://sustainabledevelopment.un.org/post2015/transformingourworld>). Subnational estimates are currently produced for a handful of countries using the Beta-binomial 8 (BB8) model described in Wu et al. (2021), but benchmarking approaches in this context have not yet been rigorously explored.

In this article, we present a novel implementation of the fully Bayesian benchmarking approach described in Zhang and Bryant (2020) that is more flexible and computationally tractable in many settings. Our approach combines an unbenchmarked model with a rejection sampler to produce fully Bayesian benchmarked posteriors. We compare benchmarking methods in the setting of modeling HIV prevalence in South Africa, as well as modeling under-5 mortality (U5MR) in Namibia. These applications were chosen to demonstrate the flexibility of the proposed fully Bayesian approach in estimating different outcomes with unique benchmarking constraints, how the method works in cases where the benchmarks are very consistent or inconsistent with the small area estimates, and the flexibility of the approach to handle both area-level and unit-level models. To emphasize the computational advantages of the proposed method over the Markov chain Monte Carlo (MCMC) samplers used in Zhang and Bryant (2020), we use integrated nested Laplace approximation (INLA) and Template Model Builder (TMB) as alternative ways to conduct Bayesian inference using Laplace approximations, that are fast and do not require users to code model-specific fitting routines (Rue et al. 2009; Kristensen et al. 2016). All code for fitting the models described in this paper is available via the R package `simultBench`, found at github.com/taylorokonek/simultBench.

2 Methods

Let y_2 be a national level estimate of the outcome of interest, possibly with uncertainty given by a confidence interval or standard error, $\hat{\boldsymbol{\theta}} = (\hat{\theta}_1, \dots, \hat{\theta}_n)^\top$ be small area estimates for areas $i = 1, \dots, n$, and w_i be population size weights that do not depend on $\boldsymbol{\theta}$, standardized so that $\sum_{i=1}^n w_i = 1$. Often, these weights are set to $w_i = N_i / \sum_{j=1}^n N_j$, where N_j is the population size for the n small areas. Note that the population sizes used should correspond to the population under study. For example, when estimating HIV prevalence using survey data, N_j should be population counts for individuals within the age range in the sampling frame. For DHS surveys, this consists of individuals

aged 15-49. To our knowledge, incorporating uncertainty from the population counts into benchmarking approaches has not yet been considered in the benchmarking literature.

Throughout the paper, we consider benchmarking constraints of the form $\sum_{i=1}^n w_i \hat{\theta}_i = y_2$. While more complex benchmarking constraints, or even multiple benchmarking constraints as noted in Zhang and Bryant (2020), may be useful in certain settings, this simple benchmarking constraint is reasonable for the HIV prevalence and U5MR applications we consider.

In the following subsections we describe a subset of existing approaches to benchmarking and propose a novel approach to fully Bayesian benchmarking.

2.1 Benchmarked Bayes Estimate Approach

The first approach we describe was developed in a Bayesian, decision theoretic framework (Datta et al. 2011; Steorts et al. 2020). This involves minimizing expected posterior loss subject to the benchmarking constraint, which results in a projection of the unbenchmarked estimates into a benchmarked (constrained) space. Methods have also recently been developed to obtain benchmarked uncertainty for these estimates under this decision theoretic framework (Patra and Dunson 2018; Patra 2019). We call this approach the Benchmarked Bayes Estimate approach.

For n small areas, let $\hat{\boldsymbol{\theta}} = (\hat{\theta}_1, \dots, \hat{\theta}_n)^\top$ be the direct estimators of the small area means $\boldsymbol{\theta} = (\theta_1, \dots, \theta_n)^\top$. We are interested in computing the benchmarked Bayes estimator $\hat{\boldsymbol{\theta}}^{BM} = (\hat{\theta}_1^{BM}, \dots, \hat{\theta}_n^{BM})^\top$ of $\boldsymbol{\theta}$ such that the constraint $\sum_{i=1}^n w_i \hat{\theta}_i^{BM} = y_2$ is satisfied.

As Datta et al. (2011) are interested in an estimate of the benchmarked posterior mean, they consider minimizing the posterior expectation of the weighted squared error loss $\sum_{i=1}^n \phi_i E[(\theta_i - e_i)^2 \mid \mathbf{y}_1]$ under the constraint $\bar{e}_w := \sum_{i=1}^n w_i e_i = y_2$, where ϕ_i are weights not necessarily equal to w_i , and \mathbf{y}_1 is the outcome of interest. They note that the weights ϕ_i could be different for different policy makers, and a simple default is setting $\phi_i = 1$ for all $i = 1, \dots, n$. The resulting benchmarked Bayes estimate is

$$\hat{\boldsymbol{\theta}}^{BM} = \hat{\boldsymbol{\theta}}^B + s^{-1}(y_2 - \bar{\hat{\theta}}_w^B)\mathbf{r}, \quad (1)$$

where $\hat{\boldsymbol{\theta}}^B = (\hat{\theta}_1^B, \dots, \hat{\theta}_n^B)^\top$ is a vector of unbenchmarked posterior means $E[\theta_i \mid \mathbf{y}_1]$ under a given prior, $\bar{\hat{\theta}}_w^B = \sum_{i=1}^n w_i \hat{\theta}_i^B$, $\mathbf{r} = (r_1, \dots, r_n)^\top$, $r_i = w_i/\phi_i$, and $s = \sum_{i=1}^n w_i^2/\phi_i$. Note that if $\phi_i = 1$ for all $i = 1, \dots, n$, the benchmarked Bayes estimate becomes $\hat{\boldsymbol{\theta}}^{BM} = \hat{\boldsymbol{\theta}}^B + (\mathbf{w}^\top \mathbf{w})^{-1}(y_2 - \bar{\hat{\theta}}_w^B)\mathbf{w}$. Thus from Equation (1) we can see that the benchmarked Bayes estimate is a function of the unbenchmarked Bayes estimate under mean squared error (MSE) loss (posterior means) and user-specified weights. This is computationally appealing, as obtaining

benchmarked estimates with this method is done via a quick post-processing step.

To obtain uncertainty around the benchmarked estimates, posterior samples can be projected into the feasible set defined by the benchmarking constraint (Patra and Dunson 2018; Patra 2019). Geometrically, we can interpret this benchmarked Bayes estimate as the point estimate within the feasible set (defined by our benchmarking constraint) that is as close to the unbenchmark Bayes estimate as possible, where closeness is measured in terms of expected weighted squared error (Steorts et al. 2020).

The benchmarked estimate from Equation (1) is an exactly benchmarked estimate, i.e., the benchmarking constraint holds exactly. Alternatively, in inexact benchmarking, the benchmarking constraint need not hold exactly. If inexact benchmarking is desired in the benchmarked Bayes estimate framework, a parameter $\lambda > 0$ is introduced, and a slightly different loss function is considered,

$$L(\boldsymbol{\theta}, \mathbf{e}) = \lambda(y_2 - \bar{e}_w)^2 + \sum_{i=1}^n \phi_i(\theta_i - e_i)^2.$$

The Bayes estimate associated with this loss is

$$\hat{\boldsymbol{\theta}}_\lambda^B = \hat{\boldsymbol{\theta}}^B + (s + \lambda^{-1})^{-1}(y_2 - \bar{\hat{\theta}}_w^B)\mathbf{r},$$

where we note that as $\lambda \rightarrow \infty$, $\hat{\boldsymbol{\theta}}_\lambda^B$ approaches the exactly benchmarked Bayes estimate in Equation (1). Considering a loss function with the addition of a penalty term for the benchmarking constraint allows the user to incorporate a predetermined level of agreement between the benchmarks and aggregated, unbenchmark model estimates that must be met, whether that be exact benchmarking (correspond to $\lambda \rightarrow \infty$) or inexact, where the resulting estimate $\hat{\boldsymbol{\theta}}_\lambda^B$ is a compromise between the exactly benchmarked and unbenchmark Bayes estimate.

In the context of U5MR and HIV prevalence, the outcome of interest lies between 0 and 1, and may be close to 0. Any estimate that falls outside of $[0, 1]$ would be invalid. In applications where the outcome of interest lies in a restricted space, the benchmarked Bayes estimate approach described above can return invalid benchmarked estimates. In particular, note that the benchmarked Bayes estimates may possibly lie below zero when $\bar{\hat{\theta}}_w^B > y_2$. Ghosh et al. (2015) note this issue and consider a variant of the Kullback-Leibler loss function rather than weighted MSE loss, which addresses the issue of estimates falling below 0 in the case of positive small area estimates. Williams and Berg (2013) and Berg and Fuller (2018) also note this issue, and the latter propose using a specific form for the weights ϕ_i in Equation (1) to deal with unbenchmark estimates that are close to the boundary. Their approach does not guarantee, however, that benchmarked estimates will lie within the required restricted space. While they

note that in many situations benchmarked estimates that lie outside the restricted space will be rare—and in such cases their approach may be sufficient—when estimating rare disease prevalence or mortality this boundary issue is a concern.

To adapt the benchmarked Bayes estimate approach to ensure that benchmarked estimates lie in $[0, 1]$, additional constraints could be included in the optimization problem, namely requiring $e_i \leq 1$ and $e_i \geq 0$ for all i , and the same weighted square error loss approach as Datta et al. (2011) could be used under these additional constraints. In this case, the benchmarked Bayes estimate will not have a closed form solution, and thus numerical optimization methods would be needed to obtain benchmarked estimates. In applications where benchmarked estimates from Equation (1) would have fallen outside $[0, 1]$, these estimates would be pulled in to the boundary of $[0, 1]$ under these additional constraints. However, this is an ugly way of trying to adapt a loss function that is fundamentally inappropriate for the problem at hand. In the context of HIV prevalence or U5MR estimation, estimates of exactly 0 or 1 in any given area are unrealistic, and thus the benchmarked Bayes estimate approach under these additional constraints is unappealing. A second adaptation to the benchmarked Bayes estimate approach could be to consider projecting a transformation of the unbenchmark estimates into the benchmarked space, where the transformed estimates lie on the real line. For example, we could consider estimates on the logit scale. Then the benchmarking constraint would be $\sum_{i=1}^m w_i \text{expit}(\hat{\theta}_i) = y_2$. However, as this benchmarking constraint is nonlinear in $\hat{\theta}_i$, the optimization problem would no longer be convex. While the benchmarked Bayes estimate approach seems reasonable in settings where estimates fall on the real line, are positive as in Ghosh et al. (2015), or lie well within the boundary of $[0, 1]$, with the loss functions considered thus far in the literature the approach will often fall short for targets that are on a restricted range.

2.2 Raking approach

The second benchmarking approach we consider is simple and popular: raking, also referred to as the ratio-adjustment method (Datta et al. 2011; Zhang and Bryant 2020; Ghosh et al. 2015). This approach is commonly applied post-hoc. The key feature of the raking approach is a ratio comparing an unbenchmark national estimate to the national level benchmark

$$\text{BENCH} = \frac{\hat{\theta}^N}{y_2}, \quad (2)$$

where $\hat{\theta}^N$ denotes some unbenchmarked national level estimate, and y_2 again denotes the national level benchmark. For the unbenchmarked national estimate, one could plug in the weighted sum of unbenchmarked small area estimates as $\hat{\theta}^N = \sum_{i=1}^n w_i \hat{\theta}_i^M$, where w_i again denote population count weights and must satisfy $\sum_{i=1}^n w_i = 1$, and $\hat{\theta}_i^M$ denote the posterior estimates (means or medians) in each area from our unbenchmarked model.

In a post-hoc raking approach and with a sampling-based method, the posterior draws of $\hat{\theta}_i$ from an unbenchmarked model are multiplied by $1/\text{BENCH}$ so that the constraint $\sum_{i=1}^n w_i \hat{\theta}_i^M = y_2$ holds. Of note, this benchmarking approach will treat the unbenchmarked estimates in every area in the same fashion, regardless of the uncertainty in the unbenchmarked estimates. As such, the ranking of regions based on posterior medians/means will be preserved between unbenchmarked and benchmarked estimates. This behavior follows because of the ad hoc nature of the raking adjustment. It may be preferable to instead treat unbenchmarked estimates with more uncertainty differently than those with less. A version of the raking approach is used by the Institute for Health Metrics and Evaluation (IHME) in a variety of applications (e.g., Osgood-Zimmerman et al. (2018) and Local Burden of Disease HIV Collaborators (2021)), and is also used in the Naomi model for estimating HIV prevalence and incidence (Eaton et al. 2021).

The raking approach to benchmarking can also be performed via the inclusion of an offset term in certain models. In the supplement of Wakefield et al. (2019) they show that, for rare outcomes, including a log offset for BENCH in a logistic regression model corresponds approximately to the same multiplicative bias adjustment that would be done in the post-hoc raking approach. We note that the form of raking involving the inclusion of a log offset for BENCH does in fact produce fully Bayesian estimates, in the sense that a full posterior distribution for the benchmarked estimates is produced. However, the approach differs from the fully Bayesian approach described in Section 2.3 in that a likelihood is not specified for the benchmarks themselves.

2.3 Fully Bayesian benchmarking approach

We define the fully Bayesian approach to benchmarking, in the same way as Zhang and Bryant (2020), to be an approach that provides full posterior distributions for benchmarked estimates. Of note, Nandram and Sayit (2011) also consider a fully Bayesian benchmarking approach for data with binomial outcomes specific to beta-binomial models, but their approach is not directly generalizable to other models, and relies on Gibbs sampling for obtaining posterior estimates which may be computationally prohibitive. Janicki and Vesper (2017) perform fully Bayesian benchmarking by minimizing the KL divergence between a benchmarked and unbenchmarked posterior using moment constraints, though they note that their approach may be computationally intractable for non-normal

outcomes. Nandram et al. (2019) perform fully Bayesian benchmarking using a transformation of the benchmarking constraint that corresponds to “deleting” a single small area, but note that benchmarked estimates vary based on which area is deleted. In the following, we describe only the fully Bayesian approach of Zhang and Bryant (2020) as it is general to a wide class of models and applicable in a variety of settings.

Consider an area-level, Bayesian hierarchical model for small area estimation. For n small areas, let the area-level parameters we wish to estimate be denoted by $\boldsymbol{\theta} = (\theta_1, \dots, \theta_n)^\top$, with a hierarchical structure specified through a model $\pi(\boldsymbol{\theta} | \boldsymbol{\phi})$ with a vector of hyperparameters $\boldsymbol{\phi}$. The area-level observations are denoted by $\mathbf{y}_1 = (y_{11}, \dots, y_{1n})^\top$. For example, the values y_{1i} may be binomial counts of HIV status, with the parameters θ_i corresponding to HIV prevalence in area i . We can write the posterior distribution as

$$\pi(\boldsymbol{\theta}, \boldsymbol{\phi} | \mathbf{y}_1) \propto \pi(\mathbf{y}_1 | \boldsymbol{\theta}, \boldsymbol{\phi})\pi(\boldsymbol{\theta} | \boldsymbol{\phi})\pi(\boldsymbol{\phi}).$$

Though Zhang and Bryant (2020) consider more complex forms of benchmarking constraints, for simplicity we again consider the constraint $\sum_{i=1}^n w_i \theta_i = y_2$, where w_i and y_2 are defined as they have been previously. The method we describe is generally applicable to a variety of benchmarking constraints, however.

To incorporate the benchmarking constraint into their hierarchical model, Zhang and Bryant (2020) define an additional likelihood term for the benchmarks, $\pi(y_2 | \boldsymbol{\theta})$. This results in the benchmarked posterior distribution

$$\pi(\boldsymbol{\theta}, \boldsymbol{\phi} | \mathbf{y}_1, y_2) \propto \pi(\mathbf{y}_1 | \boldsymbol{\theta}, \boldsymbol{\phi})\pi(y_2 | \boldsymbol{\theta})\pi(\boldsymbol{\theta} | \boldsymbol{\phi})\pi(\boldsymbol{\phi}), \quad (3)$$

with the assumption that \mathbf{y}_1 and y_2 are conditionally independent given $\boldsymbol{\theta}$. The likelihood term for the benchmarks, $\pi(y_2 | \boldsymbol{\theta})$, pulls the likelihood for the area-level observations, $\pi(\mathbf{y}_1 | \boldsymbol{\theta}, \boldsymbol{\phi})$, towards the benchmarks. Uncertainty quantification is thus straightforward, as we obtain an entire benchmarked posterior distribution as opposed to simply a benchmarked point estimate.

Under exact benchmarking, we set $\pi(y_2 | \boldsymbol{\theta}) = \mathbb{I}[\sum_{i=1}^n w_i \theta_i = y_2]$. Under inexact benchmarking, $\pi(y_2 | \boldsymbol{\theta})$ is a non-degenerate distribution specified by the user. One can incorporate a discrepancy parameter λ into this distribution to allow for varying levels of agreement between the benchmarks and the aggregate parameters if desired. For example, in the application we consider setting $\pi(y_2 | \boldsymbol{\theta})$ equal to a normal distribution with mean $\sum_{i=1}^n w_i \theta_i$ and variance equal to the variance of the national benchmark.

A benefit of this benchmarking approach is that it allows for nonlinear benchmarking constraints. This is particularly relevant for logistic models, where the benchmarking constraint may take the form $\sum_{i=1}^n w_i \theta_i =$

$\sum_{i=1}^n w_i \text{expit}(\eta_i)$ for a linear predictor η_i . Unlike the estimates from a benchmarked Bayes estimate approach, the fully Bayesian benchmarking approach ensures that benchmarked estimates remain within the boundaries of the parameter space.

The fully Bayesian benchmarking approach can be used with both area-level and unit-level models. Though Zhang and Bryant (2020) describe an extension of their fully Bayesian approach to unit-level models, an implementation of this does not currently exist. Zhang and Bryant (2020) provide code in their R package `demest` for Poisson, binomial, multinomial, and normal models, with optional point mass, Poisson, binomial, and normal distributions for the likelihood for the benchmark, found at github.com/StatisticsNZ/demest. They provide an outline for a MCMC scheme for a general model. However, implementation of this MCMC scheme will be model-specific, which can limit the uptake of the method. Statistical programs such as INLA and TMB provide alternative ways to conduct Bayesian inference which have great computational advantages over MCMC samplers (Rue et al. 2009; Kristensen et al. 2016).

The benchmarking approach we propose in the following section is a more general implementation of the inexact, fully Bayesian approach described by Zhang and Bryant (2020), and allows us to obtain fully Bayesian benchmarked estimates from any method that produces area-level samples from an unbenchmark model. The approach we propose is readily applicable to both area- and unit-level models, and can be used in conjunction with statistical programs such as INLA and TMB.

2.4 Proposed approach

We propose a rejection sampling approach to obtaining full posterior distributions conditional on a benchmarking constraint under *inexact* benchmarking. Note that from Equation (3) we can write

$$\begin{aligned}\pi(\boldsymbol{\theta}, \boldsymbol{\phi} \mid \mathbf{y}_1, y_2) &\propto \pi(\mathbf{y}_1 \mid \boldsymbol{\theta}, \boldsymbol{\phi})\pi(y_2 \mid \boldsymbol{\theta})\pi(\boldsymbol{\theta} \mid \boldsymbol{\phi})\pi(\boldsymbol{\phi}), \\ &\propto \pi(\boldsymbol{\theta}, \boldsymbol{\phi} \mid \mathbf{y}_1)\pi(y_2 \mid \boldsymbol{\theta}).\end{aligned}$$

Intuitively, we can think of $\pi(y_2 \mid \boldsymbol{\theta})$ as a likelihood for the benchmarks and $\pi(\boldsymbol{\theta}, \boldsymbol{\phi} \mid \mathbf{y}_1)$ as a prior that corresponds to the posterior based on area-level observations \mathbf{y}_1 . For concreteness we consider a normal distribution for $\pi(y_2 \mid \boldsymbol{\theta})$, i.e.

$$y_2 \mid \boldsymbol{\theta} \sim N\left(\sum_{i=1}^n w_i \theta_i, \sigma_{y_2}^2\right),$$

where w_i are population weights that sum to one across all regions, and $\sigma_{y_2}^2$ is treated as the known, national level variance for y_2 . One could consider other distributions for the benchmark likelihood, however we focus on the normal case in the following derivation. In a rejection sampling framework, we can obtain samples from $\pi(\boldsymbol{\theta}, \boldsymbol{\phi} \mid \mathbf{y}_1, y_2)$ by filtering samples from $\pi(\boldsymbol{\theta}, \boldsymbol{\phi} \mid \mathbf{y}_1)$ through the information provided by $\pi(y_2 \mid \boldsymbol{\theta})$. Importantly, $\pi(\boldsymbol{\theta}, \boldsymbol{\phi} \mid \mathbf{y}_1)$ is the posterior distribution from an unbenchmarked model. This filtering is done via the following rejection sampler (Smith and Gelfand 1992):

1. Generate $U \sim \text{Uniform}(0, 1)$ and $(\boldsymbol{\theta}, \boldsymbol{\phi}) \sim \pi(\boldsymbol{\theta}, \boldsymbol{\phi} \mid \mathbf{y}_1)$ independently.
2. Accept $(\boldsymbol{\theta}, \boldsymbol{\phi})$ if

$$U < \frac{\pi(y_2 \mid \boldsymbol{\theta})}{\sup_{\boldsymbol{\theta}} \pi(y_2 \mid \boldsymbol{\theta})} = \exp\left(-\frac{1}{2\sigma_{y_2}^2} \left(\sum_{i=1}^m w_i \theta_i - y_2\right)^2\right),$$

Otherwise, return to Step 1.

This rejection sampling approach targets the same constrained posterior distribution as the fully Bayesian benchmarking approach of Zhang and Bryant (2020) but in a computationally straightforward manner. As the rejection sampling approach only requires posterior draws from an unbenchmarked posterior distribution, this allows practitioners to use a wider array of computation tools to conduct fully Bayesian benchmarking, even when benchmarking constraints are nonlinear. A relevant example of such a computational tool is INLA, which does not allow for nonlinear predictors, and therefore the likelihood corresponding to the benchmark cannot be directly incorporated into the model (Rue et al. 2009).

The rejection sampling approach to fully Bayesian benchmarking may be inefficient in cases where benchmarks are far from the population aggregated estimates from an unbenchmarked model. It may be necessary in such cases to use an approach such as Zhang and Bryant (2020)'s in order to produce benchmarked estimates. However, we caution that if the proportion of accepted samples is very small this may be indicative of inconsistencies between the two data sources, and model elaboration may be required in this case.

Additionally, the rejection sampling approach cannot perform exact benchmarking, where we require the benchmarking constraint to hold exactly, as the likelihood $\pi(y_2 \mid \boldsymbol{\theta})$ would be a point mass. We note that exact benchmarking could be approximated by setting $\sigma_{y_2}^2$ to be very small, but the rejection sampling approach would likely be very inefficient due to the likelihood for the benchmark being very concentrated. The inexact scenario is the most practically relevant, as it is hard to think of situations where the national benchmark does not have some degree of uncertainty.

3 Application

Below we describe the data, models, and software used in the HIV prevalence application. The application to U5MR is in Section 2 of the Supplemental Data. We fit both area-level and unit-level models.

3.1 Data

Spatial boundary files for South Africa are obtained from GADM, the Database of Global Administrative Areas (Database of Global Administrative Areas (GADM) 2019).

We estimate HIV prevalence in South Africa from the 2016 South Africa DHS survey. The survey followed a multi-stage, stratified design, and was designed to provide estimates at the Administrative 1 (admin1) level, which consists of nine provinces. These nine provinces were stratified by urban/farm/traditional area status, and therefore resulted in 26 strata, as the Western Cape province does not have a traditional area geotype. The sampling frame was established from the 2011 census, and 750 primary sampling units were selected across strata. The second stage of sampling sampled dwelling units, or households, from the enumeration areas, and every individual within the household (if available) was included in the survey. Only men and women aged 15-49 were included in the HIV dataset. Households within a given enumeration area are given a single geographic location, and we denote these as clusters from here on. GPS coordinates are displaced by up to 2km for urban clusters and 5km for rural clusters, but are never displaced outside of their area of stratification.

We obtain a national level estimate for 2016 in South Africa from the national Thembisa model, an HIV epidemic projection model that produces the official estimates published by UNAIDS for South Africa (Johnson, May, et al. 2017; Mahy et al. 2019; Stover et al. 2019). The national level estimate of HIV prevalence for 2016 in South Africa is 17.1%, with a 95% confidence interval of (15.6%, 18.3%). For the benchmark likelihood for the fully Bayesian benchmarking approaches we need a standard error for this benchmarked estimate, which we take to be 0.61 based on the assumption that the national level estimate is asymptotically normally distributed.

The population count data we use for our HIV application comes from the provincial Thembisa model (Johnson, Dorrington, et al. 2017). We use this specific population data as it is currently used in UNAIDS models of subnational HIV prevalence in South Africa (Eaton et al. 2021). In Figure 1, we plot the spatial distribution of individuals aged 15-49 (the population in our HIV example) in 2016 in South Africa, i.e., out of all people aged 15-49 in South Africa, the proportion of that sub-population who live in each region is displayed.

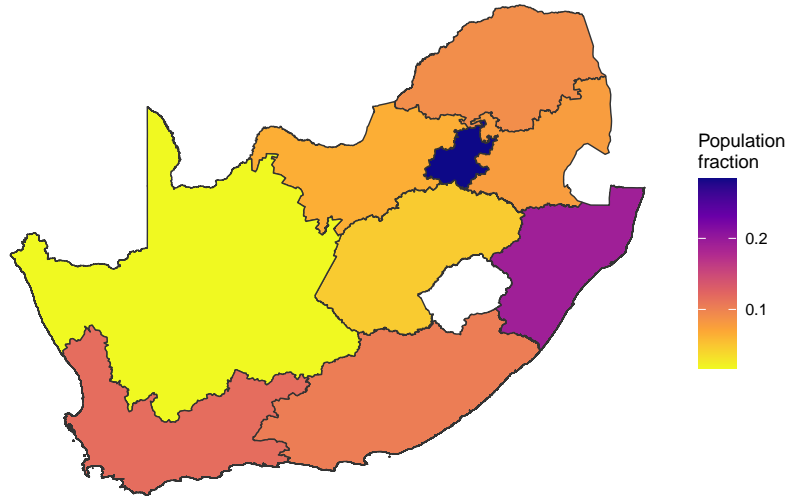


Figure 1: Proportion of the 15-49 population living in each province.

3.2 Unbenchmarked models

3.2.1 Area-level: Spatial Fay-Herriot

Following Mercer et al. (2015), we assume a working likelihood based on the distribution,

$$y_{1i}^* = \text{logit}(\hat{\theta}_i^{HT}) \sim N(\eta_i, \hat{V}_i^{DES})$$

where $\hat{\theta}_i^{HT}$ is the Horvitz-Thompson estimator for area i (Horvitz and Thompson 1952), $\hat{\sigma}^{2HT}$ is the variance of $\hat{\theta}_i^{HT}$, and $\hat{V}_i^{DES} = \frac{\hat{\sigma}_i^{2HT}}{\hat{\theta}_i^{2HT}(1-\hat{\theta}_i^{2HT})}$ is obtained via the delta method. Treating y_{1i}^* and \hat{V}_i^{DES} as fixed, we then consider the area-level model

$$y_{1i}^* \mid \eta_i \sim N(\eta_i, \hat{V}_i^{DES})$$

$$\eta_i = \beta_0 + b_i$$

where β_0 is an intercept term, and b_i follows a BYM2 model (Riebler et al. 2016), denoted $b_i \sim \text{BYM2}(\tau_b, \phi)$. A sum-to-zero constraint is placed on the structured component of the BYM2 random effect to ensure identifiability (Besag et al. 1991). For priors, we set $\beta_0 \sim N(0, 0.001^{-1})$, $\phi \sim \text{Beta}(0.5, 0.5)$. We use penalized complexity (PC) priors for the precision τ_b with values $U = 1$ and $\alpha = 0.01$, corresponding to a prior belief that the probability $\sigma_b = 1/\sqrt{\tau_b}$ is greater than 1 is 1% (Simpson et al. 2017).

We obtain $k = 1, \dots, K$ posterior draws $\hat{\eta}_i^{(k)}$ for each area i , and transform them via $\text{expit}(\hat{\eta}_i^{(k)}) = \hat{\theta}_i^{(k)}$ to obtain posterior samples for the Spatial Fay-Herriot estimates.

3.2.2 Unit-level: Binomial

We have binomial observations of HIV cases for each cluster c within area i . Let $y_{1i[c]}$ be the number of positive HIV cases observed in $n_{i[c]}$ total people in cluster c within area i . We consider the unbenchmarked, unit-level model

$$y_{1i[c]} \mid n_{i[c]}, \theta_{i[c]} \sim \text{Binomial}(n_{i[c]}, \theta_{i[c]}),$$

$$\eta_{i[c]} = \text{logit}(\theta_{i[c]}) = \beta_0 + b_i + e_{i[c]}$$

where $\theta_{i[c]}$ is HIV prevalence in area i and cluster c , β_0 is an intercept term, b_i follows a BYM2 model (Riebler et al. 2016), denoted $b_i \sim \text{BYM2}(\tau_b, \phi)$, and $e_{i[c]} \stackrel{iid}{\sim} \text{N}(0, \sigma_e^2)$ is an iid cluster-level random effect. A sum-to-zero constraint is placed on the structured component of the BYM2 random effect to ensure identifiability (Besag et al. 1991). Area-level predictions θ_i are obtained by marginalizing over the cluster random effect to get

$$\theta_i = \text{expit} \left(\frac{\alpha + \mu_i + \psi_i}{\sqrt{1 + h^2 \sigma_e^2}} \right),$$

where $h = \frac{16\sqrt{3}}{15\pi}$. The cluster-level random effect is excluded from predictions, and a so-called lono-binomial correction is done using h and σ_e^2 , as described in Dong and Wakefield (2021). The lono-binomial correction accounts for within-cluster variation that induces cluster-level overdispersion. If we instead believed the cluster-level random effect reflected true *between*-cluster differences, we could obtain predictions such as those obtained in Dong and Wakefield (2021). We let the hyperparameters (ϕ, τ) denote the spatial proportion parameter and overall precision of the BYM2 spatial random effect (Riebler et al. 2016). For priors, we set $\beta_0 \sim \text{N}(0, 0.001^{-1})$, $\phi \sim \text{Beta}(0.5, 0.5)$. We use penalized complexity (PC) priors for τ_b and $\tau_e = 1/\sigma_e^2$ with values $U = 1$ and $\alpha = 0.01$, corresponding to a prior belief that the probability $\sigma_b = 1/\sqrt{\tau_b}$ and $\sigma_e = 1/\sqrt{\tau_e}$ are greater than 1 is 1% (Simpson et al. 2017).

3.3 Benchmarked models

3.3.1 Approaches

Benchmarked Bayes Estimate:

We obtain $k = 1, \dots, K$ posterior draws $\hat{\theta}_i^{(k)}$ from an unbenchmarked model for each area i using INLA sampling capabilities, and apply Equation (1) to obtain exact, benchmarked posterior draws, $\hat{\theta}_i^{BB(k)}$.

Raking:

We obtain posterior medians $\hat{\theta}_i^M$ from an unbenchmarked model for each area i , and compute BENCH from Equation (2), using weights w_i and our benchmark y_2 , setting $\hat{\theta}^N := \sum_{i=1}^n w_i \hat{\theta}_i^M$. We then adjust unbenchmarked posterior draws $\hat{\theta}_i^{(k)}$, $k = 1, \dots, K$, to obtain benchmarked posterior draws $\hat{\theta}_i^{R(k)} = \hat{\theta}_i^{(k)}/\text{BENCH}$.

Fully Bayesian: Zhang and Bryant (2020)

Using weights w_i and our benchmark y_2 with associated standard error $\sigma_{y_2}^2$, we fit the unbenchmarked model with the additional likelihood

$$y_2 \sim \text{Normal} \left(\sum_{i=1}^m w_i \theta_i, \sigma_{y_2}^2 \right),$$

and denote benchmarked posterior draws by $\hat{\theta}_i^{FB1(k)}$.

Fully Bayesian: Rejection sampler:

We obtain $k = 1, \dots, K$ posterior draws $\hat{\theta}_i^{(k)}$ from an unbenchmarked model for each area i , and apply the algorithm described in Section 2.4 using weights w_i , and the benchmark y_2 with associated standard error $\sigma_{y_2}^2$, to obtain benchmarked posterior draws $\hat{\theta}_i^{FB2(k)}$.

3.4 Software

We implement all HIV models in Template Model Builder (TMB) (Kristensen et al. 2016) so that the fully Bayesian approach of Zhang and Bryant (2020) is directly comparable to alternative and proposed approaches, though we note in practice that one could fit an unbenchmarked model in INLA or other programmes in conjunction with the alternative and proposed approaches. TMB is a flexible modeling tool that takes advantage of Laplace approximations for computational efficiency, and allows users to specify a wide variety of models in C++. In particular, TMB allows users to specify nonlinear predictors, which is key for implementing the fully Bayesian benchmarking approach of Zhang and Bryant (2020) in settings with binary outcomes. For a review of TMB,

see Section 4 of Osgood-Zimmerman and Wakefield (2021). The rejection sampler for the proposed benchmarking approach and the Bayes estimate approach are implemented using a combination of TMB to obtain unbenchmarked posterior samples, and R to adjust them.

3.5 Results

In Figure 2, we display national level estimates from Thembisa, the unbenchmarked, and benchmarked results from the unit-level model. Results from the area-level model are very similar to those from the unit-level model, and can be found in Section 1.2 of the Supplemental Data, with direct comparisons between the unit-level and area-level models found in Section 1.3 of the Supplemental Data. We see that the Fully Bayesian benchmarking approaches produce essentially identical results, and that they are a compromise between the likelihood given by the national level benchmark and the unbenchmarked posterior estimate. The raking approach and the benchmarked Bayes estimate approach enforce exact benchmarking, which is evidenced by the overlap between the density of the Thembisa national estimate and that of the benchmarked method's national aggregated estimate. The fully Bayesian rejection sampler approach accepts 7.6% of unbenchmarked samples using the unit-level model, and 8.6% of unbenchmarked samples using the area-level model. Figure 3 displays the subnational breakdown of benchmarked and unbenchmarked estimates from the unit-level model. Additional plots and tables, including those for the area-level model, can be found in Section 1 of the Supplemental data.

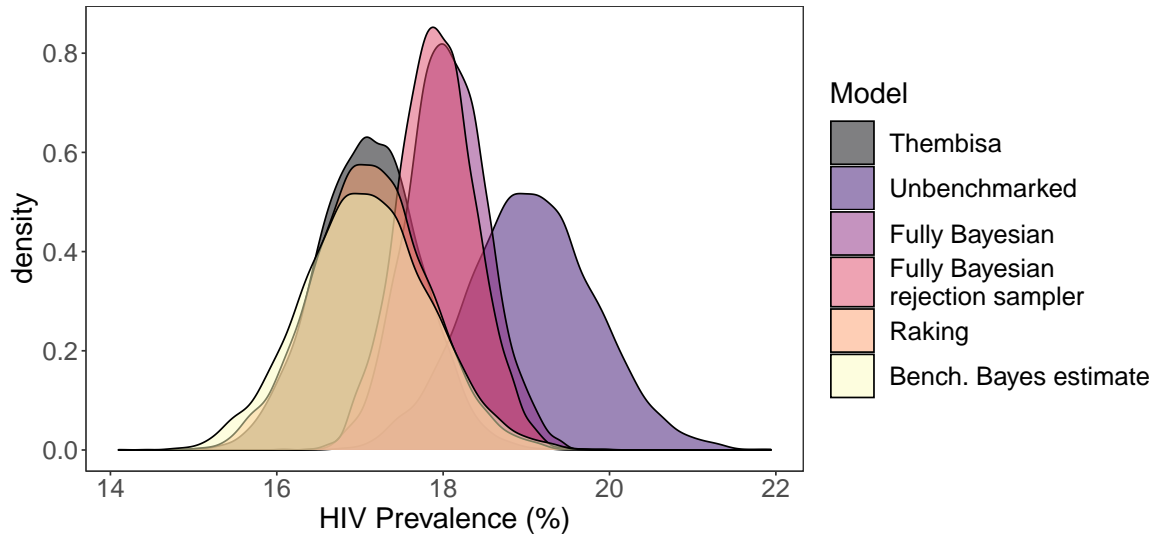


Figure 2: Aggregated national level HIV prevalence estimates from Thembisa, unbenchmark, and benchmarked results from the unit-level model. The Fully Bayesian model refers to the approach described in Zhang and Bryant (2020), and the Fully Bayesian rejection sampler refers to the proposed approach. All densities are based on 5000 samples.

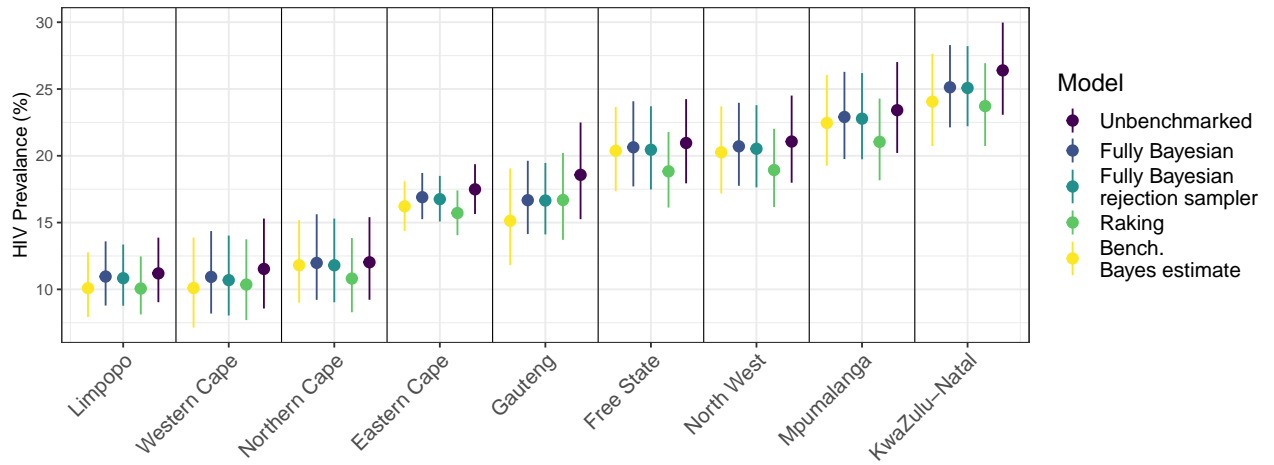


Figure 3: Comparison of HIV Prevalence estimates from benchmarked and unbenchmark unit-level models at a subnational level. Error bars correspond to 95% credible intervals, and provinces are arranged from left to right in order of unbenchmark median.

3.6 U5MR

The results for the U5MR application are in Section 2 of the Supplemental Data. Of note, 10/260 of the 95% credible intervals constructed for subnational estimates of U5MR (13 regions, 20 years) from the Bayes estimate

approach had lower bounds below zero, using either the unbenchmarked estimates from the unit-level model or the area-level model.

4 Discussion

In this paper we have summarized existing benchmarking approaches and their benefits and drawbacks with regard to data with rare binary outcomes. We consider benchmarking methods that make use of a benchmarking constraint via one-step or two-step approaches, and pay particular attention to the resulting interpretation of the benchmarked estimates, the ease of uncertainty quantification, the acknowledgement of uncertainty in national estimates, the use of non-linear constraints, and computational tractability. We believe that the proposed rejection sampling approach to fully Bayesian benchmarking best balances all of these concerns, and provides an alternative computational approach to the one-step, fully Bayesian benchmarking method developed by Zhang and Bryant (2020), which in many cases may be inflexible with regards to modeling choice and computational tractability, while targeting the same benchmarked, posterior distribution.

We show via an application of various benchmarking approaches to an HIV prevalence example that the proposed two-step approach to fully Bayesian benchmarking produces the same benchmarked estimates as the one-step Zhang and Bryant (2020) approach, and that the resulting estimates are a compromise between the national level estimate and unbenchmarked estimates. The rejection sampling approach allows us to take advantage of potentially faster computational programs than traditional MCMC samplers, such as INLA or TMB, as evidenced via our application to U5MR. Inference for spatial models (continuous models especially) using MCMC methods is computationally challenging, and our approach allows users to conduct fully Bayesian benchmarking while relying on Laplace approximation methods for inference that are more suited for such models (Osgood-Zimmerman and Wakefield 2021). Additionally, the rejection sampler approach is easily applied to both unit-level and area-level models, as evidenced in both our HIV and U5MR applications.

There are several limitations with the rejection sampling approach to fully Bayesian benchmarking. The first and potentially most pressing is the inability to conduct exact benchmarking, which may be required in some settings and is especially relevant if national benchmarks come from a census, though censuses have uncertainty in practice. Scenarios where true exact benchmarking is required may be rare. While we note that exact benchmarking can be approximated via the rejection sampling approach, it will likely be computationally inefficient. The one-step approach to fully Bayesian benchmarking may be a more useful approach if exact benchmarking is required, or a posterior projection approach using a loss function that respects the bounds on the parameters.

Additionally, our method does not account for uncertainty in the population count data. The population data used in our applications did not have reported uncertainty. If uncertainty for population count data were available, this would ideally be incorporated into the likelihood for the benchmarking constraint. Worldpop has recently started quantifying uncertainty in population data for select countries in their bottom-up Bayesian models, which may be of interest to include in future applications (Leasure et al. 2020).

References

Alkema, L., and J. R. New. 2014. “Global estimation of child mortality using a Bayesian B-spline bias-reduction model.” *The Annals of Applied Statistics* 8 (4): 2122–2149. DOI: <https://doi.org/10.1214/14-AOAS768>.

Battese, G. E., R. M. Harter, and W. A. Fuller. 1988. “An error-components model for prediction of county crop areas using survey and satellite data.” *Journal of the American Statistical Association* 83 (401): 28–36. DOI: <https://doi.org/10.2307/2288915>.

Bell, W. R., G. S. Datta, and M. Ghosh. 2013. “Benchmarking small area estimators.” *Biometrika* 100 (1): 189–202. DOI: <https://doi.org/10.1093/biomet/ass063>.

Berg, E., and W. A. Fuller. 2018. “Benchmarked small area prediction.” *Canadian Journal of Statistics* 46 (3): 482–500. DOI: <https://doi.org/10.1002/cjs.11461>.

Besag, J., J. York, and A. Mollié. 1991. “Bayesian image restoration, with two applications in spatial statistics.” *Annals of the Institute of Statistical Mathematics* 43 (1): 1–20. DOI: <https://doi.org/10.1007/BF00116466>.

Database of Global Administrative Areas (GADM). 2019. *Global Administrative Areas [Shapefiles]*. Available at: <https://www.gadm.org>. Downloaded January 2020.

Datta, G., M. Ghosh, R. Steorts, and J. Maples. 2011. “Bayesian benchmarking with applications to small area estimation.” *TEST* 20 (3): 574–588. DOI: <https://doi.org/10.1007/s11749-010-0218-y>.

Dong, T. Q., and J. Wakefield. 2021. “Modeling and presentation of vaccination coverage estimates using data from household surveys.” *Vaccine* 39 (18): 2584–2594. DOI: <https://doi.org/10.1016/j.vaccine.2021.03.007>.

Eaton, J. W., L. Dwyer-Lindgren, S. Gutreuter, M. O'Driscoll, O. Stevens, S. Bajaj, R. Ashton, A. Hill, E. Russell, R. Esra, et al. 2021. "Naomi: a new modelling tool for estimating HIV epidemic indicators at the district level in sub-Saharan Africa." *Journal of the International AIDS Society* 24:e25788. DOI: <https://doi.org/10.1002/jia2.25788>.

Fay, R. E., and R. A. Herriot. 1979. "Estimates of income for small places: an application of James-Stein procedures to census data." *Journal of the American Statistical Association* 74 (366a): 269–277. DOI: <https://doi.org/10.2307/2286322>.

Ghosh, M., T. Kubokawa, and Y. Kawakubo. 2015. "Benchmarked empirical Bayes methods in multiplicative area-level models with risk evaluation." *Biometrika* 102 (3): 647–659. DOI: <https://doi.org/10.1093/BIOMET/ASV010>.

Horvitz, D. G., and D. J. Thompson. 1952. "A generalization of sampling without replacement from a finite universe." *Journal of the American Statistical Association* 47 (260): 663–685. DOI: <https://doi.org/10.2307/2280784>.

Janicki, R., and A. Vesper. 2017. "Benchmarking techniques for reconciling Bayesian small area models at distinct geographic levels." *Statistical Methods and Applications* 26 (4): 557–581. DOI: <https://doi.org/10.1007/s10260-017-0379-x>.

Johnson, L. F., R. E. Dorrington, and H. Moola. 2017. "Progress towards the 2020 targets for HIV diagnosis and antiretroviral treatment in South Africa." *Southern African Journal of HIV Medicine* 18 (1): 1–8. DOI: <https://doi.org/10.4102/sajhivmed.v18i1.694>.

Johnson, L. F., M. T. May, R. E. Dorrington, M. Cornell, A. Boulle, M. Egger, and M.-A. Davies. 2017. "Estimating the impact of antiretroviral treatment on adult mortality trends in South Africa: A mathematical modelling study." *PLoS Medicine* 14 (12): e1002468. DOI: <https://doi.org/10.1371/journal.pmed.1002468>.

Kristensen, K., A. Nielsen, C. W. Berg, H. J. Skaug, and B. Bell. 2016. "TMB: Automatic differentiation and Laplace approximation." *Journal of Statistical Software* 70 (5): 1–21. DOI: <https://doi.org/10.18637/jss.v070.i05>.

Leasure, D. R., W. C. Jochum, E. M. Weber, V. Seaman, and A. J. Tatem. 2020. “National population mapping from sparse survey data: A hierarchical Bayesian modeling framework to account for uncertainty.” *Proceedings of the National Academy of Sciences* 117 (39): 24173–24179. DOI: <https://doi.org/10.1073/pnas.1913050117>.

Local Burden of Disease HIV Collaborators. 2021. “Mapping subnational HIV mortality in six Latin American countries with incomplete vital registration systems.” *BMC Medicine* 19:1–25. DOI: <https://doi.org/10.1186/s12916-020-01876-4>.

Mahy, M., K. Marsh, K. Sabin, I. Wanyeki, J. Daher, and P. D. Ghys. 2019. “HIV estimates through 2018: data for decision-making.” *AIDS (London, England)* 33 (Suppl 3): S203. DOI: <https://doi.org/10.1097/QAD.0000000000002321>.

Mercer, L. D., J. Wakefield, A. Pantazis, A. M. Lutambi, H. Masanja, and S. Clark. 2015. “Space-time smoothing of complex survey data: small area estimation for child mortality.” *The Annals of Applied Statistics* 9 (4): 1889. DOI: <https://doi.org/10.1214/15-AOAS872>.

Nandram, B., A. L. Erciulescu, and N. B. Cruze. 2019. “Bayesian benchmarking of the Fay-Herriot model using random deletion.” *Survey Methodology* 45 (2): 365–391. Available at: <https://www150.statcan.gc.ca/n1/pub/12-001-x/2019002/article/00004-eng.htm> (accessed March 2022).

Nandram, B., and H. Sayit. 2011. “A Bayesian analysis of small area probabilities under a constraint.” *Survey Methodology* 37 (2): 137–152. Available at: <https://www150.statcan.gc.ca/n1/pub/12-001-x/2011002/article/11603-eng.pdf> (accessed March 2022).

Osgood-Zimmerman, A., A. I. Millear, R. W. Stubbs, C. Shields, B. V. Pickering, L. Earl, N. Graetz, D. K. Kinyoki, S. E. Ray, S. Bhatt, et al. 2018. “Mapping child growth failure in Africa between 2000 and 2015.” *Nature* 555 (7694): 41–47. DOI: <https://doi.org/10.1038/nature25760>.

Osgood-Zimmerman, A., and J. Wakefield. 2021. “A Statistical Introduction to Template Model Builder: A Flexible Tool for Spatial Modeling.” *arXiv:2103.09929v1*, DOI: <https://doi.org/10.48550/arXiv.2103.09929>.

Patra, S. 2019. “Constrained Bayesian Inference through Posterior Projection with Applications.” PhD diss., Duke University. Available at: <https://hdl.handle.net/10161/19864> (accessed March 2022).

Patra, S., and D. B. Dunson. 2018. “Constrained Bayesian inference through posterior projections.” *arXiv:1812.05741v3*, DOI: <https://doi.org/10.48550/arXiv.1812.05741>.

Rao, J. N., and I. Molina. 2015. *Small Area Estimation*. John Wiley & Sons.

Riebler, A., S. H. Sørbye, D. Simpson, and H. Rue. 2016. “An intuitive Bayesian spatial model for disease mapping that accounts for scaling.” *Statistical Methods in Medical Research* 25 (4): 1145–1165. DOI: <https://doi.org/10.1177/0962280216660421>.

Rue, H., S. Martino, and N. Chopin. 2009. “Approximate Bayesian inference for latent Gaussian models by using integrated nested Laplace approximations.” *Journal of the Royal Statistical Society: Series B (statistical methodology)* 71 (2): 319–392. DOI: <https://doi.org/10.1111/j.1467-9868.2008.00700.x>.

Simpson, D., H. Rue, A. Riebler, T. G. Martins, S. H. Sørbye, et al. 2017. “Penalising model component complexity: A principled, practical approach to constructing priors.” *Statistical Science* 32 (1): 1–28. DOI: <https://doi.org/10.1214/16-STS576>.

Smith, A. F., and A. E. Gelfand. 1992. “Bayesian statistics without tears: a sampling–resampling perspective.” *The American Statistician* 46 (2): 84–88. DOI: <https://doi.org/10.2307/2684170>.

Stefan, M., and M. A. Hidiroglou. 2021. “Small area benchmarked estimation under the basic unit level model when the sampling rates are non-negligible.” *Survey Methodology* 47 (1): 123–150. Available at: <https://www150.statcan.gc.ca/n1/pub/12-001-x/2021001/article/00007-eng.htm> (accessed March 2022).

Steorts, R. C., T. Schmid, and N. Tzavidis. 2020. “Smoothing and Benchmarking for Small Area Estimation.” *International Statistical Review*, DOI: <https://doi.org/10.1111/insr.12373>.

Stover, J., R. Glaubius, L. Mofenson, C. M. Dugdale, M.-A. Davies, G. Patten, and C. Yiannoutsos. 2019. “Updates to the Spectrum/AIM model for estimating key HIV indicators at national and subnational levels.” *AIDS (London, England)* 33:S227. DOI: <https://doi.org/10.1097/QAD.0000000000002357>.

Wakefield, J., G.-A. Fuglstad, A. Riebler, J. Godwin, K. Wilson, and S. J. Clark. 2019. “Estimating under-five mortality in space and time in a developing world context.” *Statistical Methods in Medical Research* 28 (9): 2614–2634. DOI: <https://doi.org/10.1177/0962280218767988>.

Williams, M., and E. Berg. 2013. “Incorporating user input into optimal constraining procedures for survey estimates.” *Journal of Official Statistics* 29 (3): 375. DOI: <https://doi.org/10.2478/jos-2013-0032>.

Wu, Y., Z. R. Li, B. K. Mayala, H. Wang, P. Gao, J. Paige, G.-A. Fuglstad, et al. 2021. “Spatial Modeling for Subnational Administrative Level 2 Small-Area Estimation.” *DHS Spatial Analysis Reports* 21. Available at: <https://dhsprogram.com/publications/publication-SAR21-Spatial-Analysis-Reports.cfm> (accessed March 2022).

Zhang, J. L., and J. Bryant. 2020. “Fully Bayesian Benchmarking of Small Area Estimation Models.” *Journal of Official Statistics* 36 (1): 197–223. DOI: <https://doi.org/10.2478/jos-2020-0010>.

Supplemental data for “A Computationally Efficient Approach to Fully Bayesian Benchmarking”

1 HIV Application

1.1 Unit-level figures and tables

The subnational breakdown of unbenchmarked and benchmarked, unit-level models can be seen in Figure 1 and Table 1.

Table 1: Admin1 HIV prevalence estimates from unbenchmarked and benchmarked unit-level models. Point estimates provided are medians, with 95% credible intervals. Provinces are arranged in the order of lowest unbenchmarked median to highest.

Province	Unbenched (%)	FB (%)	FB: Rejection sampler (%)	Raking (%)	Bayes Estimate (%)
Limpopo	11.2 (8.9, 13.9)	10.9 (8.8, 13.5)	10.9 (8.7, 13.3)	10.3 (8.2, 12.8)	10.1 (7.8, 12.8)
Western Cape	11.5 (8.7, 15.4)	10.9 (8.2, 14.2)	10.8 (8.1, 13.9)	10.5 (7.8, 14)	10.1 (7.3, 14.0)
Northern Cape	12.1 (9.2, 15.7)	12.0 (9.1, 15.8)	11.8 (9.0, 15.3)	11.0 (8.4, 14.4)	11.9 (9.0, 15.5)
Eastern Cape	17.5 (15.8, 19.4)	16.9 (15.2, 18.7)	16.7 (15.2, 18.4)	16.1 (14.4, 17.9)	16.2 (14.5, 18.1)
Gauteng	18.5 (15.2, 22.4)	16.7 (14.2, 19.6)	16.6 (14.1, 19.3)	17.0 (13.9, 20.7)	15.1 (11.8, 19.0)
Free State	20.9 (17.9, 24.4)	20.6 (17.6, 23.9)	20.5 (17.5, 23.9)	19.3 (16.4, 22.5)	20.4 (17.3, 23.8)
North West	21.0 (18.0, 24.4)	20.7 (17.7, 24.0)	20.5 (17.5, 23.8)	19.4 (16.6, 22.6)	20.2 (17.2, 23.6)
Mpumalanga	23.4 (20.2, 27.1)	22.9 (19.8, 26.3)	22.8 (19.6, 26.2)	21.7 (18.7, 24.9)	22.5 (19.2, 26.1)
KwaZulu-Natal	26.4 (23.1, 29.9)	25.1 (22.2, 28.5)	25.0 (22.1, 28.2)	24.5 (21.3, 28.0)	24.1 (20.8, 27.6)

A table representation of the aggregated national estimates presented in Figure 2 in the main body of the paper can be found in Figure 2.

1.2 Area-level figures and tables

In Figure 2, we display national level estimates from Thembisa, the unbenchmarked, and benchmarked results from the area-level model. Results from this model are very similar to results from the unit-level model, found in the

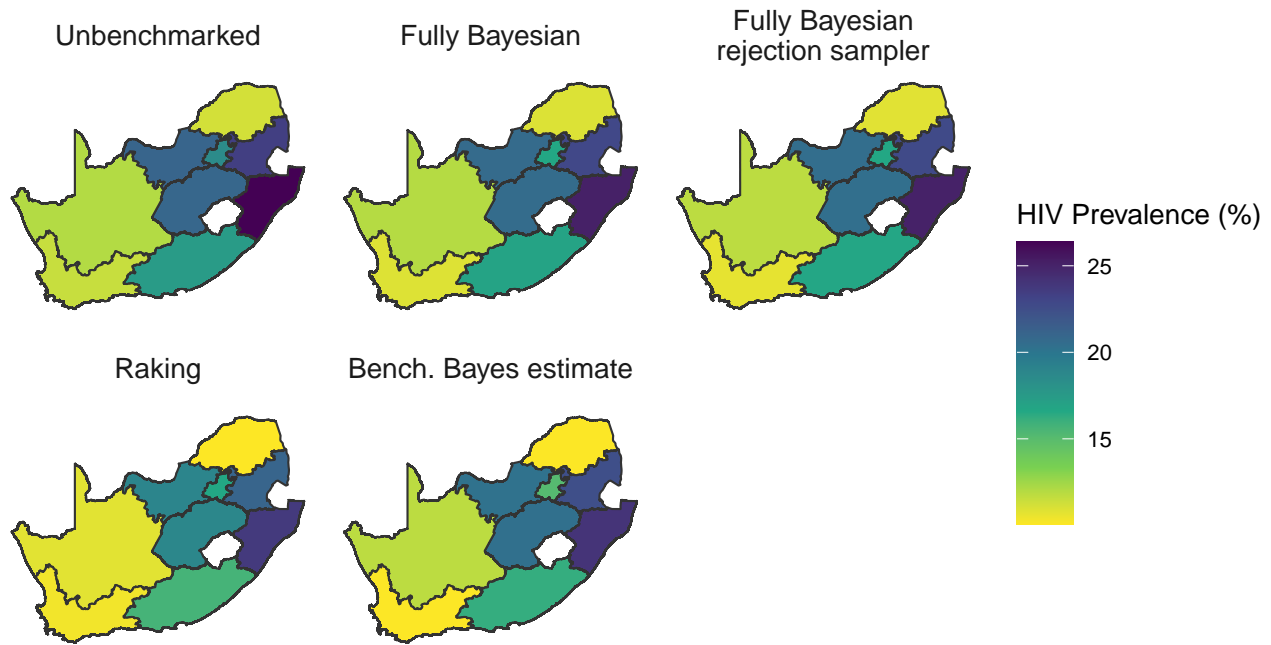


Figure 1: Comparison of HIV prevalence estimates from benchmarked and unbenchmark model.

Table 2: Aggregated national level HIV prevalence estimates from Thembisa, unbenchmarked, and benchmarked results from the unit-level model. 95% credible intervals are given next to posterior medians.

Model	Median (%)	SD (%)
Thembisa	17.1 (15.6, 18.3)	0.61
Unbenched	19.1 (17.6, 20.6)	0.76
FB	18.0 (17.1, 19.0)	0.48
FB: Rejection sampler	17.9 (17.0, 18.9)	0.46
Raking	17.1 (15.8, 18.5)	0.68
Bayes estimate	17.1 (15.6, 18.6)	0.76

main body of the paper.

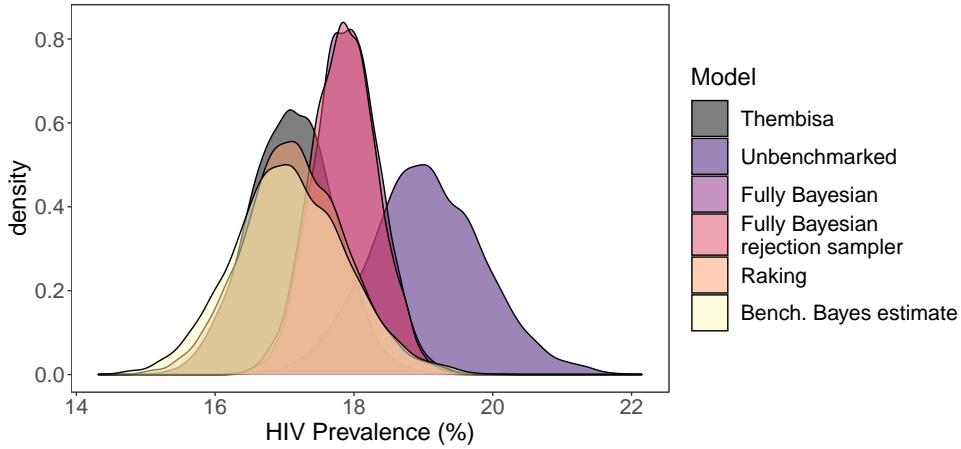


Figure 2: Aggregated national level HIV prevalence estimates from Thembisa, unbenchmarked, and benchmarked results from the area-level model. All densities are based on 5000 samples

Table 3: Aggregated national level HIV prevalence estimates from Thembisa, unbenchmarked, and benchmarked results from the area-level model. 95% credible intervals are given next to posterior medians.

Model	Median (%)	SD (%)
Thembisa	17.1 (15.6, 18.3)	0.61
Unbenchmarked	19.0 (17.5, 20.7)	0.81
FB	17.9 (17.0, 18.8)	0.47
FB: Rejection sampler	17.9 (17.0, 18.8)	0.47
Raking	17.1 (15.8, 18.7)	0.73
Bayes estimate	17.1 (15.5, 18.7)	0.81

Table 4: Admin1 HIV prevalence estimates from unbenchmarked and benchmarked area-level models. Point estimates provided are medians, with 95% credible intervals. Provinces are arranged in the order of lowest unbenchmarked median to highest.

Province	Unbenched (%)	FB	FB: Rejection sampler (%)	Raking (%)	Bayes Estimate (%)
Limpopo	10.4 (8.3, 13.1)	10.1 (8.0, 12.8)	10.2 (8.0, 12.8)	9.4 (7.5, 11.8)	9.3 (7.2, 12.0)
Northern Cape	12.5 (8.9, 17.4)	12.2 (8.6, 17.0)	12.3 (8.7, 17.1)	11.3 (8.0, 15.7)	12.3 (8.6, 17.2)
Western Cape	12.6 (8.2, 18.8)	11.1 (7.5, 16.4)	11.0 (7.4, 16.2)	11.3 (7.4, 17.0)	11.1 (6.8, 17.4)
Eastern Cape	16.8 (14.6, 19.4)	16.3 (14.3, 18.5)	16.3 (14.1, 18.7)	15.1 (13.1, 17.4)	15.5 (13.3, 18.1)
Gauteng	19.3 (15.9, 23.6)	17.5 (14.7, 20.6)	17.4 (14.7, 20.5)	17.4 (14.3, 21.2)	15.9 (12.5, 20.1)
North West	20.2 (17.5, 23.3)	19.9 (17.2, 22.8)	19.9 (17.2, 22.9)	18.2 (15.7, 21.0)	19.4 (16.7, 22.5)
Free State	21.0 (17.9, 24.4)	20.6 (17.7, 24.1)	20.7 (17.6, 24.0)	18.9 (16.1, 21.9)	20.4 (17.3, 23.8)
Mpumalanga	23.4 (20.2, 27.0)	22.9 (19.7, 26.4)	22.9 (19.6, 26.4)	21.1 (18.2, 24.3)	22.5 (19.2, 26.1)
KwaZulu-Natal	25.5 (21.7, 29.4)	24.0 (20.7, 27.6)	24.0 (20.7, 27.4)	22.9 (19.5, 26.5)	23.1 (19.3, 27.1)

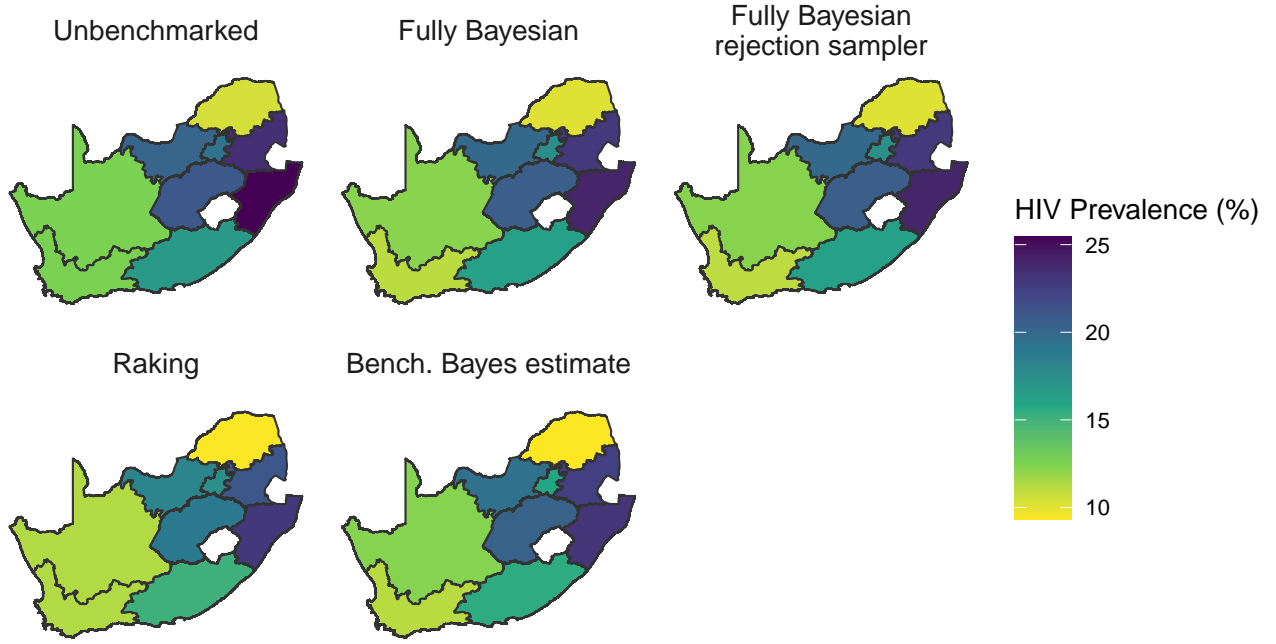


Figure 3: Comparison of HIV prevalence estimates from benchmarked and unbenchmark model.

1.3 Area-level and unit-level comparison plots

In Figure 4 we display the densities for the national aggregated HIV prevalence estimates from unbenchmark and benchmark models, comparing across unit-level and area-level models. As noted in the main text, the differences between unit-level and area-level estimates are very small, although there are relatively large differences between the unbenchmark and benchmark models themselves.

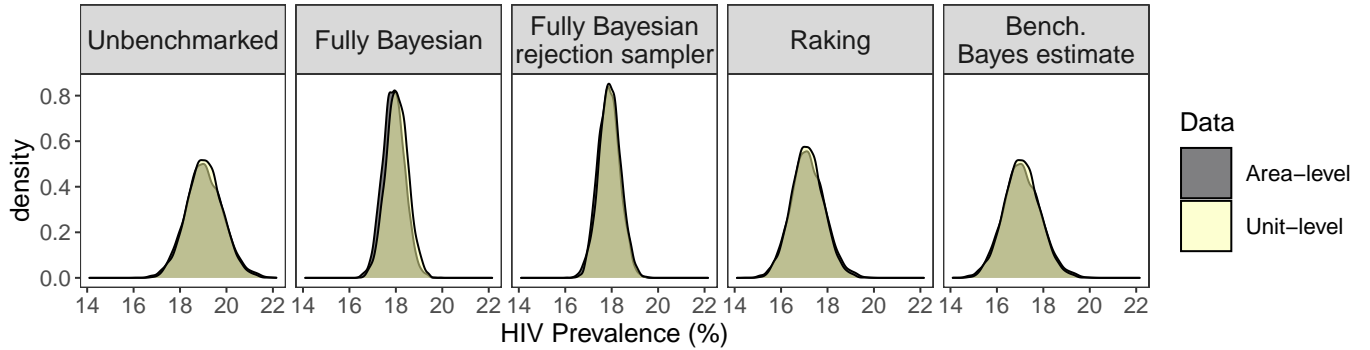


Figure 4: Aggregated national level HIV prevalence estimates from unbenchmarked and benchmarked models. All densities are based on 5000 samples.

In Figures 5 through 13, we show the differences between the unit-level and area-level, benchmarked and unbenchmarked sub-national estimates for each of the nine provinces. For most provinces, the differences between area-level and unit-level models are small, though we note that estimates from the unit-level models may have higher precision.

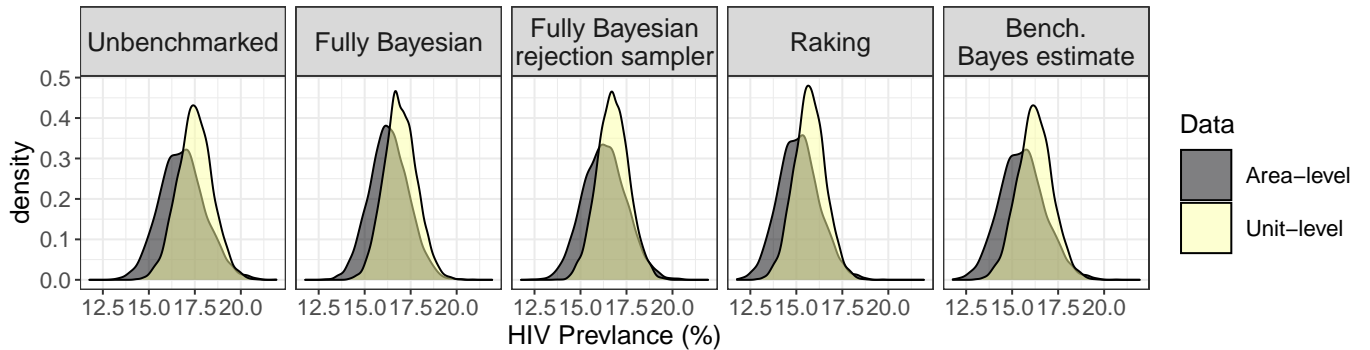


Figure 5: Subnational HIV prevalence estimates for the Eastern Cape province from unbenchmarked and benchmarked models. All densities are based on 5000 samples.

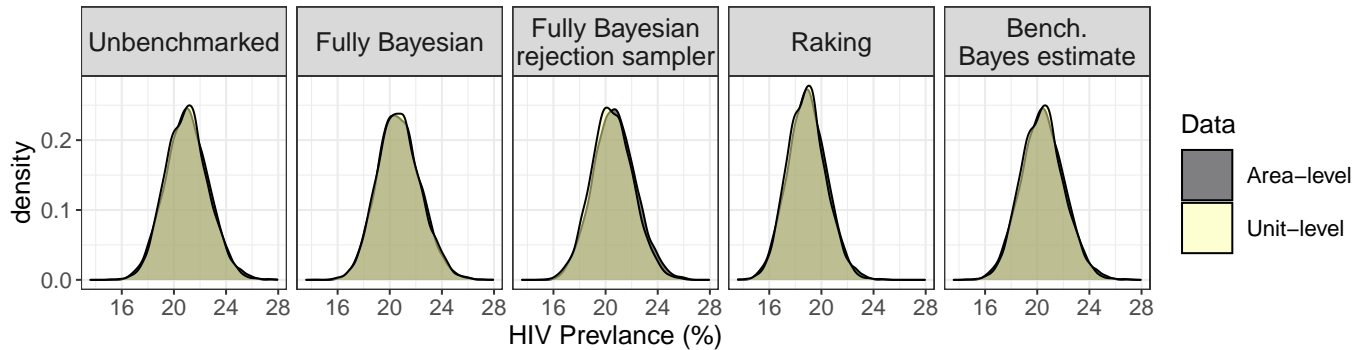


Figure 6: Subnational HIV prevalence estimates for the Free State province from unbenchmarked and benchmarked models. All densities are based on 5000 samples.

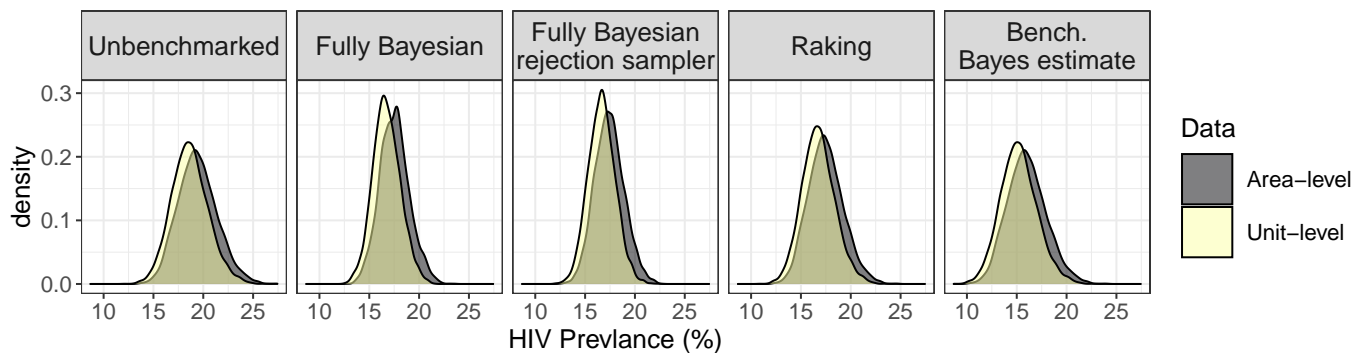


Figure 7: Subnational HIV prevalence estimates for the Gauteng province from unbenchmarked and benchmarked models. All densities are based on 5000 samples.

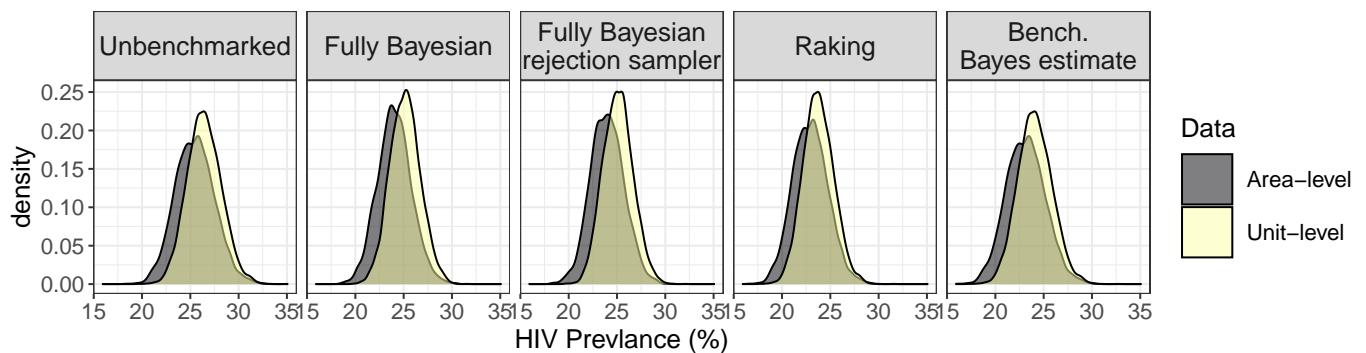


Figure 8: Subnational HIV prevalence estimates for the KwaZulu-Natal province from unbenchmarked and benchmarked models. All densities are based on 5000 samples.

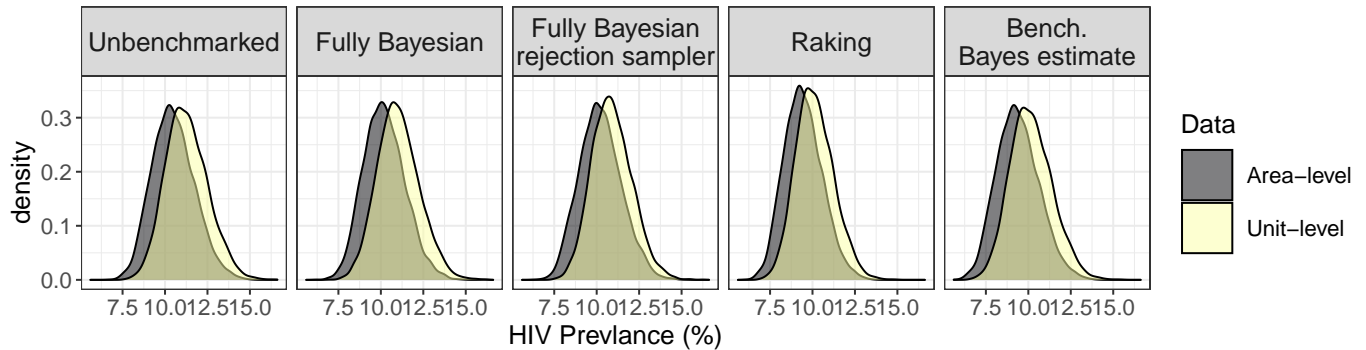


Figure 9: Subnational HIV prevalence estimates for the Limpopo province from unbenchmarked and benchmarked models. All densities are based on 5000 samples.

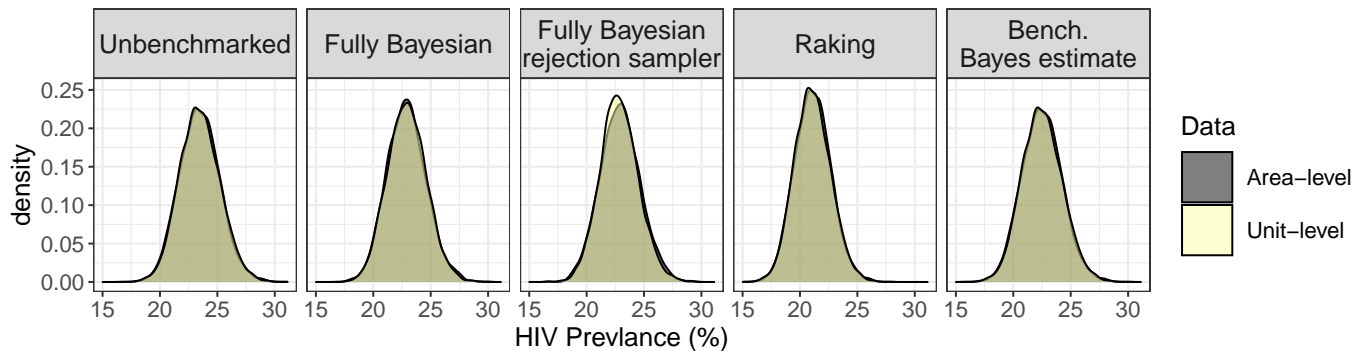


Figure 10: Subnational HIV prevalence estimates for the Mpumalanga province from unbenchmarked and benchmarked models. All densities are based on 5000 samples.

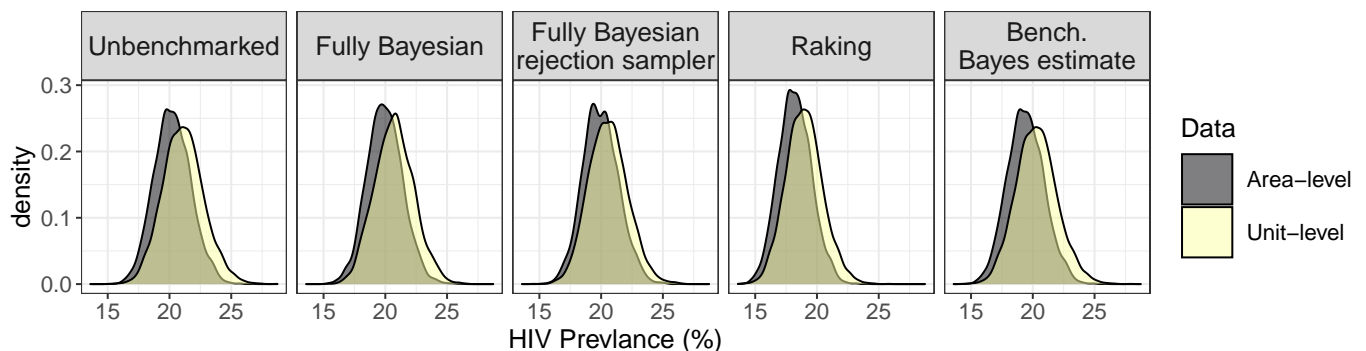


Figure 11: Subnational HIV prevalence estimates for the North West province from unbenchmarked and benchmarked models. All densities are based on 5000 samples.

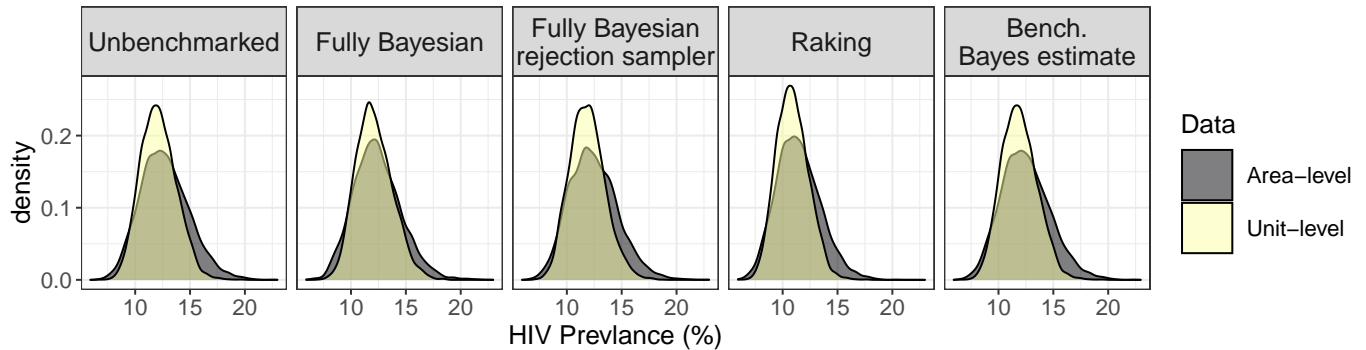


Figure 12: Subnational HIV prevalence estimates for the Northern Cape province from unbenchmarked and benchmarked models. All densities are based on 5000 samples.

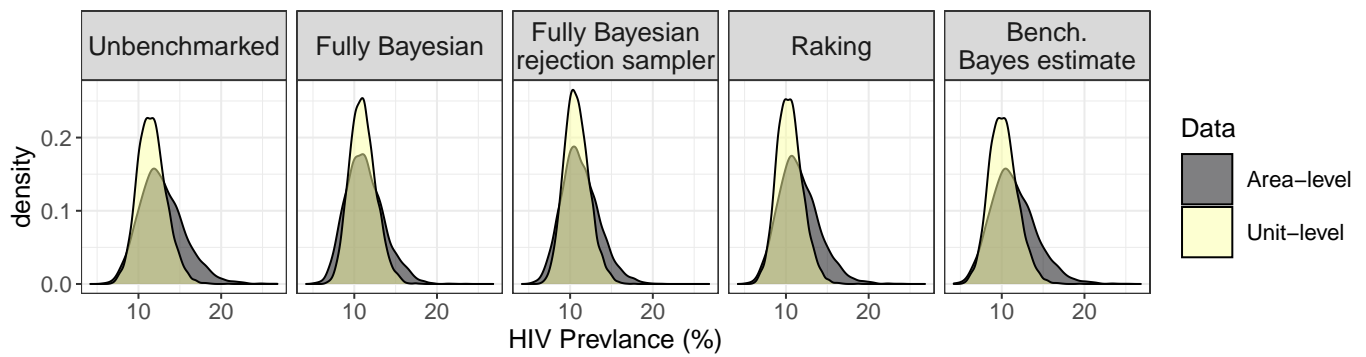


Figure 13: Subnational HIV prevalence estimates for the Western Cape province from unbenchmarked and benchmarked models. All densities are based on 5000 samples.

In Figures 14 through 16, we compare benchmarked and unbenchmarked estimates and their uncertainty for area-level and unit-level models.

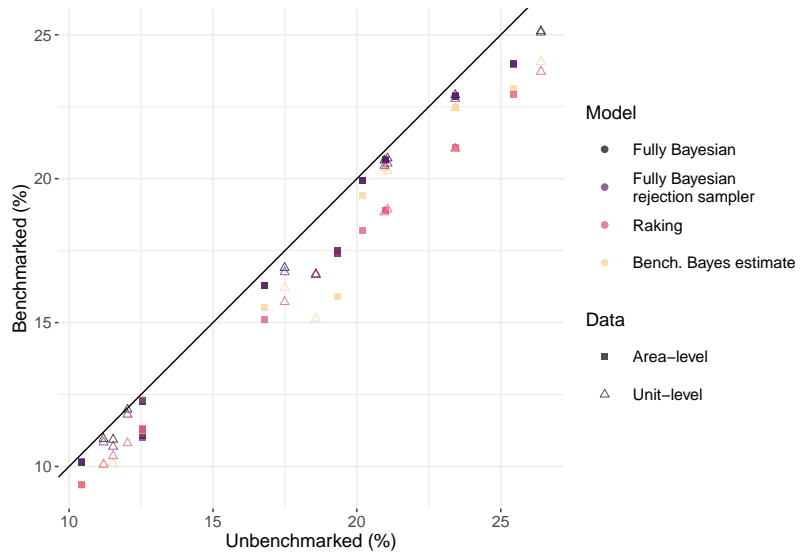


Figure 14: Comparison of unbenchmarkmed and benchmarkmed posterior medians by model and data type at a subnational level.

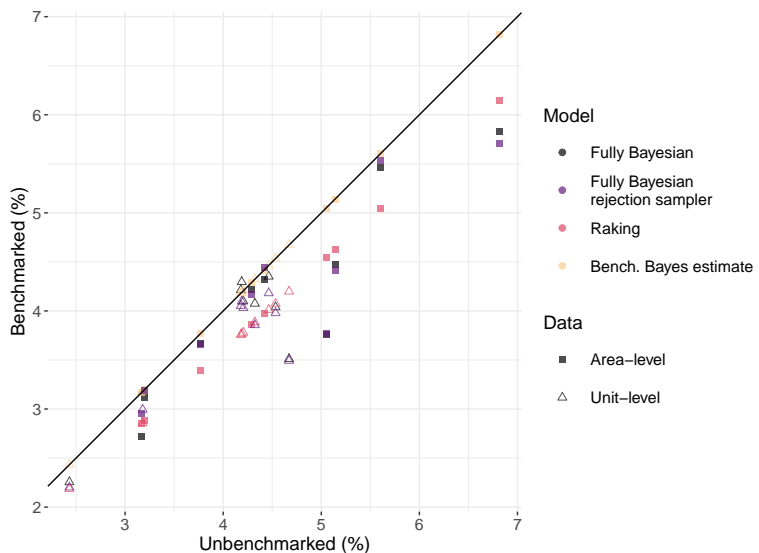


Figure 15: Comparison of unbenchmarkmed and benchmarkmed posterior 95% CI widths by model and data type at a subnational level.

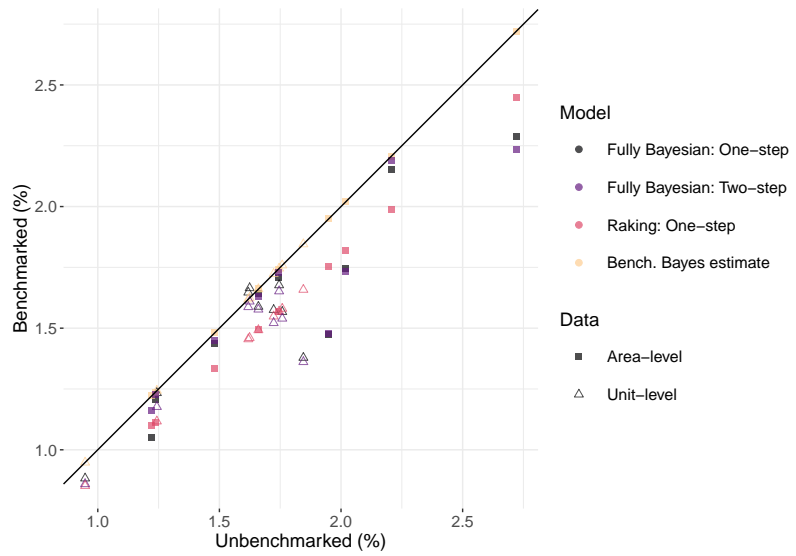


Figure 16: Comparison of unbenchmarkmarked and benchmarked posterior standard deviations by model and data type at a subnational level.

In Figures 17 through 19, we display benchmarked and unbenchmarkmarked estimates and their uncertainty for area-level and unit-level models.

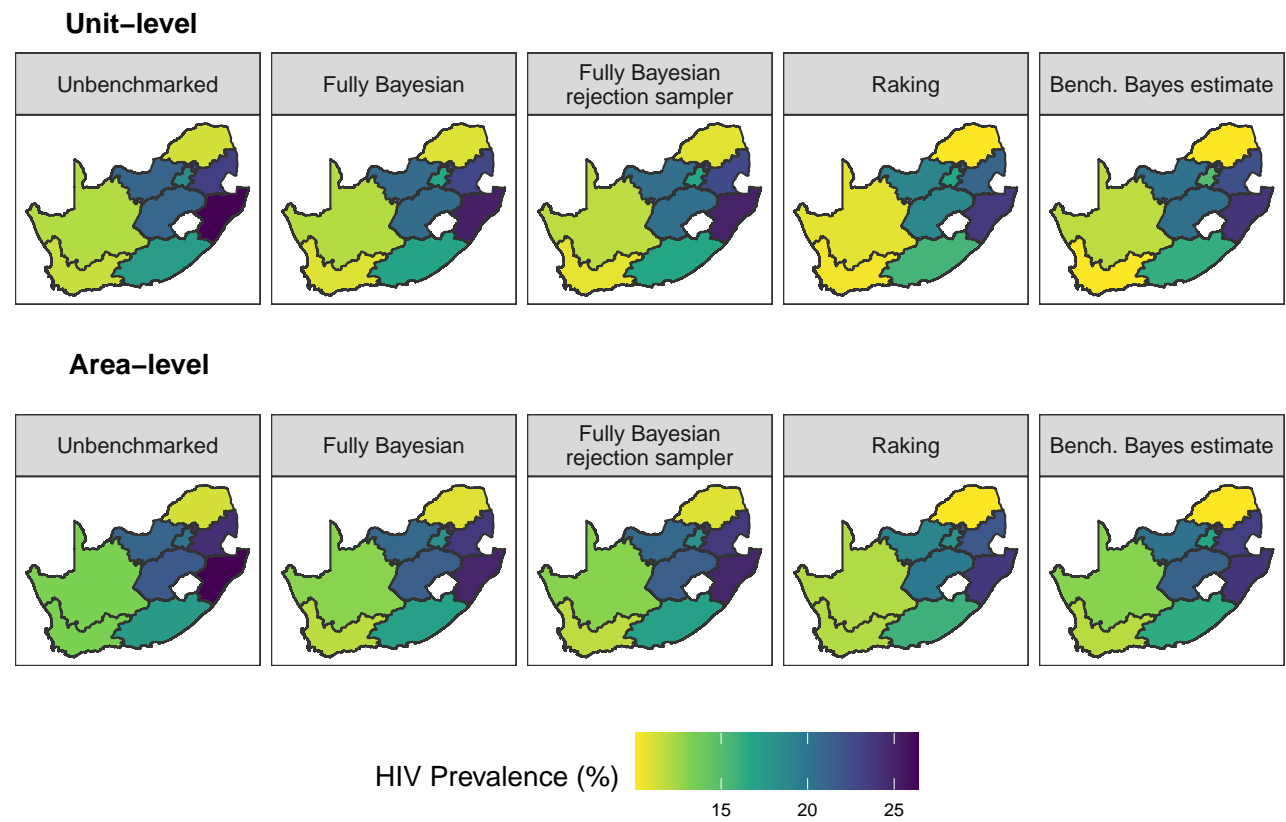


Figure 17: Unbenchmarked and benchmarked posterior medians by model and data type at a subnational level.

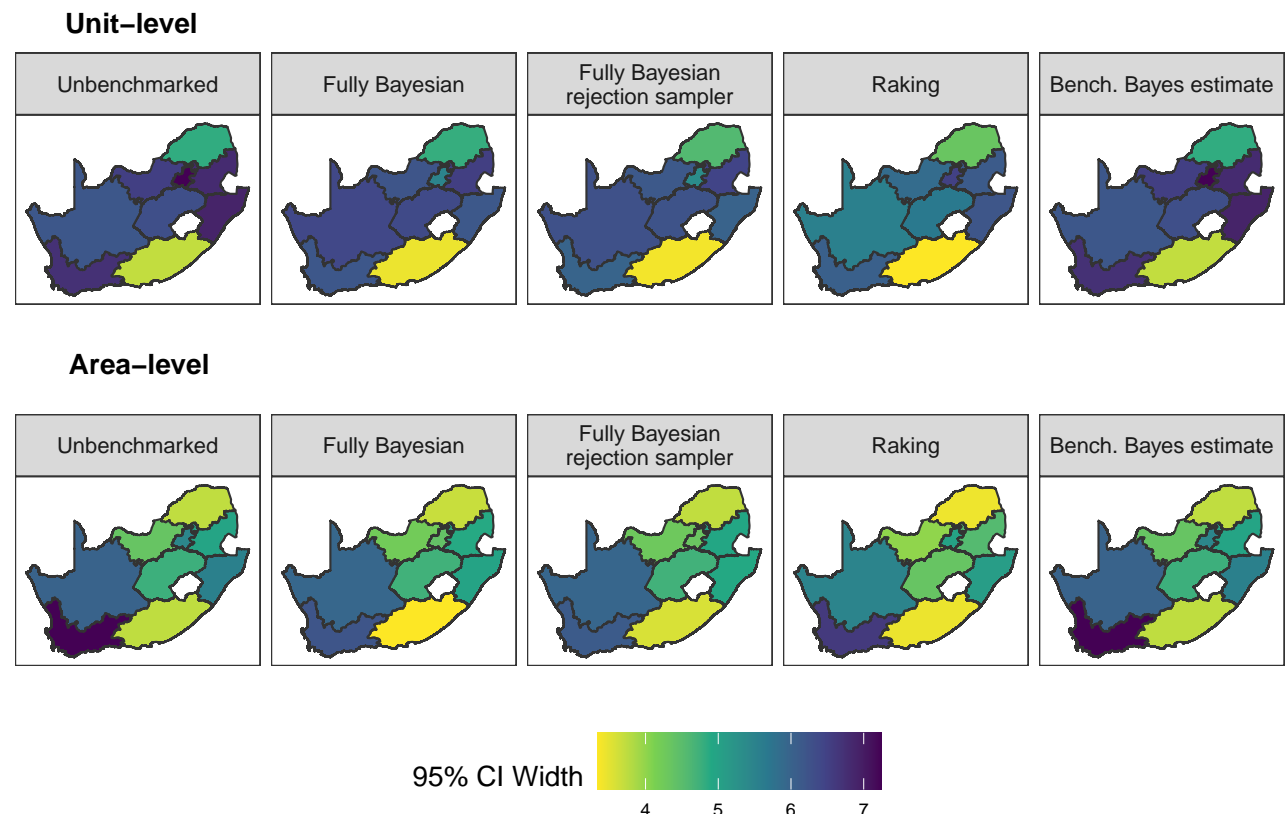


Figure 18: Unbenchmarked and benchmarked posterior 95% CI widths by model and data type at a subnational level.

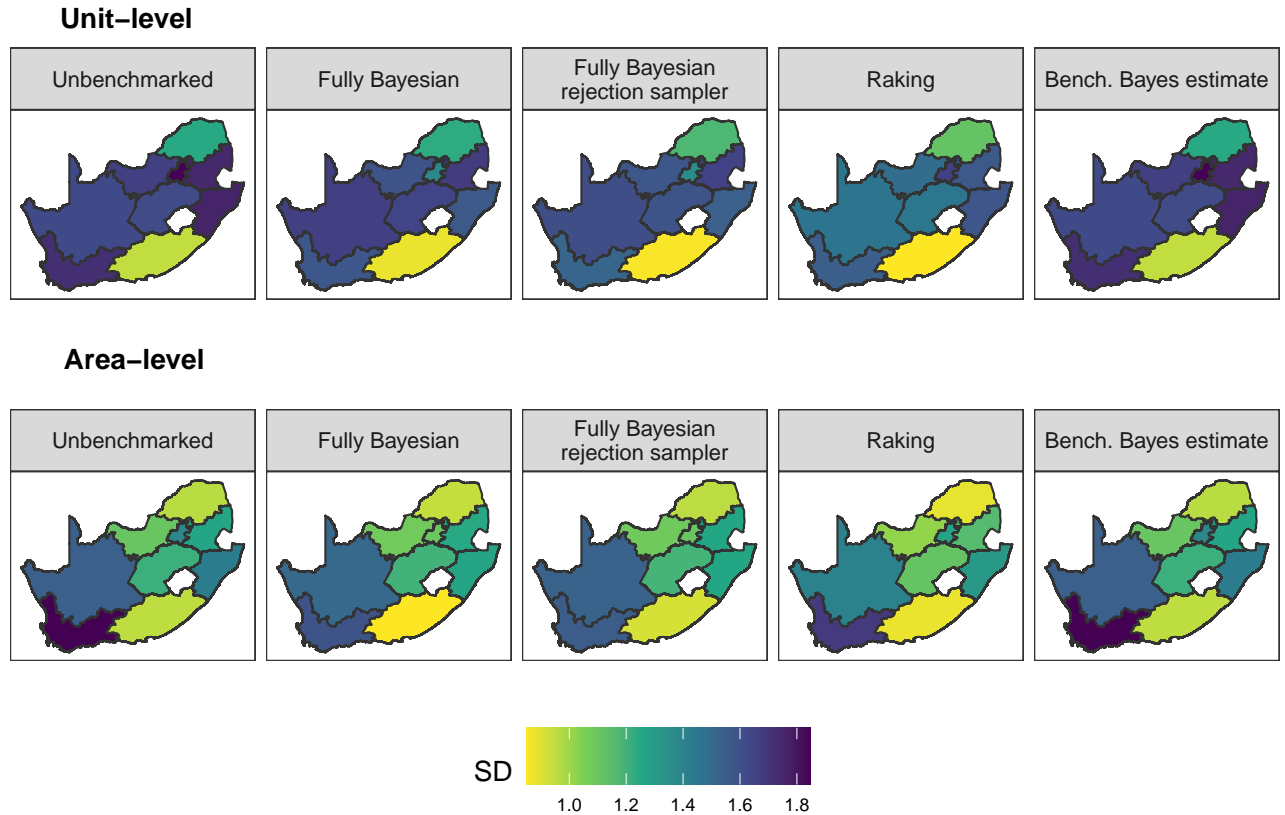


Figure 19: Unbenchmarked and benchmarked posterior standard deviations by model and data type at a subnational level.

2 U5MR Application

Below we describe the data, models, and software used in the U5MR application.

2.1 Data

Spatial boundary files for Namibia are obtained from GADM, the Database of Global Administrative Areas (Database of Global Administrative Areas (GADM) 2019). We use the 2013 administrative boundary (the most recent DHS survey year) for all years in our U5MR model for Namibia, and note that this implies 13 Administrative 1 (admin1) regions. Of note, the Kavango region split in 2013 to form Kavango East and Kavango West. We obtain estimates for the Kavango region as a whole, as this is consistent with the 2013 GADM file, the most recent DHS survey we have available for Namibia, and current subnational UN IGME estimates for Namibia.

For our U5MR application, we use data from the 2000, 2006-2007, and 2013 DHS surveys for Namibia. These

three surveys were chosen for their GPS data availability, and to align with the analysis carried out to produce official subnational U5MR estimates by UN IGME (Inter-agency Group for Child Mortality Estimation 2020), and therefore allow for comparison between the benchmarking methods used in that paper and those proposed here. The surveys followed a multi-stage, stratified design and were designed to provide estimates at the admin1 level, which consists of 13 regions. Again for consistency with official UN IGME estimates, we make predictions for years 2014-2019.

We obtain national level benchmarks for 2000-2019 in Namibia from the UN IGME national estimates from the B3 model (Alkema and New 2014). The national level U5MR estimates and their 95% confidence intervals can be found in Table 6. The likelihood for our benchmarks for the fully Bayesian benchmarking approach requires standard errors for the benchmarks, which we approximate via the assumption that the benchmark is asymptotically normally distributed. These standard errors are presented in Table 6. The data sources used to produce the B3 estimates include surveys/censuses with full birth histories, summary birth histories, and household deaths. A full table of the data sources used is presented in Table 5. Of note, the three full birth history DHS surveys we use for our model (2000, 2006-2007, 2013) are included in the B3 model. As many additional data sources went into the UN IGME estimates, we consider this setting to be external benchmarking and therefore treat our estimates as independent of the national level benchmarks despite this inclusion. Implications of the potential internal benchmarking scenario are outside the scope of this paper.

Table 5: Data sources included in the B3 model for Namibia. MM = maternal mortality.

Survey/Census	Year	Collection Method
Census	1991	Summary Birth History
DHS (MM adjusted)	1992	Full Birth History
DHS	1992	Summary Birth History
DHS	1992	Full Birth History
DHS (MM adjusted)	2000	Full Birth History
DHS	2000	Summary Birth History
DHS	2000	Full Birth History
Census	2001	Household Deaths
DHS (MM adjusted)	2006-2007	Full Birth History
DHS	2006-2007	Summary Birth History
DHS	2006-2007	Full Birth History
DHS	2006-2007	Household Deaths
Census	2011	Summary Birth History
Census	2011	Household Deaths
DHS (MM adjusted)	2013	Full Birth History
DHS	2013	Full Birth History
Inter-censal Demographic Survey	2016	Summary Birth History
Inter-censal Demographic Survey	2016	Household Deaths

Table 6: National benchmarks for U5MR from the UN IGME B3 model for Namibia. Standard errors are computed using the upper bound of the 95% confidence interval via the assumption that the benchmark is normally distributed. U5MR is reported as deaths per 1000 live births.

Year	U5MR	CI (95%)	SE (%)*
2000	75.4	(67.9, 84.4)	4.6
2001	74.9	(67.5, 83.8)	4.5
2002	74.3	(67.0, 83.2)	4.5
2003	74.0	(66.5, 82.8)	4.4
2004	73.7	(66.1, 82.3)	4.4
2005	70.2	(62.8, 78.6)	4.3
2006	65.6	(58.4, 73.8)	4.2
2007	60.7	(53.3, 69.4)	4.4
2008	55.8	(47.9, 65.0)	4.7
2009	51.8	(43.5, 62.3)	5.3
2010	49.7	(40.4, 62.0)	6.3
2011	50.4	(39.4, 66.0)	8.0
2012	52.2	(39.3, 71.4)	9.8
2013	50.1	(36.3, 71.8)	11.1
2014	48.1	(33.7, 72.3)	12.3
2015	47.8	(32.3, 74.7)	13.7
2016	46.3	(30.0, 75.6)	14.9
2017	44.5	(28.0, 75.1)	15.6
2018	43.3	(26.2, 76.0)	16.7
2019	42.4	(24.8, 77.0)	17.7

We use population count data from WorldPop for our U5MR application (Tatem 2017; Stevens et al. 2015). Population counts are available at a 100 meter resolution, and using spatial boundary files from GADM, we aggregate population counts to the admin1 level. The population count data from WorldPop prior to 2020 is not provided with any measure of uncertainty, and so we treat the estimated population proportions as fixed. The spatial distribution of the under five population from 2000-2019 in Namibia can be seen in Figure 20. In Figure 21, the same data is displayed as a stacked bar chart over time.

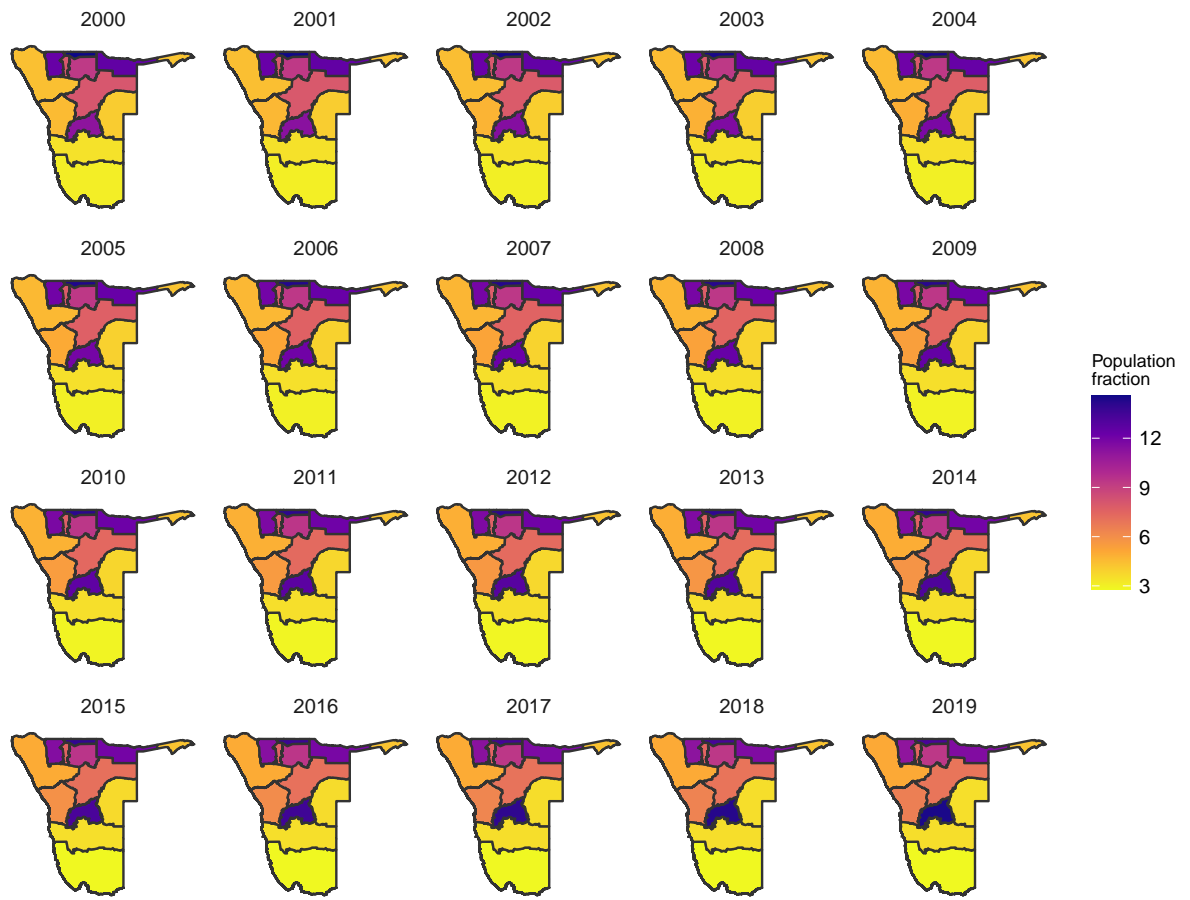


Figure 20: Percentage of the under-5 population living in each region by year.

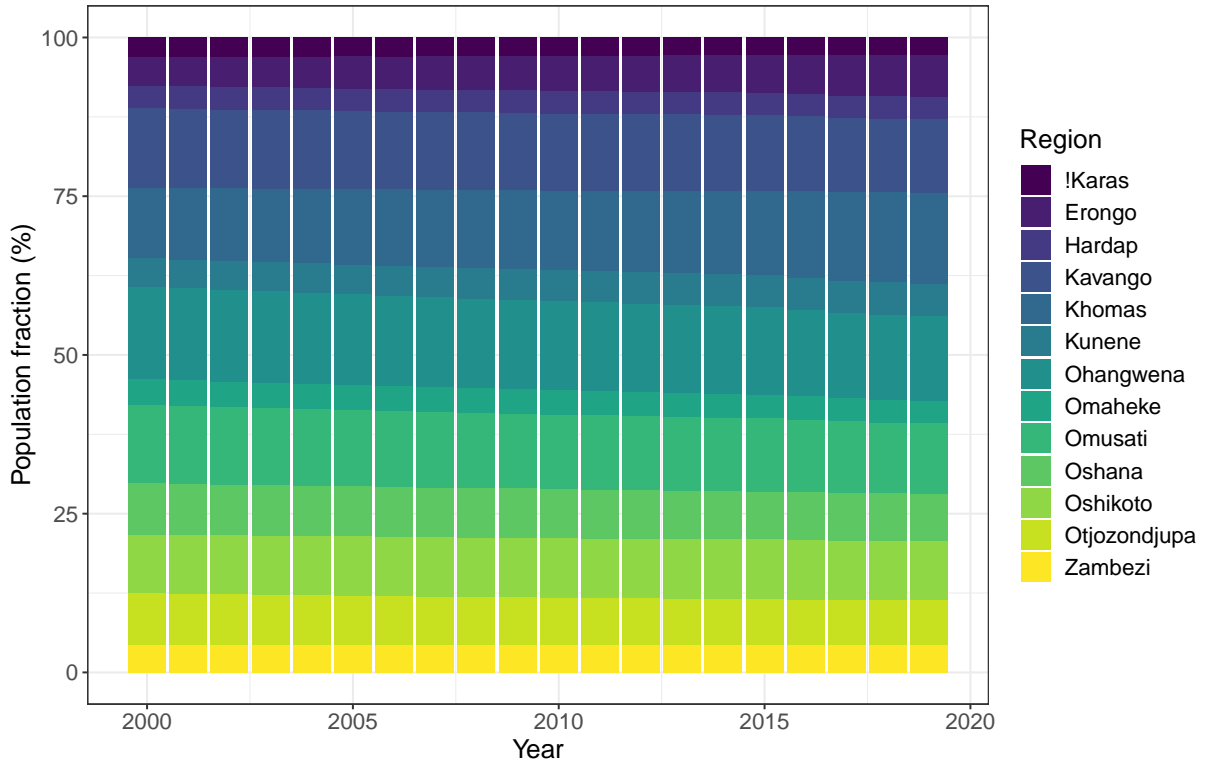


Figure 21: Percentage of the under-5 population living in each region by year.

2.2 Unbenchmarked models

2.2.1 Area-level: Spatial Fay-Herriot

We obtain design-based, direct estimates ${}_{60}\hat{q}_{0it}^{HT}$ of U5MR and their variances for each area i and time t , and smooth the direct estimates via a spatio-temporal extension to the classic Fay-Herriot model described in Z. Li et al. 2019 (Fay and Herriot 1979; Mercer et al. 2015). Direct estimates are combined across surveys using a standard meta-analysis approach and an HIV bias correction is done, both of which are described in Z. Li et al. 2019 in detail.

2.2.2 Unit-level: Binomial

From each DHS survey, we have records of birth and death dates for each child born to a mother sampled in the survey. These records are expanded into monthly binary outcomes that indicate whether death occurs for a given child in a given month, allowing us to perform a discrete time survival analysis with discrete hazards by age groups. In this way, children who survive longer contribute more observations to our data. The binary outcomes

are collapsed to binomial observations in clusters c within area i in year t from survey s for age groups defined as 0-1, 1-11, 12-23, 24-35, 36-47, and 48-59 months. Let $m = 0, 1, \dots, 59$ denote age in months, and let

$$a[m] = \begin{cases} 1, 0 \leq m < 1 \\ 2, 1 \leq m < 12 \\ 3, 12 \leq m < 24 \\ 4, 24 \leq m < 36 \\ 5, 36 \leq m < 48 \\ 6, 48 \leq m < 60 \end{cases} \quad a^*[m] = \begin{cases} 1, 0 \leq m < 1 \\ 2, 1 \leq m < 12 \\ 3, 12 \leq m < 60 \end{cases}$$

We have number of deaths observed $y_{1m,i[c]ts}$ in $n_{m,i[c]ts}$ months of life in cluster c within area i , year t in agemonth m from survey s . We consider the unbenchmark model

$$\begin{aligned} y_{1m,i[c]ts} \mid n_{m,i[c]ts}, {}_1q_{m,i[c]ts} &\sim \text{Binomial}(n_{m,i[c]ts}, {}_1q_{m,i[c]ts}) \\ \eta_{m,i[c]ts} = \text{logit}({}_1q_{m,i[c]ts}) &= \mu_{a[m]} + \alpha_t + \gamma_{a^*[m]t} + b_i \\ &\quad + \beta_i \times t + \delta_{it} + \nu_s + e_{i[c]} + \log(\text{HIV}_{ts}), \end{aligned} \tag{1}$$

and aggregate to a space/time/age level via

$${}_1q_{m,it} = \text{expit} \left(\frac{\mu_{a[m]} + \alpha_t + \gamma_{a^*[m]t} + b_i + \beta_i \times t + \delta_{it}}{\sqrt{1 + h^2 \sigma_e^2}} \right),$$

where ${}_1q_{m,it}$ is the monthly hazard of death for age m . The linear predictor contains fixed intercepts for age bands $\mu_{a[m]}$, an iid temporal random effect $\alpha_t \sim N(0, \tau_\alpha)$, and age group-specific temporal random effects following a random walk 2 (RW2) $\gamma_{a^*[m]t}$ (Lindgren and Rue 2008). The term b_i is a spatial random effect following a BYM2 prior (Riebler et al. 2016; Besag et al. 1991). A sum-to-zero constraint is placed on the structured component of the BYM2 random effect to ensure identifiability. Two separate terms allow for space-time interactions: β_i are random, area-specific slopes, and δ_{it} is a Type IV Knorr-Held interaction term (Knorr-Held 2000). Finally we have a survey fixed effect ν_s which we constrain to sum to zero, and a log offset for HIV, varying by survey and time. These log offsets account for the differing survival probabilities of children born to HIV-positive mothers (Walker et al. 2012). The inclusion of a log offset term in our linear predictor corresponds approximately to a multiplicative

bias correction for mothers who could not be sampled due to death from HIV (Wakefield et al. 2019).

We obtain predictions of U5MR at each time point ${}_{60}q_{0t}$ by calculating posterior draws $k = 1, \dots, K$ of all terms from Equation 1 and the formula

$${}_{60}q_{0it}^{(k)} = 1 - \prod_{m=1}^{59} \left(1 - \text{expit} \left(\frac{\mu_{a[m]}^{(k)} + \alpha_t^{(k)} + \gamma_{a^*[m]t}^{(k)} + b_i^{(k)} + \beta_i^{(k)} \times t + \delta_{it}^{(k)}}{\sqrt{1 + h^2 \sigma_e^{2(k)}}} \right) \right).$$

Note that we do not include the survey fixed effect, cluster random effect, or log offset in our predictions.

For the variance parameters in all random effects, we use PC priors with parameters $U = 1$, $\alpha = 0.01$. For the age-specific intercepts, we use the default INLA prior, which is normal, centered at 0 with precision 0.001. For the ϕ parameter in the BYM2 spatial random effect, we use a PC prior with parameters $U = 0.5$, $\alpha = 2/3$. These prior and hyperprior choices are used in all benchmarked models below, when applicable.

2.3 Benchmarked models

2.3.1 Approaches

Benchmarked Bayes Estimate:

We obtain $k = 1, \dots, K$ posterior draws ${}_{60}\hat{q}_{0it}^{(k)}$ from the unbenchmarked model for each area i , and apply Equation (1) in the main body of the paper to obtain exact, benchmarked posterior draws, ${}_{60}\hat{q}_{0it}^{BB(k)}$.

Raking:

For the unit-level model, we obtain posterior medians ${}_{60}\hat{q}_{0it}^M$ from the unbenchmarked model for each area i and time point t , and compute

$$\text{BENCH}_t^{R1} = \frac{\sum_{i=1}^m w_{it} \times {}_{60}\hat{q}_{0it}^M}{y_{2t}}$$

using weights w_{it} and national benchmarks are each time point y_{2t} . We then refit the unbenchmarked model including BENCH_t^{R1} as a log offset term in the linear predictor to obtain benchmarked posterior draws ${}_{60}\hat{q}_{0it}^{R1(k)}$.

For the area-level model, we adjust the unbenchmarked direct estimates with the ratio BENCH_t^{R1} in the same manner we adjust for HIV, as described in Z. Li et al. 2019, and then proceed fitting the smoothed direct model with these HIV- and benchmark-adjusted direct estimates.

Fully Bayesian: Rejection sampler:

We obtain $k = 1, \dots, K$ posterior draws ${}_{60}\hat{q}_{0it}^{(k)}$ from the unbenchmarked model for each area i and year t , and apply the algorithm described in the proposed approach section of the main body of the paper to obtain benchmarked posterior draws ${}_{60}\hat{q}_{0it}^{FB2}$.

2.4 Software

We implement the unbenchmarked and raking benchmarked U5MR models in INLA via the R package **SUMMER** (Rue et al. 2009; Z. R. Li et al. 2020), and the proposed benchmarking approach and Bayes estimate approach using a combination of INLA and R. INLA is a popular tool for conducting Bayesian, space-time analyses, and provides great computational gains compared to traditional MCMC methods. While nonlinear predictors can be incorporated via the R package **inlabru**, INLA itself cannot make use of nonlinear predictors by design (Bachl et al. 2019). As such, the fully Bayesian benchmarking approach described in Zhang and Bryant 2020 cannot be fit in INLA. Since the unbenchmarked U5MR model is straightforward to fit in INLA using the **SUMMER** package, this application serves as an example of how the proposed rejection sampling approach to fully Bayesian benchmarking may be particularly useful for modelers who have already produced unbenchmarked estimates in an a programme that doesn't allow them to incorporate additional likelihood(s) for the benchmarks.

2.5 U5MR Results

The proposed rejection sampling approach to fully Bayesian benchmarking performs similarly in the U5MR example to the HIV prevalence example in that the posterior density of the aggregated national level estimate is a compromise between the national IGME density and the unbenchmarked density for both the unit-level and area-level models. Figure 23 displays the ratio of unbenchmarked medians from the unit-level and area-level models to IGME national medians across time, with estimates and their confidence intervals shown in 22. During “prediction” years where there is no data informing estimates (2014 onward), the ratio for the unit-level model is particularly large, and we expect to see the greatest effect in benchmarking during these years. The ratio is particularly large likely due to the flexibility of the RW2 in time in this model, and the ratio is less large in prediction years for the area-level model. The ratio for the area-level model overall is greater for almost all years than the ratio for the unit-level model.

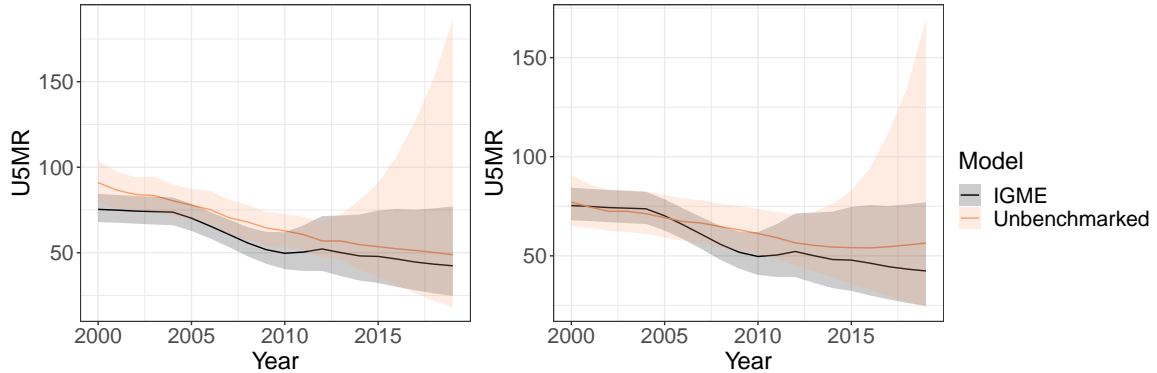


Figure 22: Aggregated national unbenchmarkmed medians from the area-level model (left) and unit-level model (right) compared to IGME national medians across time.

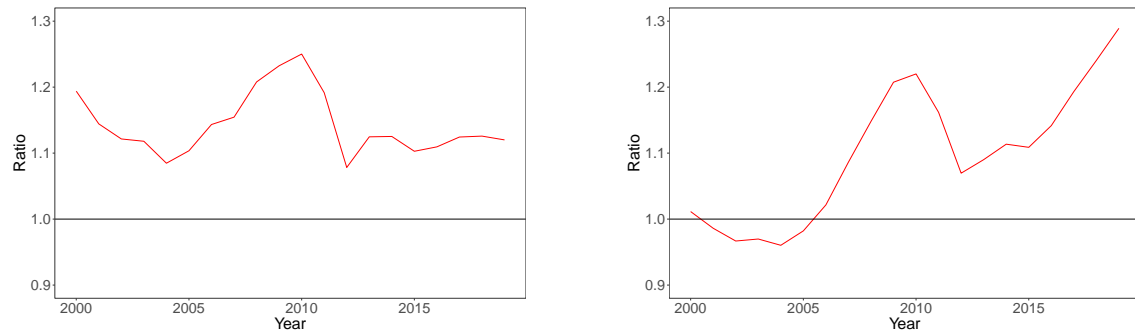


Figure 23: Ratio of aggregated national unbenchmarkmed medians from the area-level model (left) and unit-level model (right) to IGME national medians across time. A value greater than 1 corresponds to the unbenchmarkmed estimate being higher than the IGME estimate.

Figures 24 through 43 display the aggregated national level estimates produced from each benchmarked and unbenchmarkmed method for both unit- and area-level models. The posterior densities from the fully Bayesian rejection sampling approach are less uncertain than the posterior densities from the unbenchmarkmed model due to the additional information contained in the benchmarking constraint being incorporated in the benchmarked approach. The overlap between the IGME density and the Bayes estimate approach is expected as the Bayes estimate approach performs exact benchmarking. A table of these national estimates for all years and models can be found in Table 7.

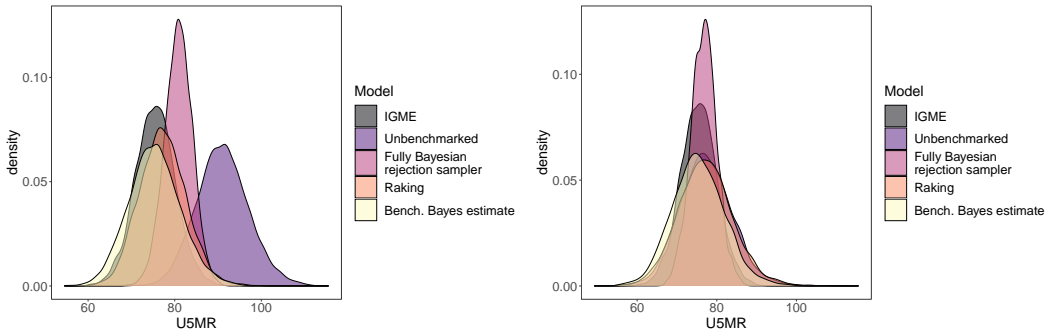


Figure 24: Aggregated national level U5MR estimates from IGME, unbenchmarked, and benchmarked models for area-level (left) and unit-level (right) models, for 2000. All densities are based on 5000 samples. U5MR is reported as deaths per 1000 live births.

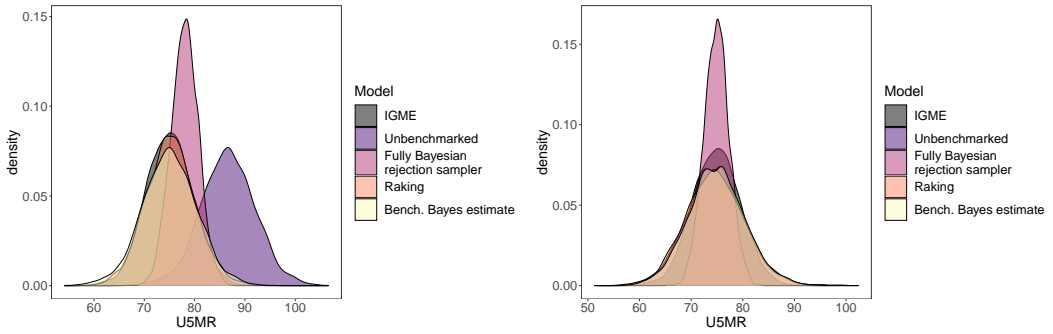


Figure 25: Aggregated national level U5MR estimates from IGME, unbenchmarked, and benchmarked models for area-level (left) and unit-level (right) models, for 2001. All densities are based on 5000 samples. U5MR is reported as deaths per 1000 live births.

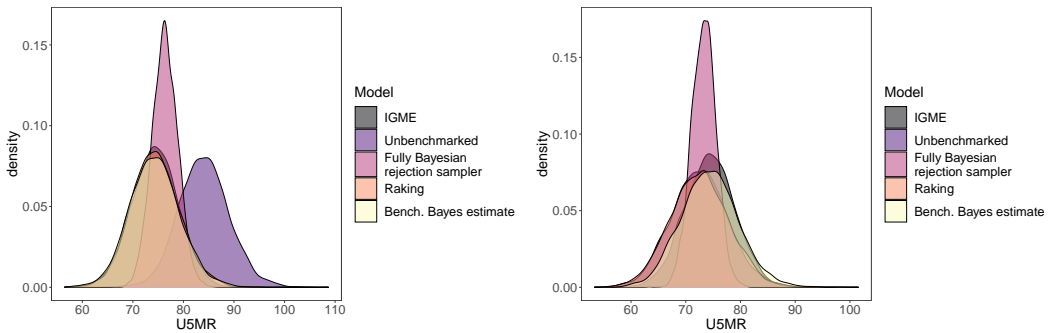


Figure 26: Aggregated national level U5MR estimates from IGME, unbenchmarked, and benchmarked models for area-level (left) and unit-level (right) models, for 2002. All densities are based on 5000 samples. U5MR is reported as deaths per 1000 live births.

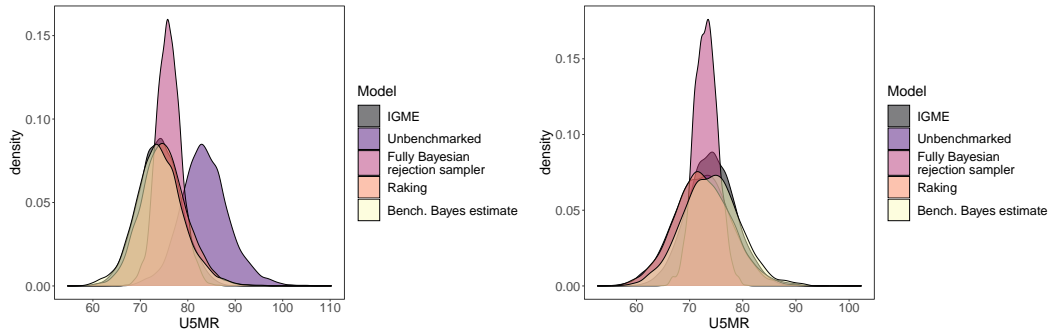


Figure 27: Aggregated national level U5MR estimates from IGME, unbenchmarked, and benchmarked models for area-level (left) and unit-level (right) models, for 2003. All densities are based on 5000 samples. U5MR is reported as deaths per 1000 live births.

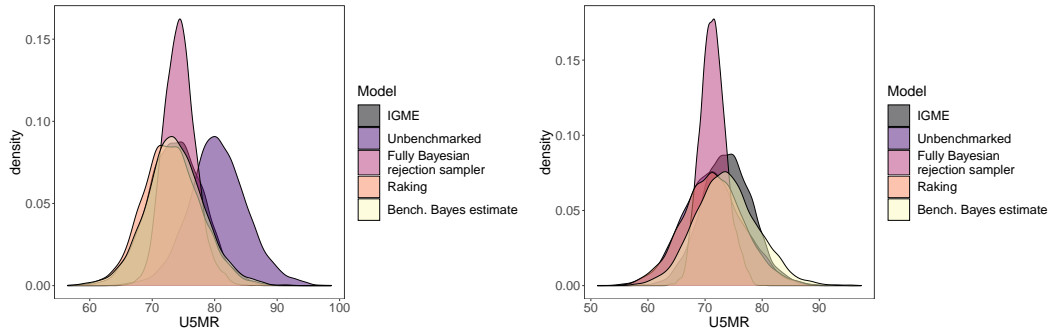


Figure 28: Aggregated national level U5MR estimates from IGME, unbenchmarked, and benchmarked models for area-level (left) and unit-level (right) models, for 2004. All densities are based on 5000 samples. U5MR is reported as deaths per 1000 live births.

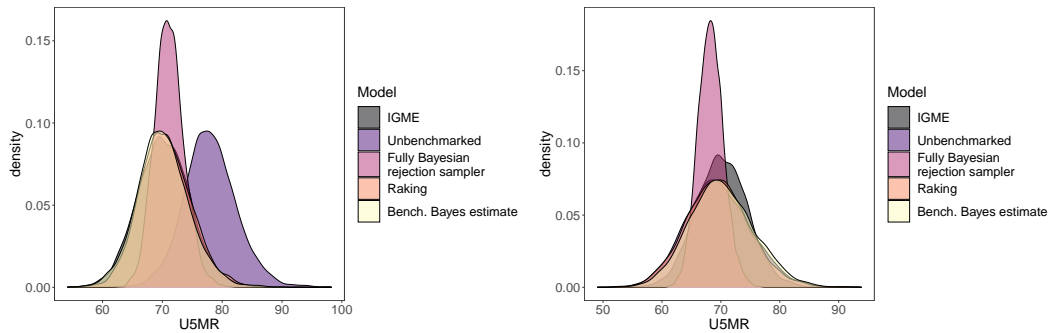


Figure 29: Aggregated national level U5MR estimates from IGME, unbenchmarked, and benchmarked models for area-level (left) and unit-level (right) models, for 2005. All densities are based on 5000 samples. U5MR is reported as deaths per 1000 live births.

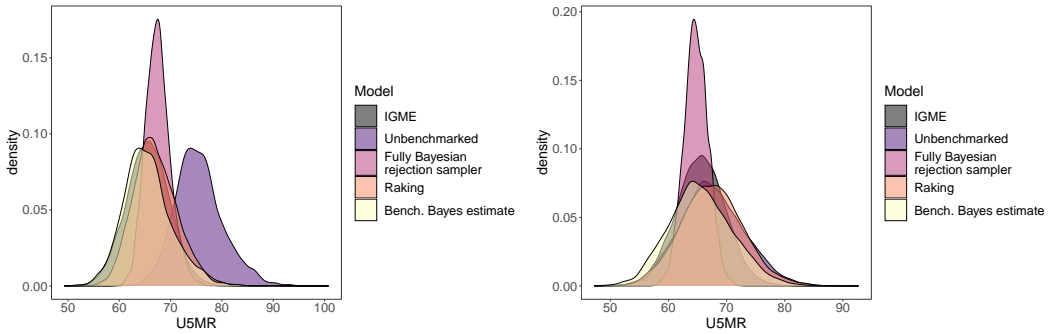


Figure 30: Aggregated national level U5MR estimates from IGME, unbenchmarked, and benchmarked models for area-level (left) and unit-level (right) models, for 2006. All densities are based on 5000 samples. U5MR is reported as deaths per 1000 live births.

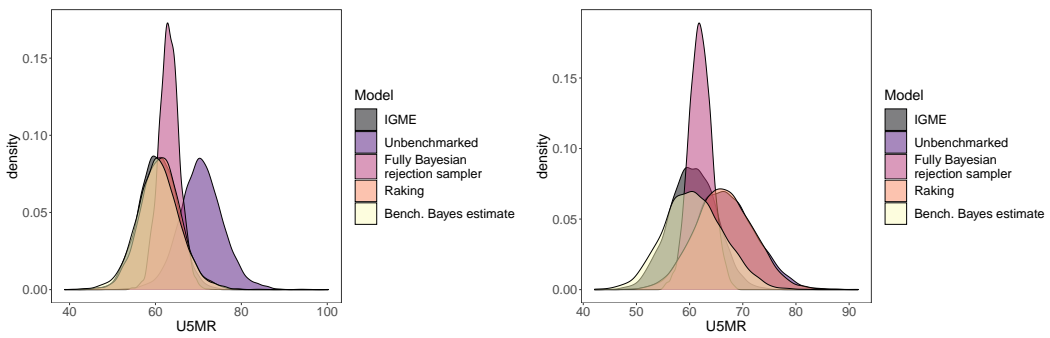


Figure 31: Aggregated national level U5MR estimates from IGME, unbenchmarked, and benchmarked models for area-level (left) and unit-level (right) models, for 2007. All densities are based on 5000 samples. U5MR is reported as deaths per 1000 live births.

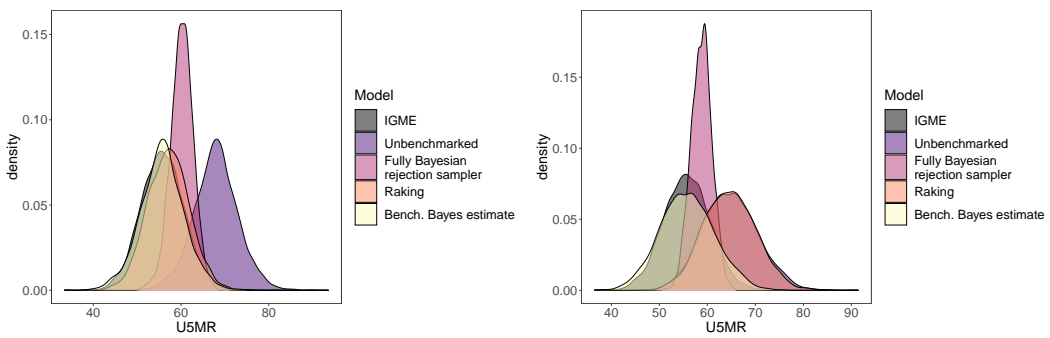


Figure 32: Aggregated national level U5MR estimates from IGME, unbenchmarked, and benchmarked models for area-level (left) and unit-level (right) models, for 2008. All densities are based on 5000 samples. U5MR is reported as deaths per 1000 live births.

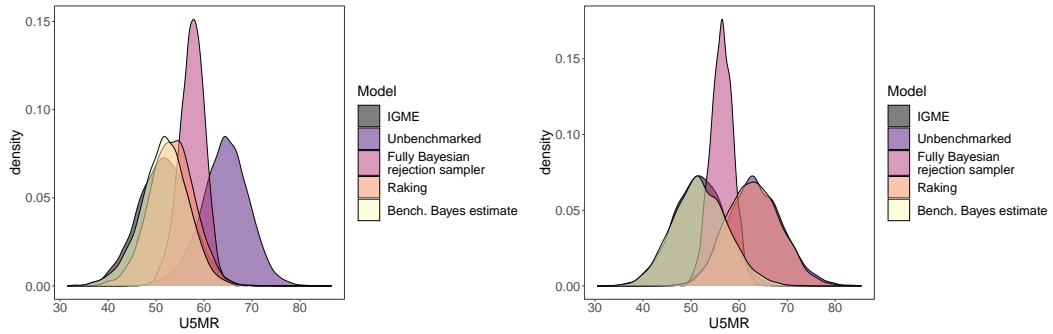


Figure 33: Aggregated national level U5MR estimates from IGME, unbenchmarked, and benchmarked models for area-level (left) and unit-level (right) models, for 2009. All densities are based on 5000 samples. U5MR is reported as deaths per 1000 live births.

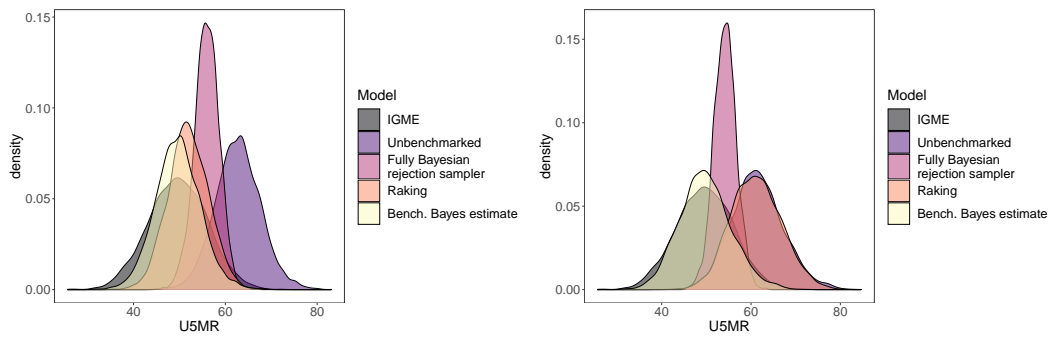


Figure 34: Aggregated national level U5MR estimates from IGME, unbenchmarked, and benchmarked models for area-level (left) and unit-level (right) models, for 2010. All densities are based on 5000 samples. U5MR is reported as deaths per 1000 live births.

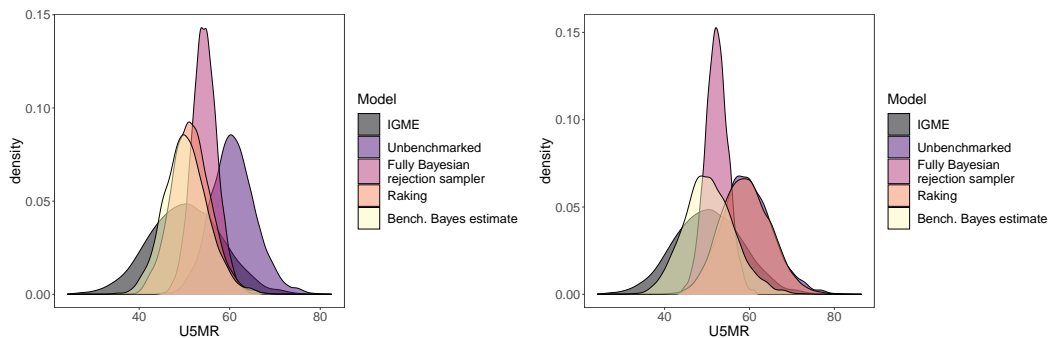


Figure 35: Aggregated national level U5MR estimates from IGME, unbenchmarked, and benchmarked models for area-level (left) and unit-level (right) models, for 2011. All densities are based on 5000 samples. U5MR is reported as deaths per 1000 live births.

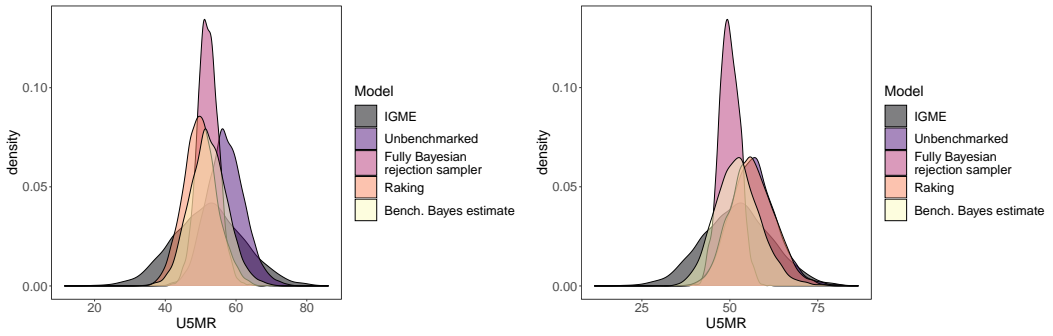


Figure 36: Aggregated national level U5MR estimates from IGME, unbenchmarked, and benchmarked models for area-level (left) and unit-level (right) models, for 2012. All densities are based on 5000 samples. U5MR is reported as deaths per 1000 live births.

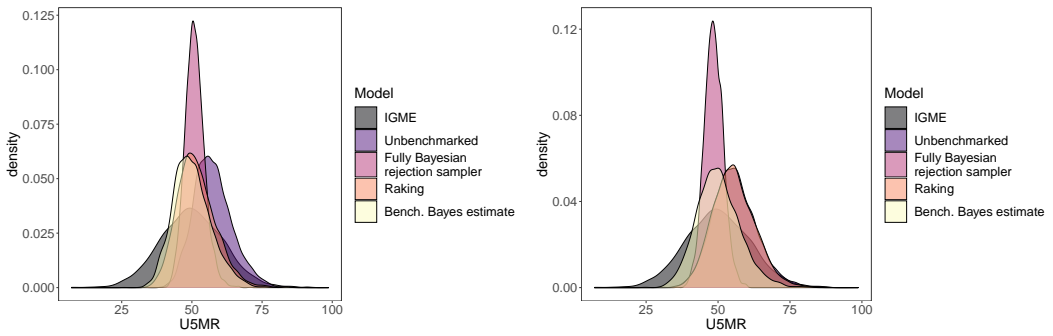


Figure 37: Aggregated national level U5MR estimates from IGME, unbenchmarked, and benchmarked models for area-level (left) and unit-level (right) models, for 2013. All densities are based on 5000 samples. U5MR is reported as deaths per 1000 live births.

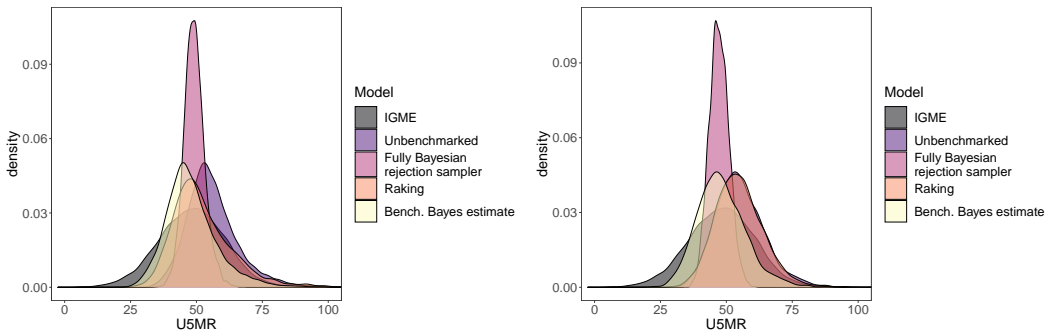


Figure 38: Aggregated national level U5MR estimates from IGME, unbenchmarked, and benchmarked models for area-level (left) and unit-level (right) models, for 2014. All densities are based on 5000 samples. U5MR is reported as deaths per 1000 live births.

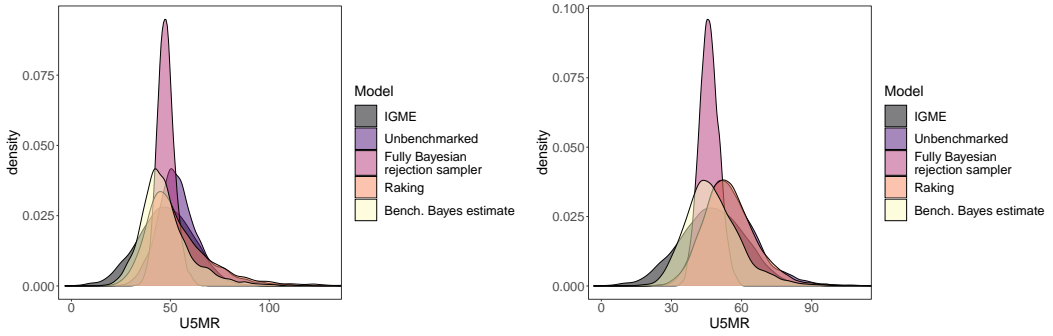


Figure 39: Aggregated national level U5MR estimates from IGME, unbenchmarked, and benchmarked models for area-level (left) and unit-level (right) models, for 2015. All densities are based on 5000 samples. U5MR is reported as deaths per 1000 live births.

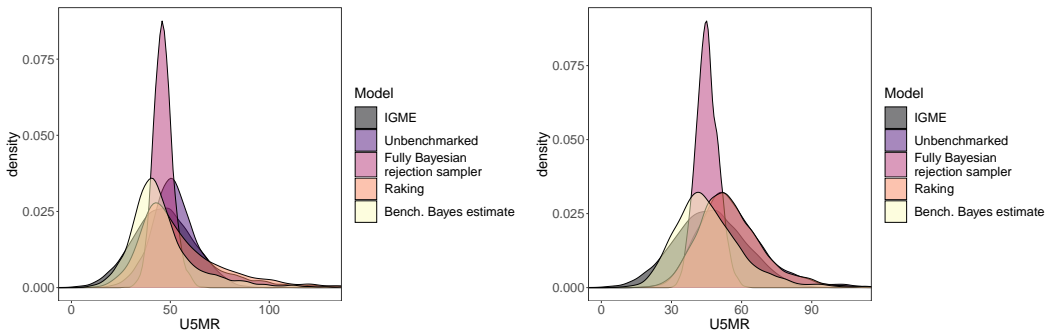


Figure 40: Aggregated national level U5MR estimates from IGME, unbenchmarked, and benchmarked models for area-level (left) and unit-level (right) models, for 2016. All densities are based on 5000 samples. U5MR is reported as deaths per 1000 live births.

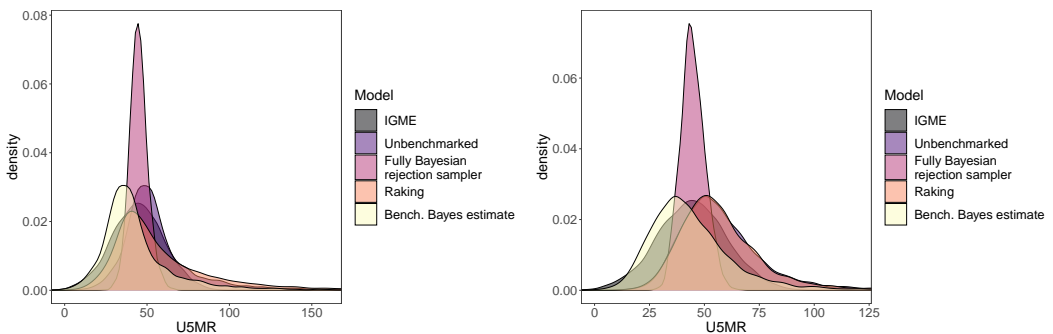


Figure 41: Aggregated national level U5MR estimates from IGME, unbenchmarked, and benchmarked models for area-level (left) and unit-level (right) models, for 2017. All densities are based on 5000 samples. U5MR is reported as deaths per 1000 live births.

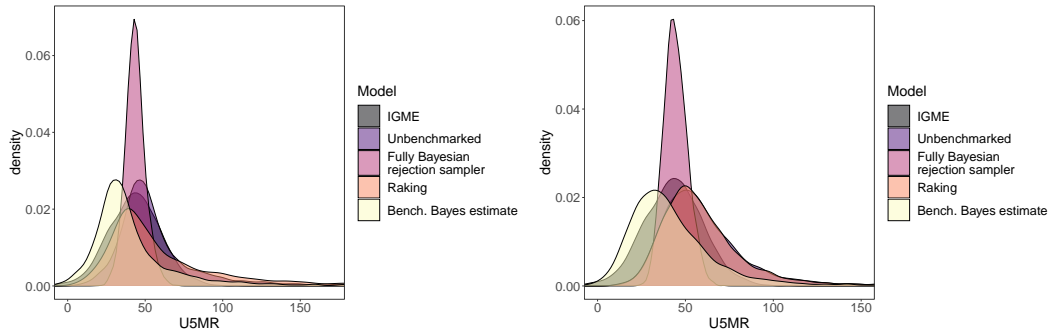


Figure 42: Aggregated national level U5MR estimates from IGME, unbenchmarked, and benchmarked models for area-level (left) and unit-level (right) models, for 2018. All densities are based on 5000 samples. U5MR is reported as deaths per 1000 live births.

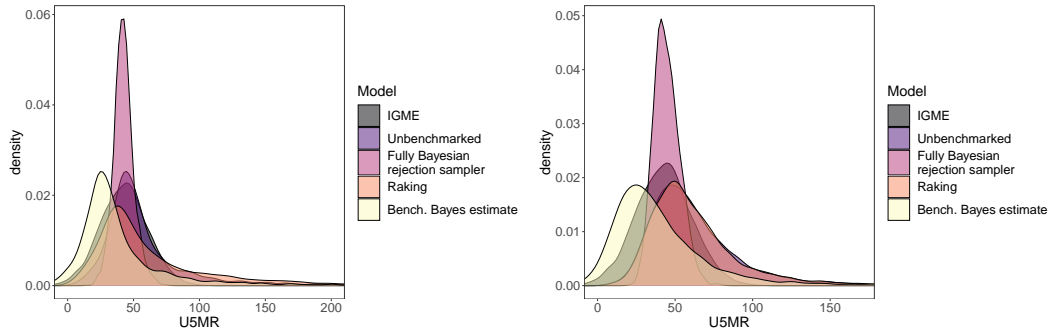


Figure 43: Aggregated national level U5MR estimates from IGME, unbenchmarked, and benchmarked models for area-level (left) and unit-level (right) models, for 2019. All densities are based on 5000 samples. U5MR is reported as deaths per 1000 live births.

The proportion of samples accepted in the fully Bayesian rejection sampler approach was 0.41% for the unit-level model, and 0.0001% for the area-level model.

Table 7: Aggregated national level U5MR estimates from IGME, unbenchmarked, and benchmarked models for 2010. 95% credible intervals are given next to posterior medians. U5MR is reported as deaths per 1000 live births. AL = Area-level, UL = Unit-level.

Year	Model	AL: Median	UL: Median	AL: SD	UL: SD
2000	IGME	75.4 (67.9, 84.4)	75.4 (67.9, 84.4)	4.6	4.6
	Unbenchmarked	91 (79.9, 103.6)	77.1 (65, 90.8)	6.0	6.6
	FB: Rejection Sampler	81.4 (74.6, 88.7)	75.7 (68.3, 83.1)	3.6	3.8
	Raking	77.2 (67.2, 87.9)	77.1 (64.2, 91.1)	5.4	6.8
	Bayes Estimate	75.3 (64.2, 87.9)	75.3 (63.2, 89)	6.0	6.6
2001	IGME	74.9 (67.5, 83.8)	74.9 (67.5, 83.8)	4.5	4.5
	Unbenchmarked	86.6 (76, 97.4)	74.6 (64, 86)	5.4	5.5
	FB: Rejection Sampler	79.8 (72.5, 86.5)	74.6 (67.9, 81.3)	3.6	3.5
	Raking	75.2 (65.6, 85.1)	74.6 (64, 86.2)	4.9	5.7
	Bayes Estimate	75 (64.4, 85.8)	74.9 (64.3, 86.3)	5.4	5.5
2002	IGME	74.3 (67, 83.2)	74.3 (67, 83.2)	4.5	4.5
	Unbenchmarked	84 (74.7, 94.2)	72.5 (62.6, 83.3)	5.0	5.3
	FB: Rejection Sampler	79 (72.7, 85.6)	73.1 (66.5, 80.1)	3.3	3.4
	Raking	74.3 (65.5, 84.4)	72.6 (62.3, 83)	4.8	5.3
	Bayes Estimate	74.3 (65, 84.5)	74.3 (64.4, 85.1)	5.0	5.3
2003	IGME	74 (66.5, 82.8)	74 (66.5, 82.8)	4.4	4.4
	Unbenchmarked	83.4 (74, 94.5)	72.5 (62, 83.2)	5.1	5.4
	FB: Rejection Sampler	78.6 (72.6, 84.7)	73.1 (66.6, 79.7)	3.1	3.4
	Raking	74.8 (66, 85.3)	72.4 (62.2, 83.4)	4.9	5.4
	Bayes Estimate	73.9 (64.5, 85)	74 (63.6, 84.8)	5.1	5.4
2004	IGME	73.7 (66.1, 82.3)	73.7 (66.1, 82.3)	4.4	4.4
	Unbenchmarked	80.4 (71.5, 90.1)	71.2 (61.1, 82.4)	4.6	5.5
	FB: Rejection Sampler	77.2 (71.4, 83.2)	72.5 (65.9, 79.2)	3.0	3.4
	Raking	73 (64.5, 82.5)	71.4 (61.1, 82.5)	4.6	5.4
	Bayes Estimate	73.5 (64.6, 83.2)	73.5 (63.4, 84.7)	4.6	5.5
2005	IGME	70.2 (62.8, 78.6)	70.2 (62.8, 78.6)	4.3	4.3
	Unbenchmarked	77.8 (69.8, 87.3)	69.3 (59.2, 80.7)	4.4	5.5
	FB: Rejection Sampler	74.1 (68.4, 80)	69.5 (63.2, 76.1)	3.0	3.3
	Raking	70.4 (62.7, 79.6)	69.4 (59.2, 80.4)	4.3	5.4
	Bayes Estimate	70 (61.9, 79.4)	69.9 (59.9, 81.4)	4.4	5.5
2006	IGME	65.6 (58.4, 73.8)	65.6 (58.4, 73.8)	4.2	4.2
	Unbenchmarked	75.2 (67.3, 86.2)	67.3 (57.5, 78.9)	4.7	5.5
	FB: Rejection Sampler	70.4 (64.9, 76.4)	66 (59.8, 72.4)	2.8	3.2
	Raking	66.7 (59.4, 76.4)	67.5 (57.2, 78.6)	4.3	5.4
	Bayes Estimate	65.2 (57.3, 76.1)	65.3 (55.6, 77)	4.7	5.5
2007	IGME	60.7 (53.3, 69.4)	60.7 (53.3, 69.4)	4.4	4.4
	Unbenchmarked	70.6 (60.8, 81.2)	66.5 (56.3, 78.1)	5.1	5.6
	FB: Rejection Sampler	65.5 (58.9, 71.7)	62.7 (56, 69.5)	3.3	3.4
	Raking	61.2 (52.1, 71)	66.4 (56.1, 77.5)	4.7	5.5
	Bayes Estimate	60.6 (50.7, 71.1)	60.6 (50.4, 72.2)	5.1	5.6
2008	IGME	55.8 (47.9, 65)	55.8 (47.9, 65)	4.7	4.7
	Unbenchmarked	68 (57.6, 78.2)	64.7 (54, 76.2)	5.0	5.7
	FB: Rejection Sampler	62.2 (54.3, 68.8)	59.5 (52.6, 66.7)	3.7	3.5
	Raking	57.1 (48, 66.5)	64.6 (54, 75.5)	4.8	5.5
	Bayes Estimate	55.7 (45.4, 65.9)	55.7 (45.1, 67.3)	5.0	5.7
2009	IGME	51.8 (43.5, 62.3)	51.8 (43.5, 62.3)	5.3	5.3
	Unbenchmarked	64.5 (53.9, 73.8)	63.2 (52.5, 75.1)	5.0	5.7
	FB: Rejection Sampler	58.9 (50, 65.8)	57.4 (50.1, 64.9)	4.1	3.7
	Raking	53.3 (44, 62.3)	63 (52.8, 74.2)	4.7	5.6
	Bayes Estimate	51.9 (41.2, 61.2)	51.7 (41, 63.6)	5.0	5.7

Year	Model	AL: Median	UL: Median	AL: SD	UL: SD
2010	IGME	49.7 (40.4, 62)	49.7 (40.4, 62)	6.3	6.3
	Unbenchmarked	62.8 (53.2, 72.7)	61.2 (50.8, 73.6)	4.9	5.8
	FB: Rejection Sampler	58.5 (50.8, 65.4)	56.1 (48.4, 64.2)	3.7	4.0
	Raking	51.9 (43.5, 60.7)	61 (50.6, 72.7)	4.4	5.6
	Bayes Estimate	49.6 (40.1, 59.6)	49.6 (39.1, 61.9)	4.9	5.8
2011	IGME	50.4 (39.4, 66)	50.4 (39.4, 66)	8.0	8.0
	Unbenchmarked	60.7 (51.7, 71.1)	59.2 (48.4, 72.3)	4.9	6.0
	FB: Rejection Sampler	58.1 (50.8, 65.9)	55.6 (47.2, 65)	3.8	4.5
	Raking	51.4 (43.3, 60.8)	58.9 (48.3, 70.9)	4.4	5.8
	Bayes Estimate	50.2 (41.2, 60.6)	50.3 (39.5, 63.4)	4.9	6.0
2012	IGME	52.2 (39.3, 71.4)	52.2 (39.3, 71.4)	9.8	9.8
	Unbenchmarked	56.9 (47, 68)	56.5 (45, 70.3)	5.3	6.5
	FB: Rejection Sampler	55.7 (47.5, 64.7)	54.8 (45.2, 65.6)	4.4	5.1
	Raking	49.7 (40.7, 60)	56.2 (45, 69.2)	4.8	6.3
	Bayes Estimate	52 (42.2, 63.1)	52.1 (40.5, 65.8)	5.3	6.5
2013	IGME	50.1 (36.3, 71.8)	50.1 (36.3, 71.8)	11.1	11.1
	Unbenchmarked	56.9 (45.8, 72.5)	55.3 (42.3, 72.1)	6.9	7.5
	FB: Rejection Sampler	54.4 (45, 65.2)	53.2 (42.4, 65.7)	5.2	5.9
	Raking	51 (40, 66.7)	55.2 (42.3, 70.9)	6.9	7.3
	Bayes Estimate	49.4 (38.3, 65.1)	49.7 (36.7, 66.5)	6.9	7.5
2014	IGME	48.1 (33.7, 72.3)	48.1 (33.7, 72.3)	12.3	12.3
	Unbenchmarked	54.7 (40.1, 80.6)	54.4 (39.4, 76.4)	10.2	9.4
	FB: Rejection Sampler	52 (40.4, 65.6)	51.7 (39.2, 66.4)	6.4	6.9
	Raking	50.2 (35.3, 80.8)	54.3 (39, 74.7)	11.7	9.2
	Bayes Estimate	46.7 (32.1, 72.6)	47.4 (32.3, 69.4)	10.2	9.4
2015	IGME	47.8 (32.3, 74.7)	47.8 (32.3, 74.7)	13.7	13.7
	Unbenchmarked	53.5 (35.7, 90.8)	54.1 (36.1, 82.9)	14.9	12.2
	FB: Rejection Sampler	50.6 (36.9, 67.2)	51.1 (36.3, 68.2)	7.6	8.0
	Raking	50 (31, 101.7)	53.9 (35.6, 81.1)	18.9	12.1
	Bayes Estimate	45.4 (27.6, 82.7)	46.7 (28.6, 75.4)	14.9	12.2
2016	IGME	46.3 (30, 75.6)	46.3 (30, 75.6)	14.9	14.9
	Unbenchmarked	52.3 (31, 106.8)	54 (32.8, 94.2)	21.5	16.5
	FB: Rejection Sampler	48.8 (33.5, 67.4)	50 (33.9, 69.3)	8.7	9.0
	Raking	49.7 (25.9, 132.1)	53.8 (32.3, 92.1)	30.7	16.7
	Bayes Estimate	42.4 (21.1, 96.8)	44 (22.8, 84.2)	21.5	16.5
2017	IGME	44.5 (28, 75.1)	44.5 (28, 75.1)	15.6	15.6
	Unbenchmarked	51.3 (26.3, 127.4)	54.6 (30.1, 112.2)	30.1	23.0
	FB: Rejection Sampler	46.8 (30, 67.9)	48.9 (31.2, 70.4)	9.7	10.0
	Raking	49.4 (21.6, 169.1)	54.3 (29.4, 109.8)	46.4	23.6
	Bayes Estimate	38.7 (13.6, 114.7)	40.9 (16.4, 98.5)	30.1	23.0
2018	IGME	43.3 (26.2, 76)	43.3 (26.2, 76)	16.7	16.7
	Unbenchmarked	50.1 (21.7, 152.7)	55.5 (26.9, 135.3)	41.2	31.7
	FB: Rejection Sampler	45.1 (26.7, 68.9)	47.4 (27.5, 71.9)	10.8	11.4
	Raking	49.1 (17, 220.1)	55 (26.7, 133.2)	64.8	33.1
	Bayes Estimate	34.7 (6.3, 137.2)	37.5 (8.9, 117.3)	41.2	31.7
2019	IGME	42.4 (24.8, 77)	42.4 (24.8, 77)	17.7	17.7
	Unbenchmarked	48.8 (18.2, 186.6)	56.4 (24.2, 169.5)	53.6	43.0
	FB: Rejection Sampler	43.8 (23.8, 69.8)	46.7 (25, 72.4)	11.8	12.2
	Raking	48.4 (13.5, 284.7)	55.9 (23.8, 164.4)	83.9	45.7
	Bayes Estimate	30.2 (-0.4, 168.1)	33.2 (0.9, 146.2)	53.6	43.0

Comparisons between unit-level and area-level models for each admin1 region across time can be found in Figures 44 through 47.

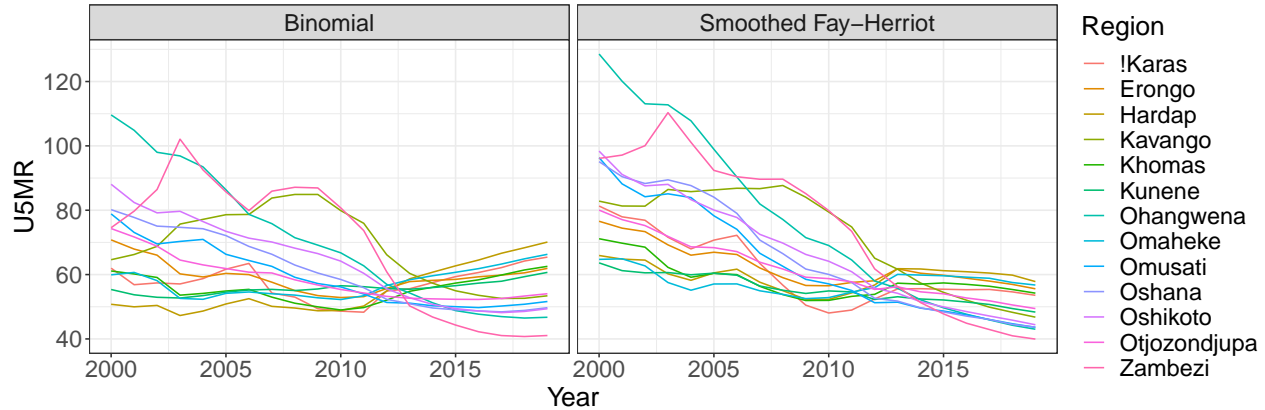


Figure 44: Comparison of median, unbenchmarked U5MR estimates from unit- and area-level models across time. U5MR is reported as deaths per 1000 live births.

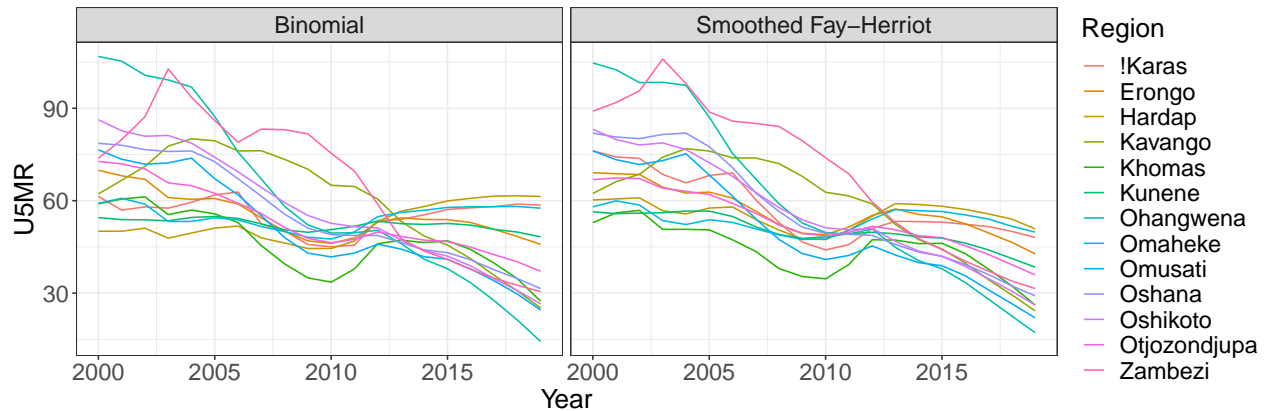


Figure 45: Comparison of median, benchmarked U5MR estimates from unit- and area-level models across time for the benchmarked Bayes estimate approach. U5MR is reported as deaths per 1000 live births.

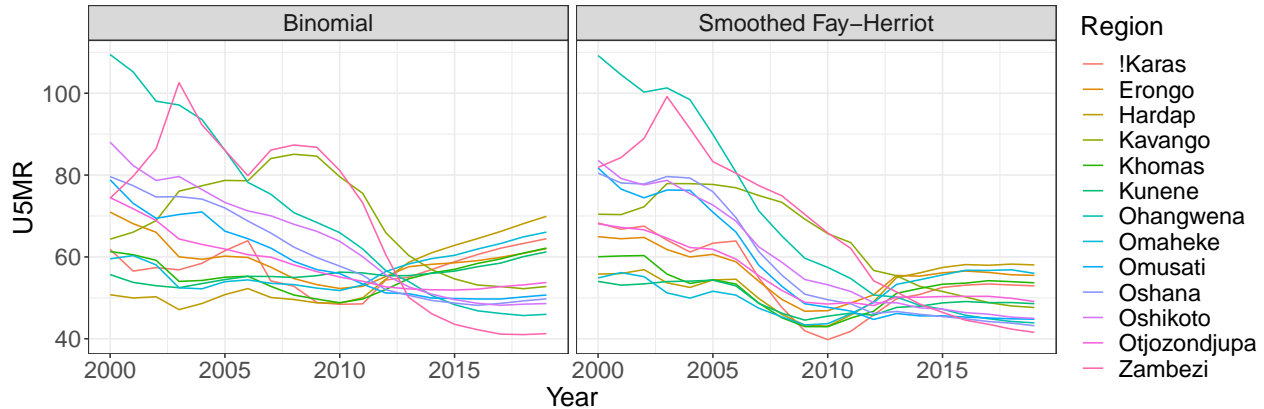


Figure 46: Comparison of median, benchmarked U5MR estimates from unit- and area-level models across time for the raking approach. U5MR is reported as deaths per 1000 live births.

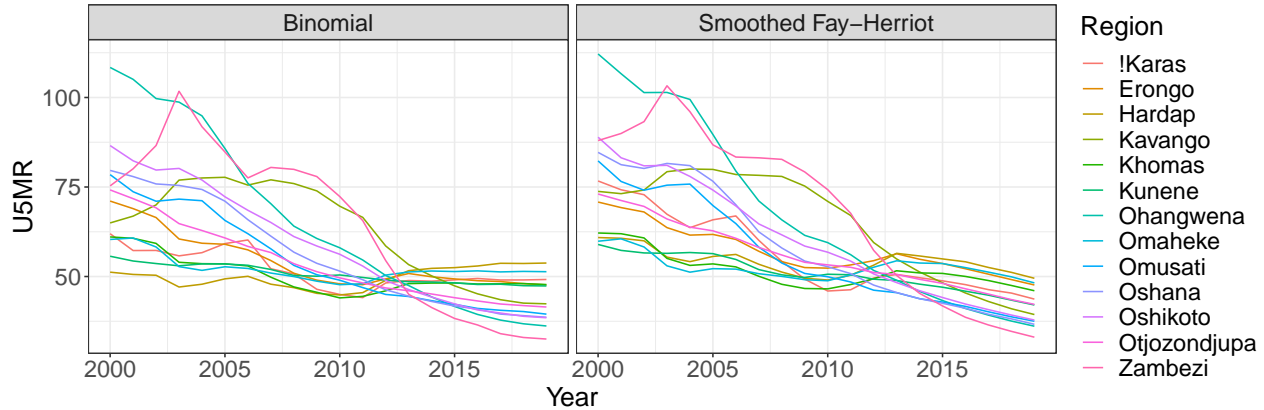


Figure 47: Comparison of median, benchmarked U5MR estimates from unit- and area-level models across time for the rejection sampler approach. U5MR is reported as deaths per 1000 live births.

Subnational maps of unbenchmarked and benchmarked estimates from 2000 to 2019 can be found in Figures 48 through 67.

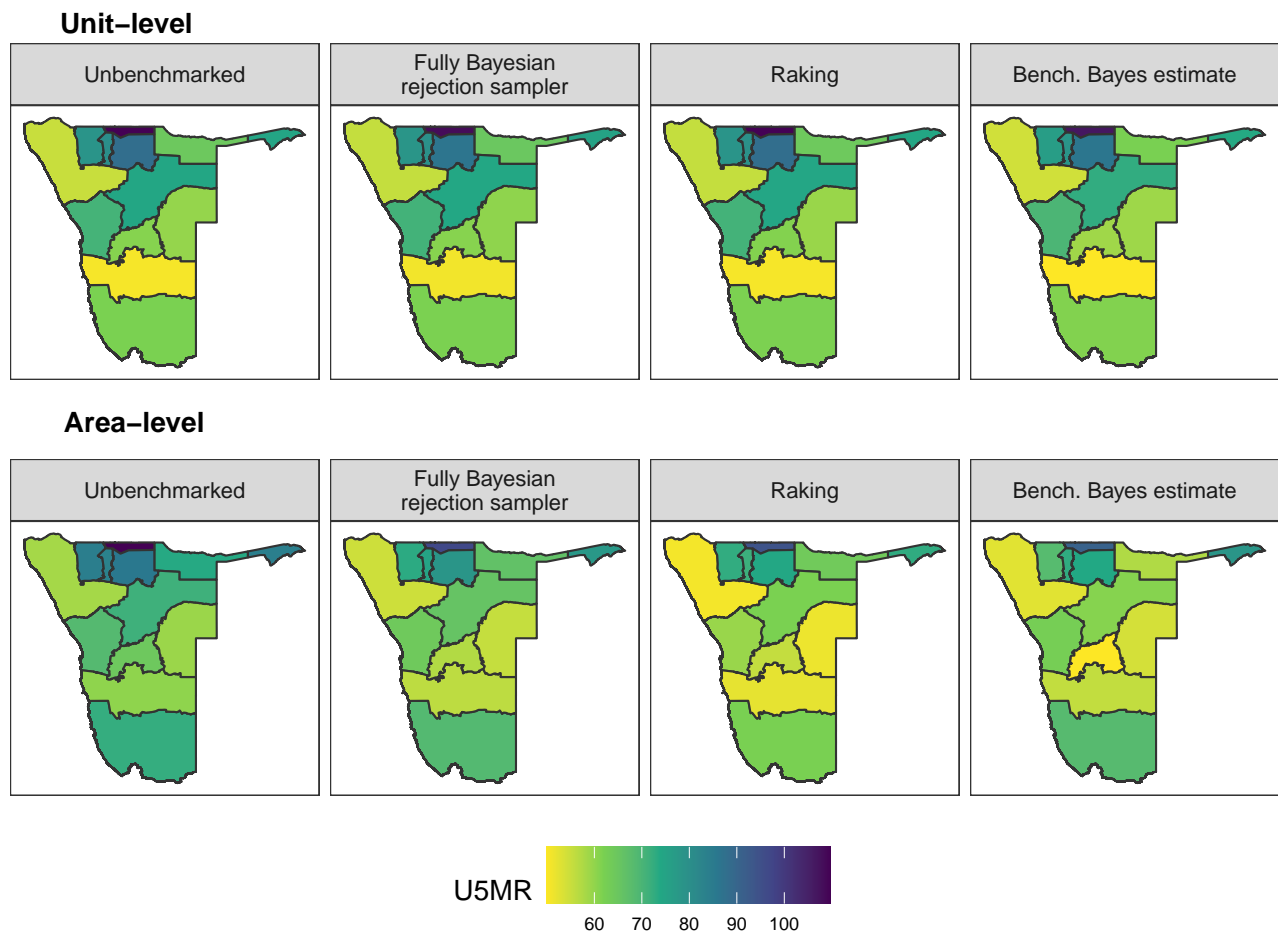


Figure 48: Comparison of median U5MR estimates from benchmarked and unbenchmarked unit- and area-level models for 2000. U5MR is reported as deaths per 1000 live births.

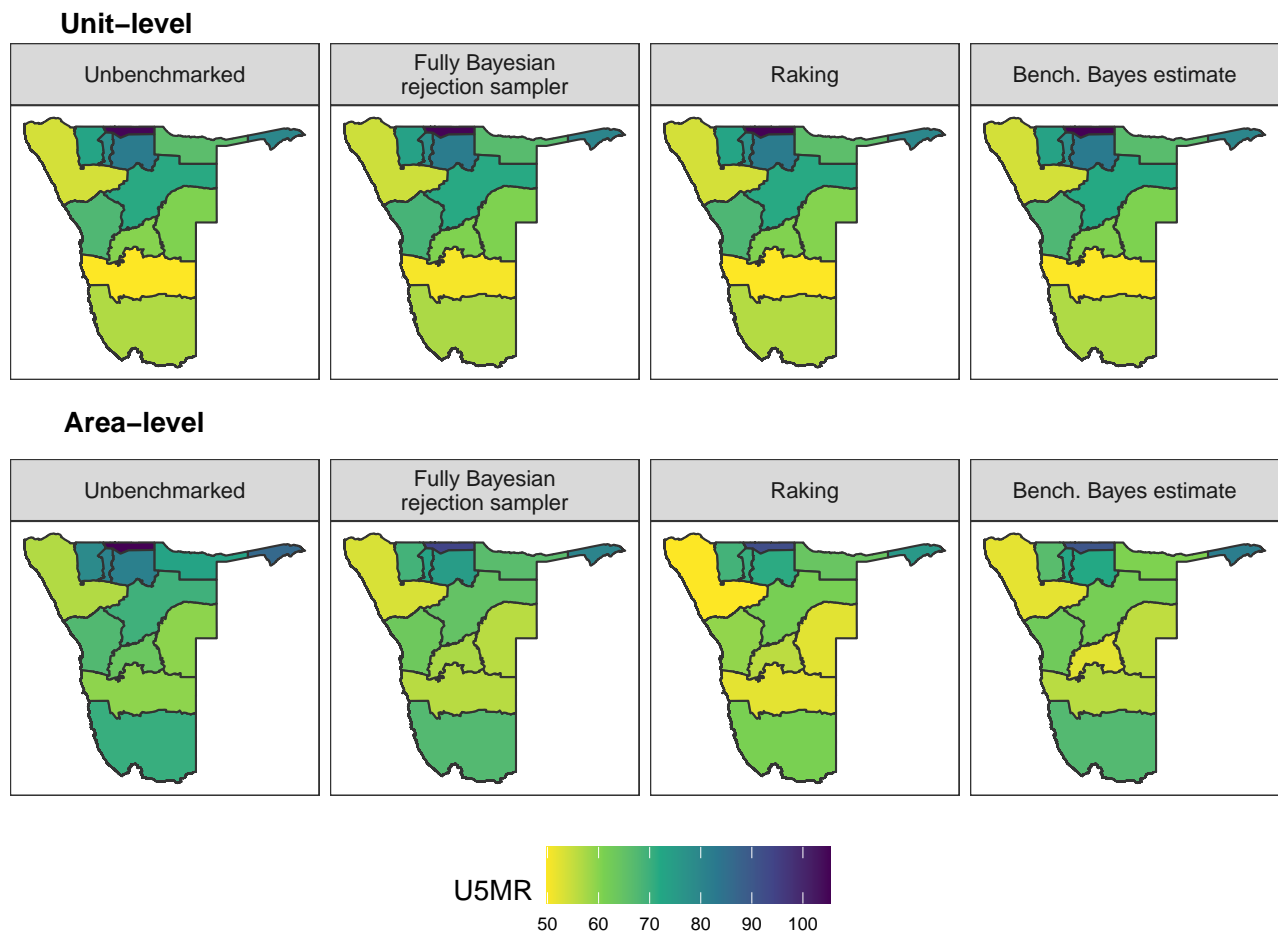


Figure 49: Comparison of median U5MR estimates from benchmarked and unbenchmarked unit- and area-level models for 2001. U5MR is reported as deaths per 1000 live births.

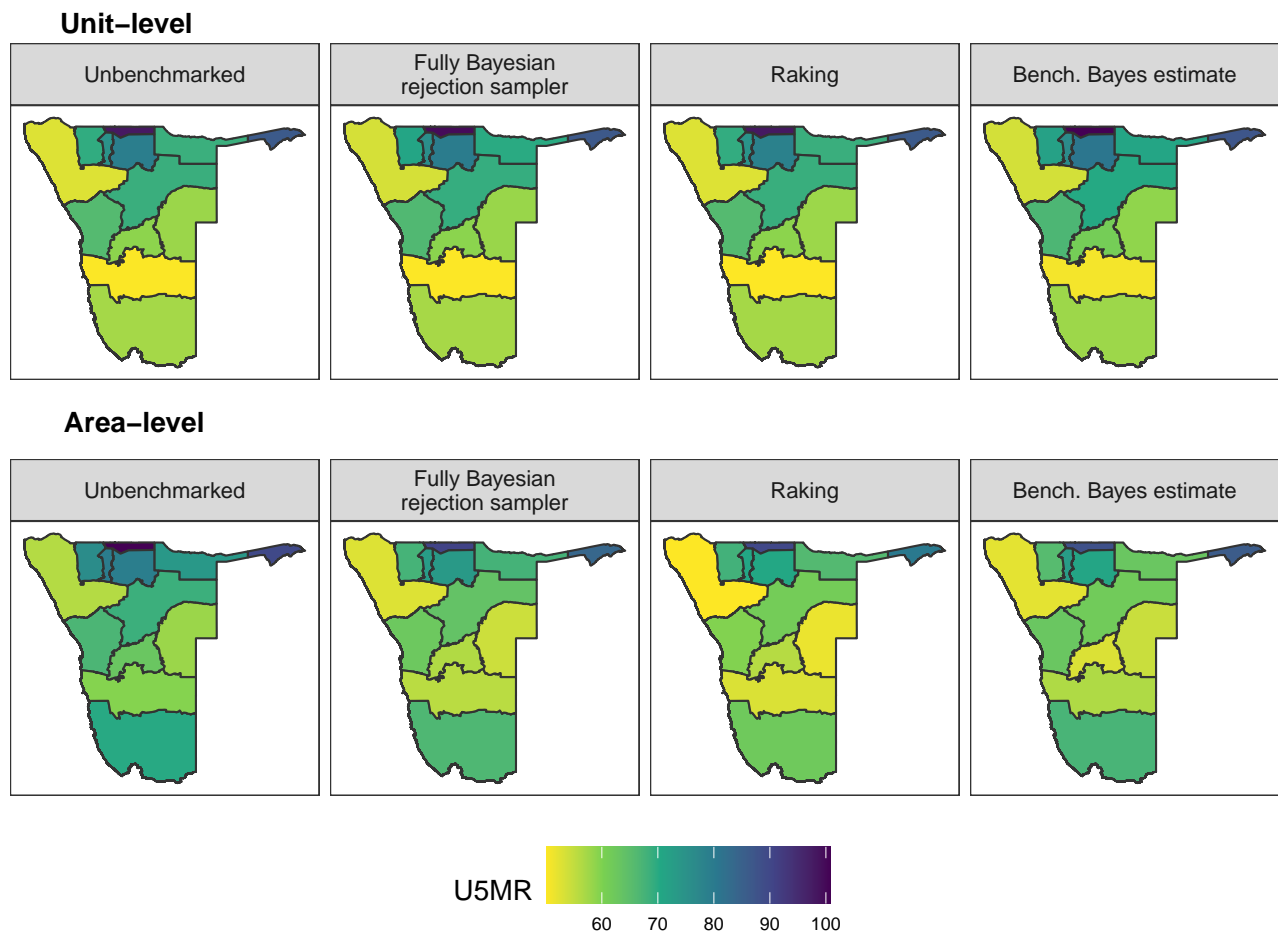


Figure 50: Comparison of median U5MR estimates from benchmarked and unbenchmarked unit- and area-level models for 2002. U5MR is reported as deaths per 1000 live births.

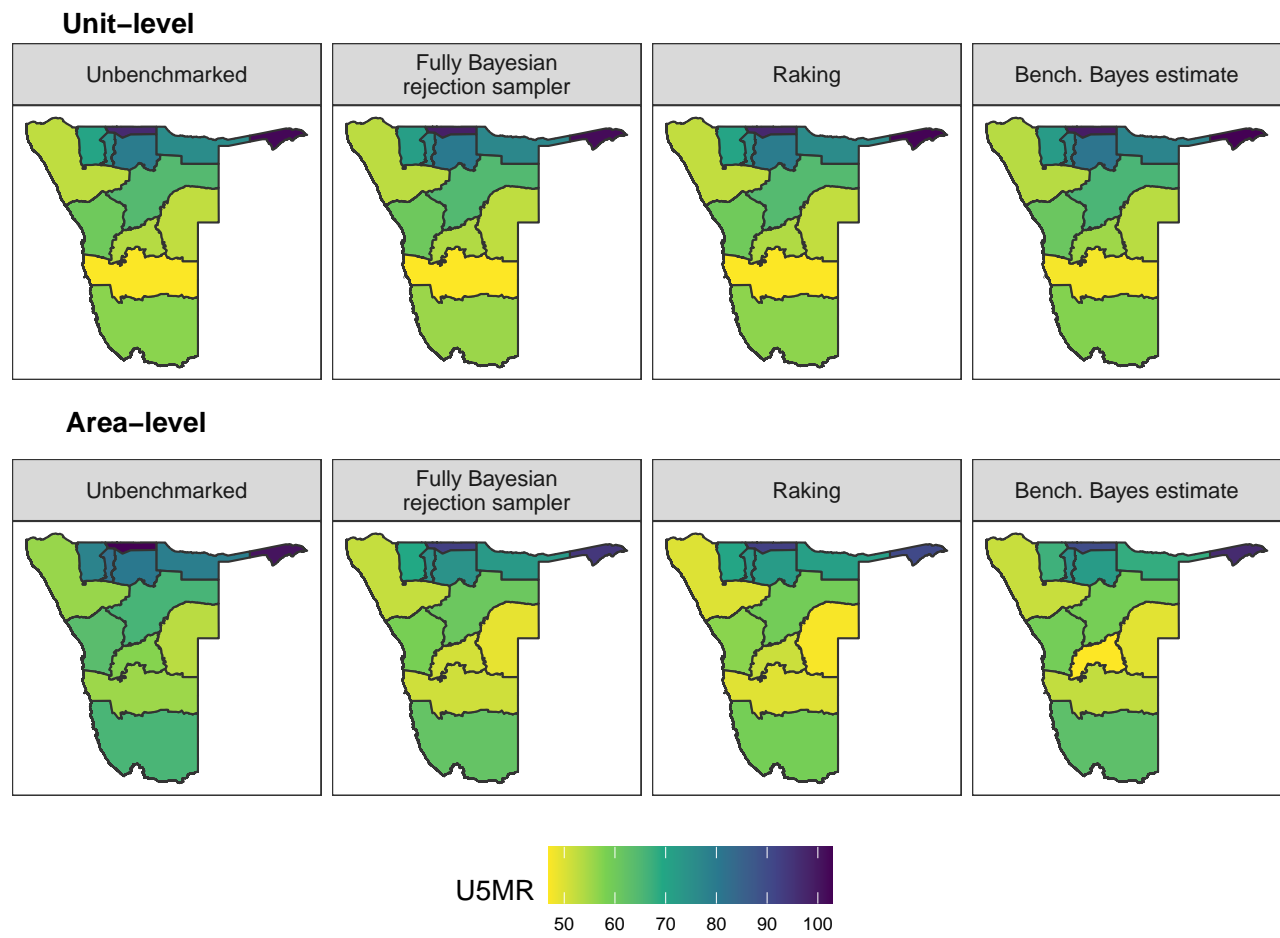


Figure 51: Comparison of median U5MR estimates from benchmarked and unbenchmarked unit- and area-level models for 2003. U5MR is reported as deaths per 1000 live births.

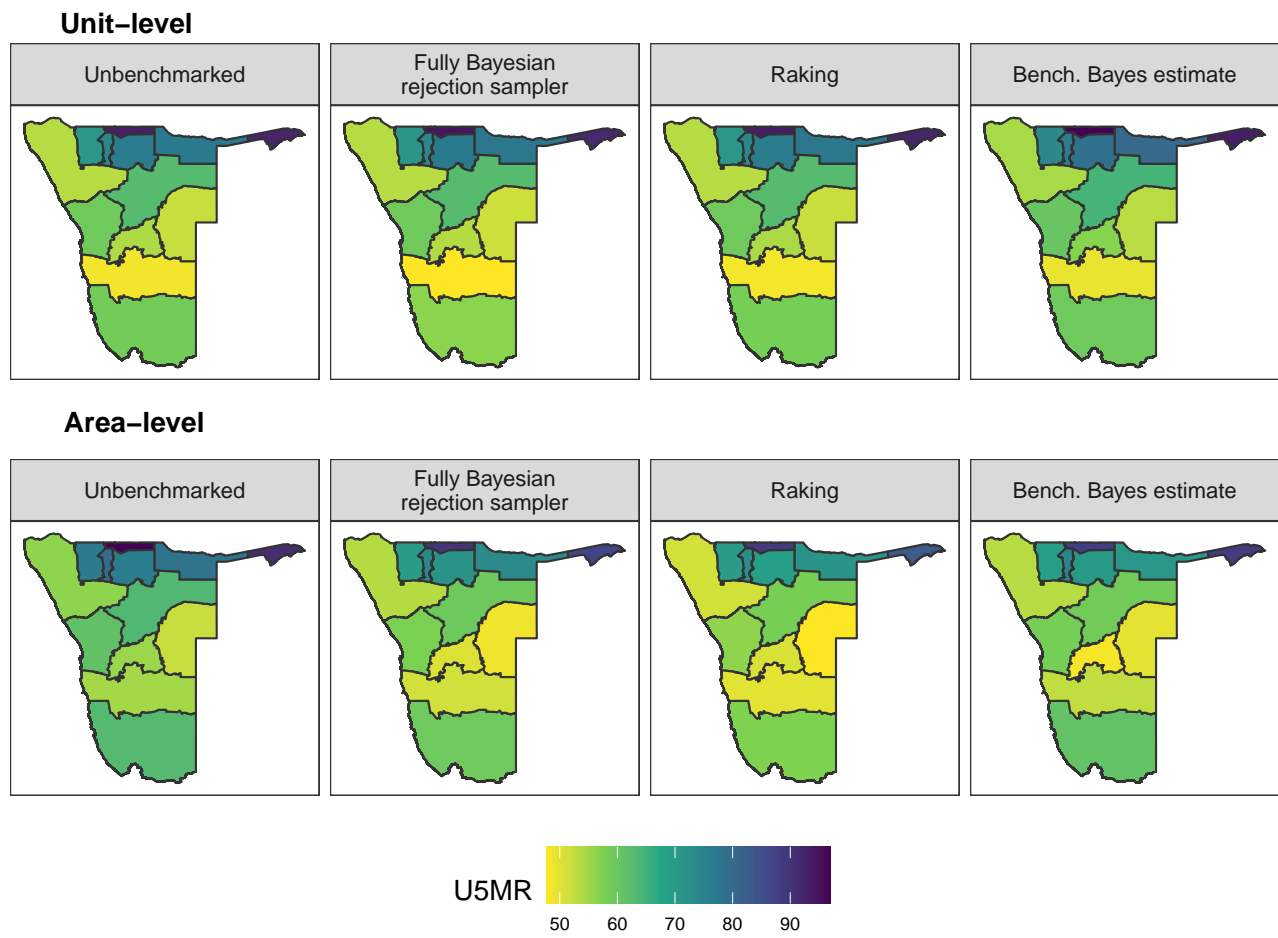


Figure 52: Comparison of median U5MR estimates from benchmarked and unbenchmarked unit- and area-level models for 2004. U5MR is reported as deaths per 1000 live births.

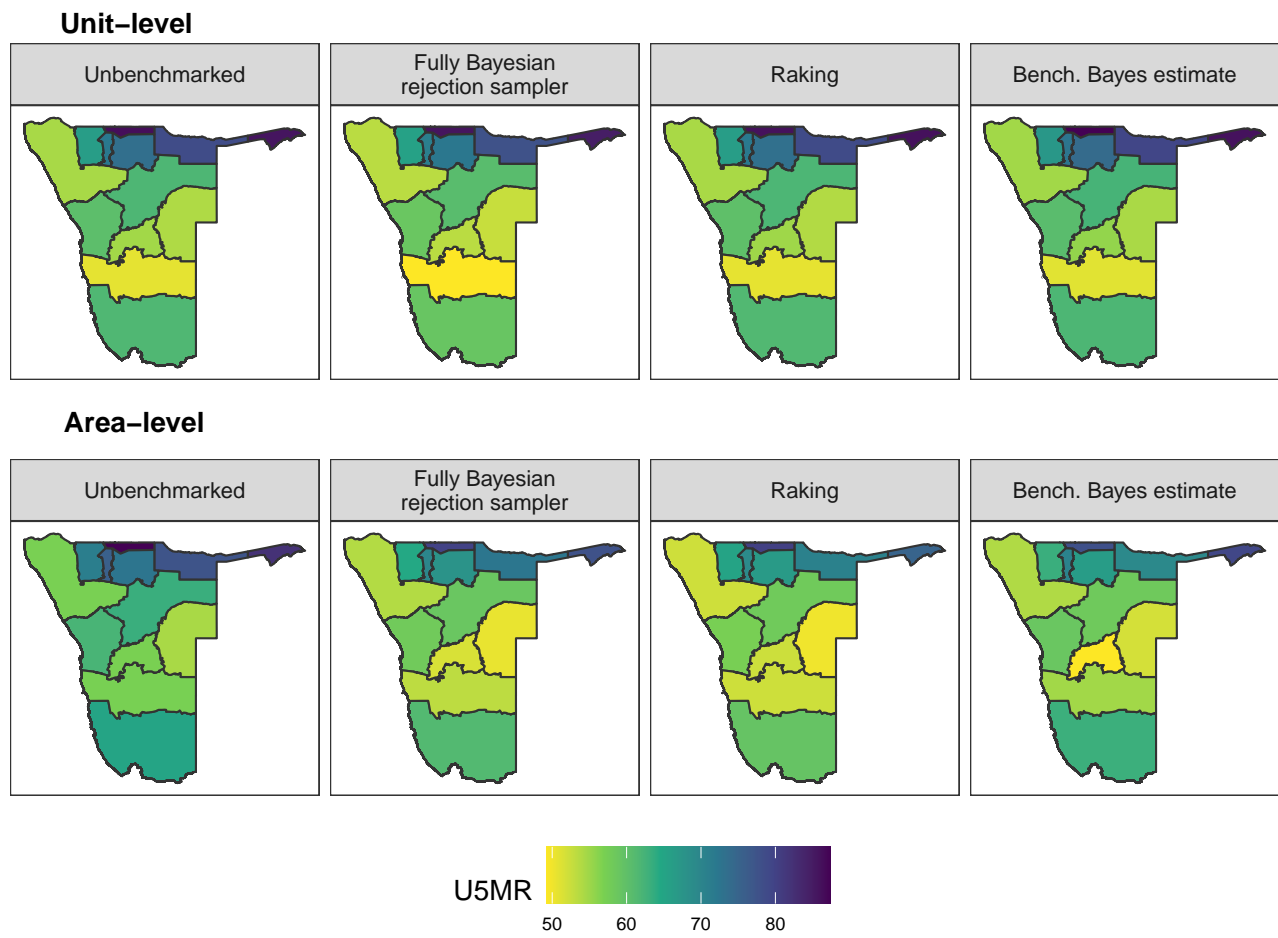


Figure 53: Comparison of median U5MR estimates from benchmarked and unbenchmarked unit- and area-level models for 2005. U5MR is reported as deaths per 1000 live births.

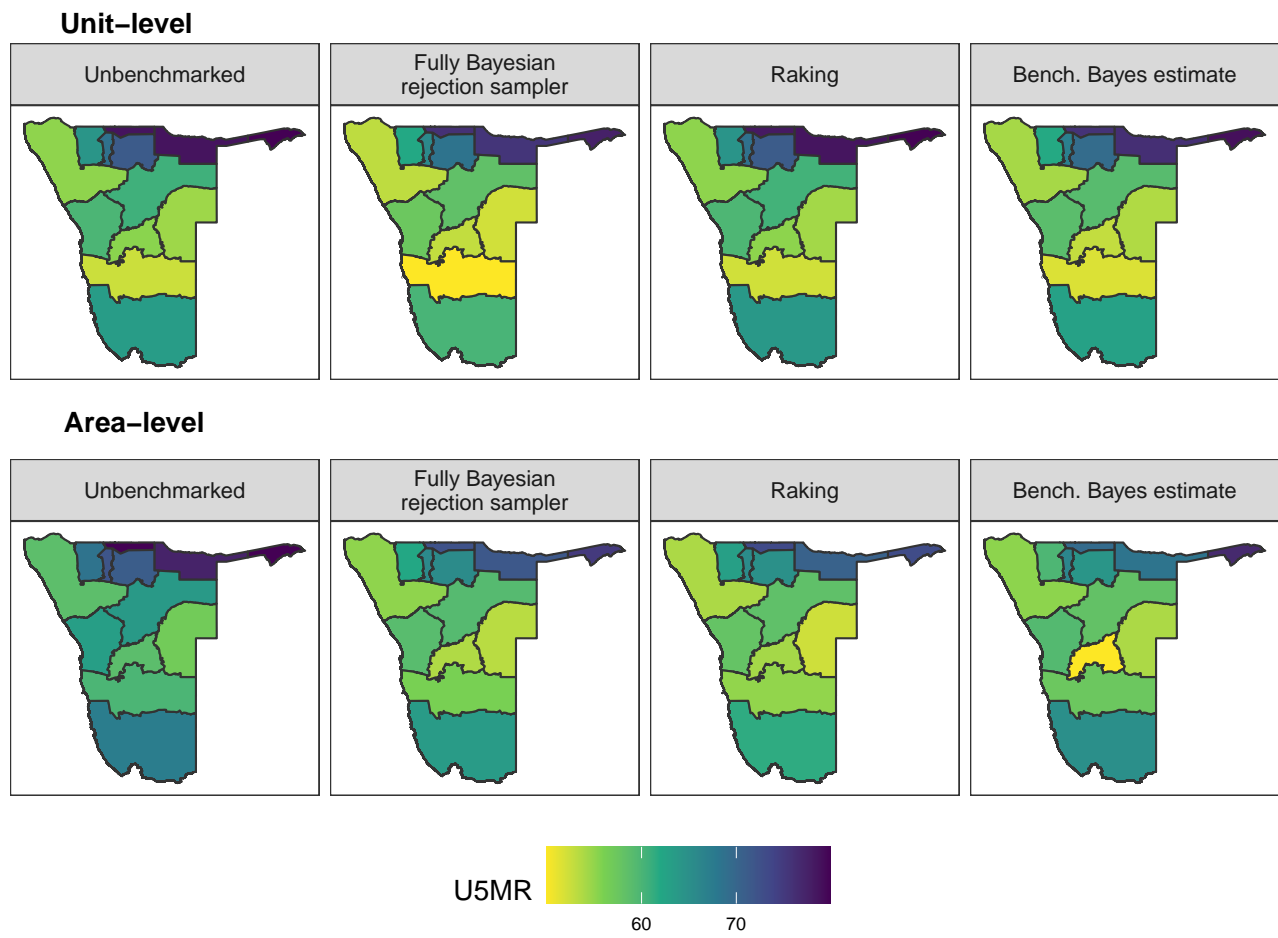


Figure 54: Comparison of median U5MR estimates from benchmarked and unbenchmarked unit- and area-level models for 2006. U5MR is reported as deaths per 1000 live births.

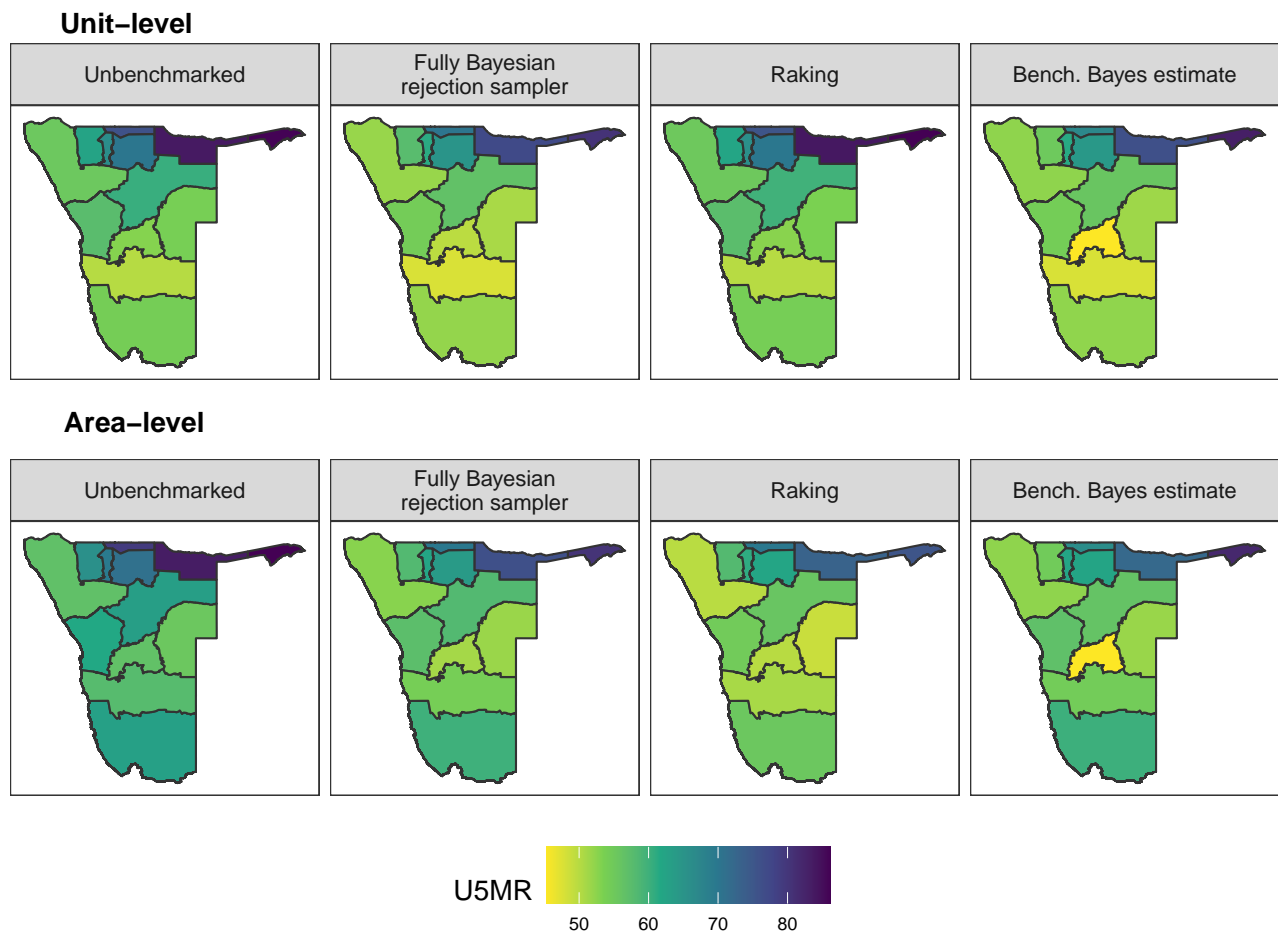


Figure 55: Comparison of median U5MR estimates from benchmarked and unbenchmarked unit- and area-level models for 2007. U5MR is reported as deaths per 1000 live births.

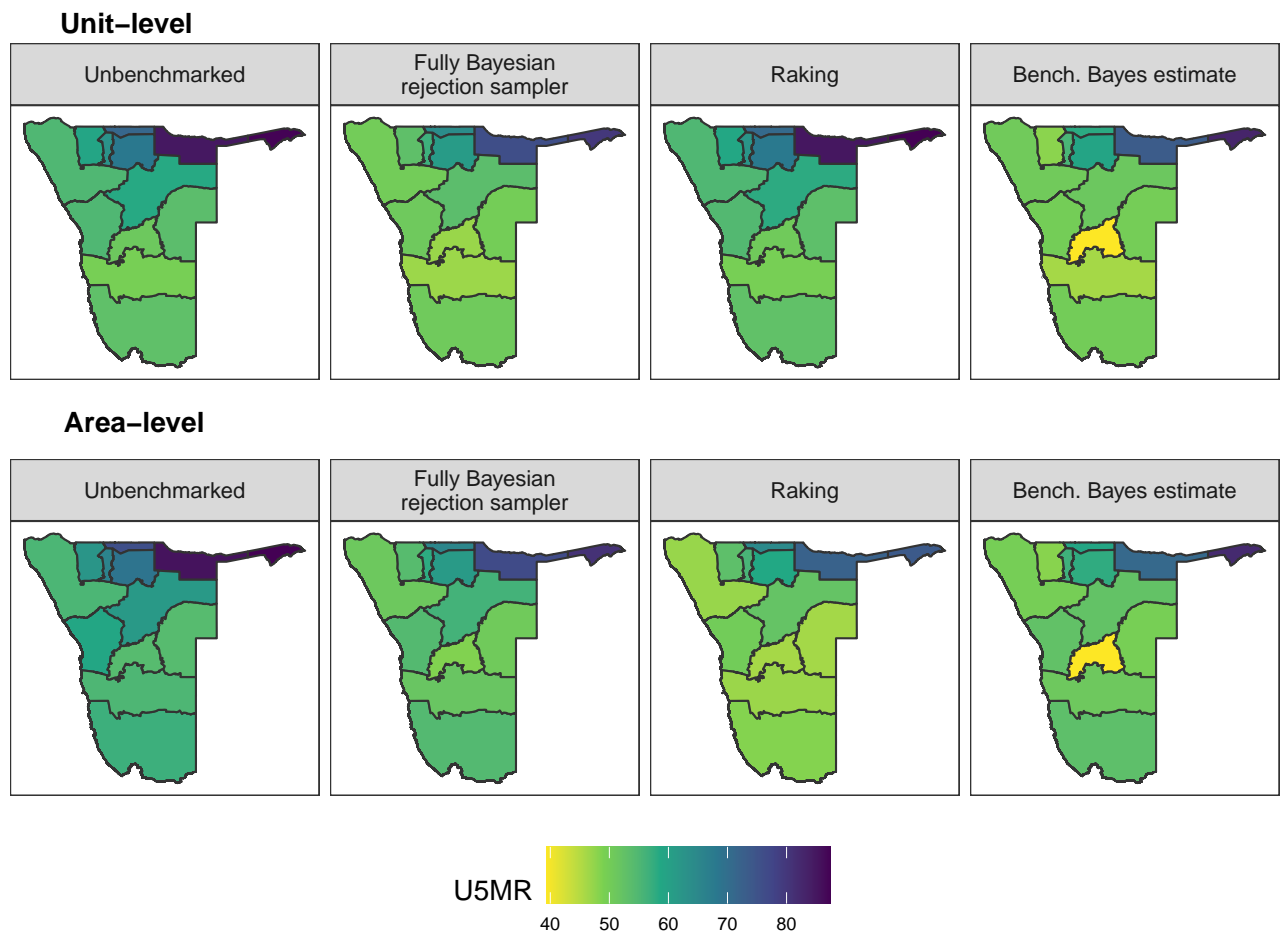


Figure 56: Comparison of median U5MR estimates from benchmarked and unbenchmarked unit- and area-level models for 2008. U5MR is reported as deaths per 1000 live births.

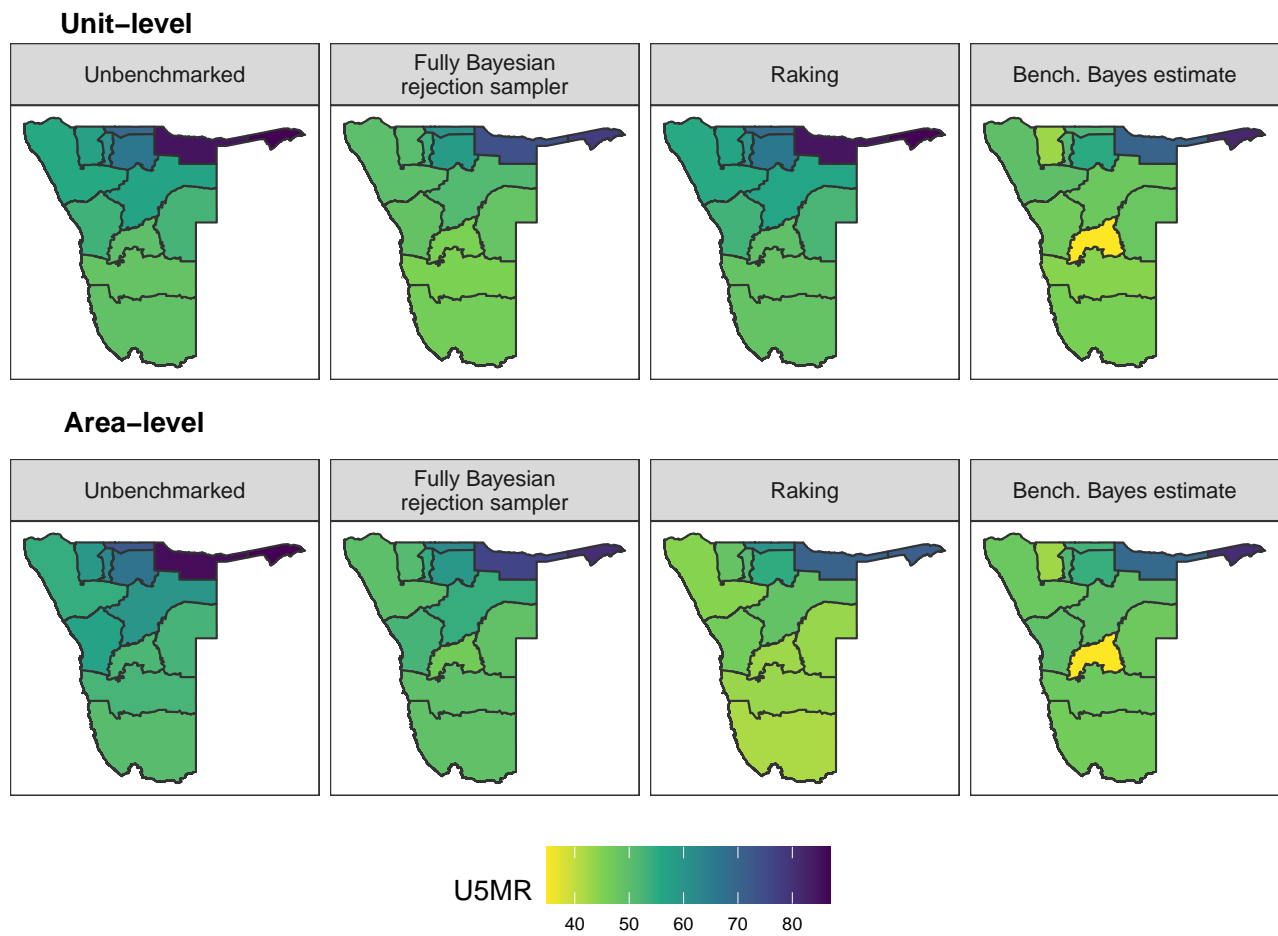


Figure 57: Comparison of median U5MR estimates from benchmarked and unbenchmarked unit- and area-level models for 2009. U5MR is reported as deaths per 1000 live births.

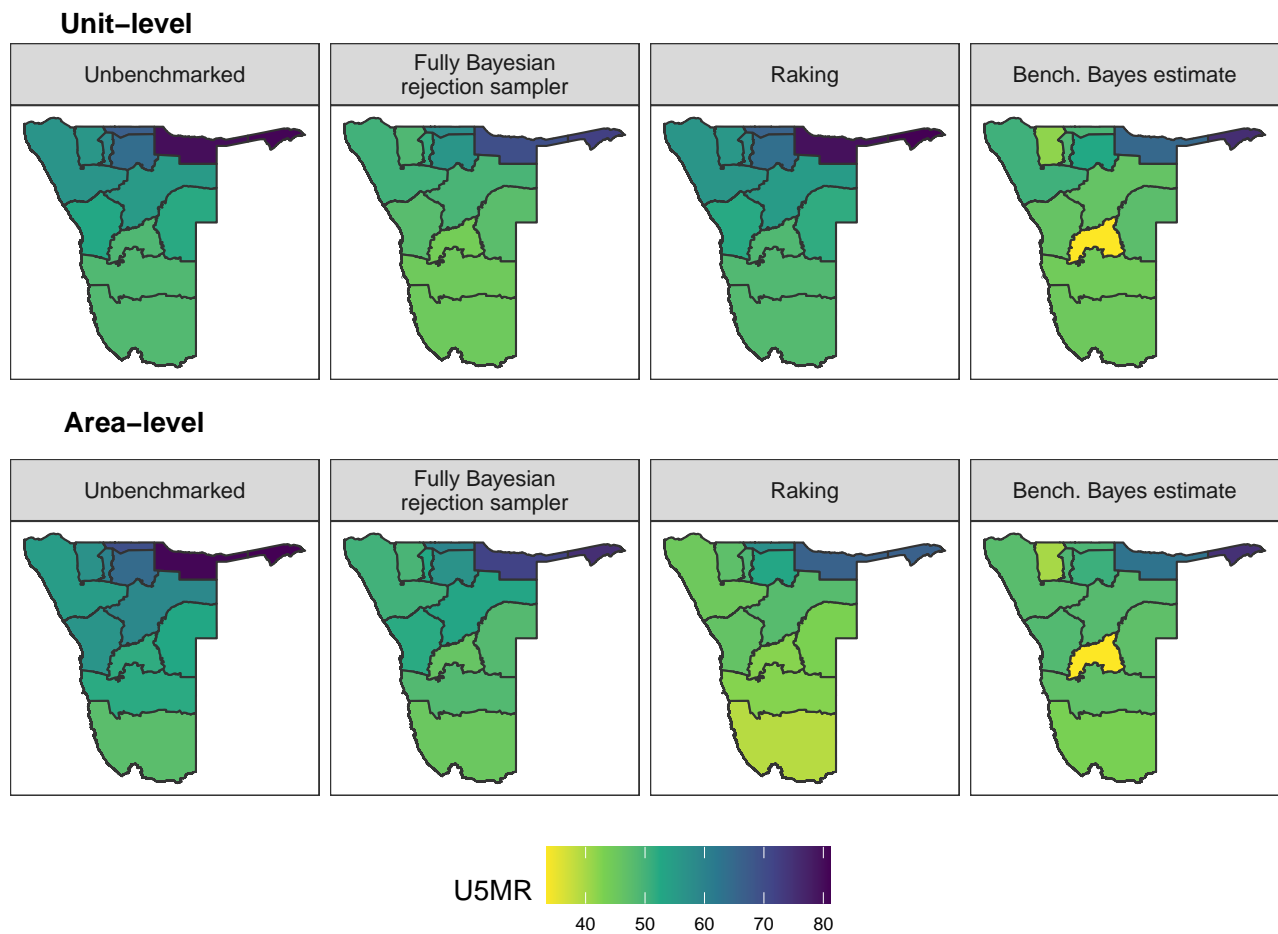


Figure 58: Comparison of median U5MR estimates from benchmarked and unbenchmarked unit- and area-level models for 2010. U5MR is reported as deaths per 1000 live births.

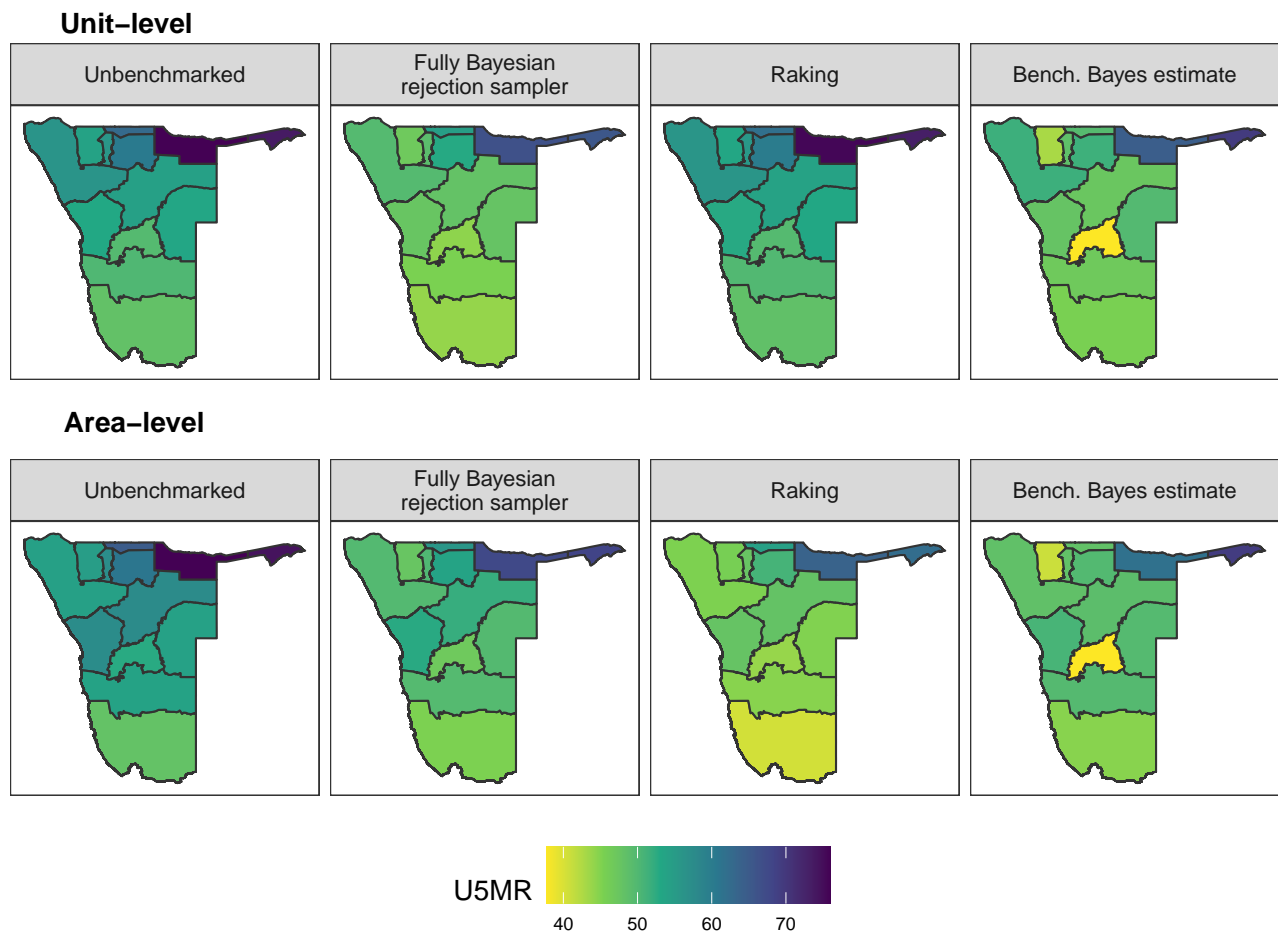


Figure 59: Comparison of median U5MR estimates from benchmarked and unbenchmarked unit- and area-level models for 2011. U5MR is reported as deaths per 1000 live births.

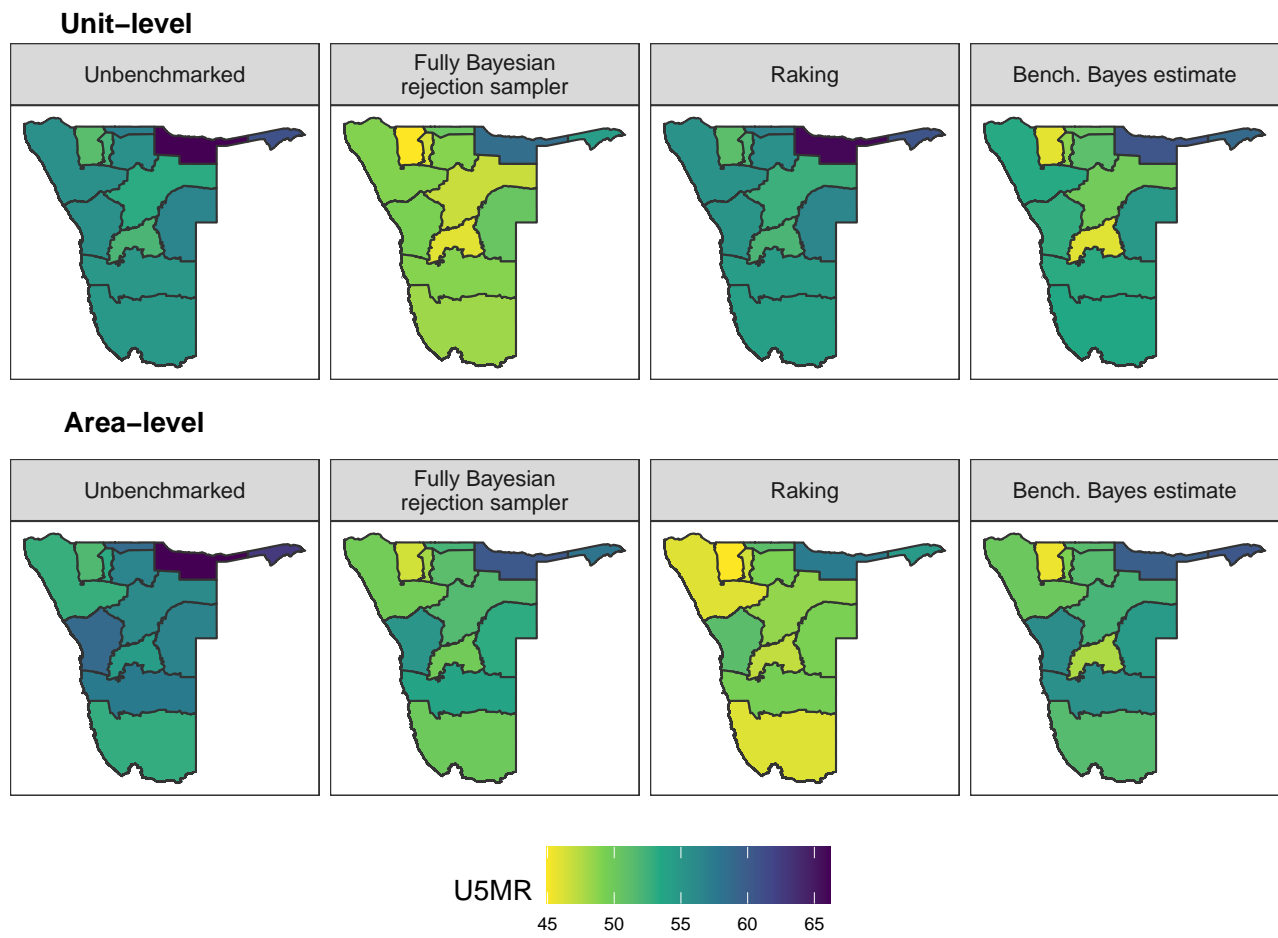


Figure 60: Comparison of median U5MR estimates from benchmarked and unbenchmarked unit- and area-level models for 2012. U5MR is reported as deaths per 1000 live births.

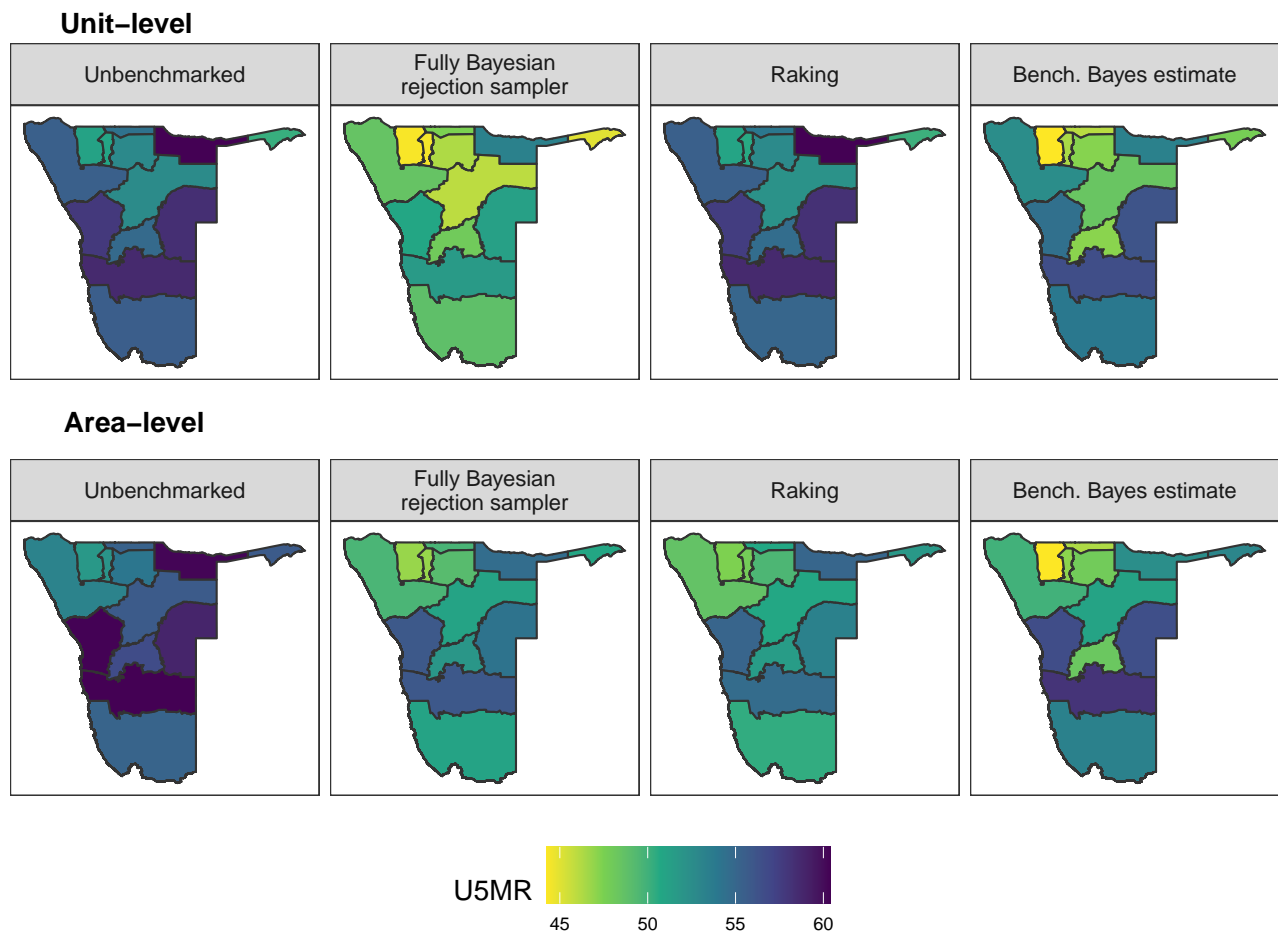


Figure 61: Comparison of median U5MR estimates from benchmarked and unbenchmarked unit- and area-level models for 2013. U5MR is reported as deaths per 1000 live births.

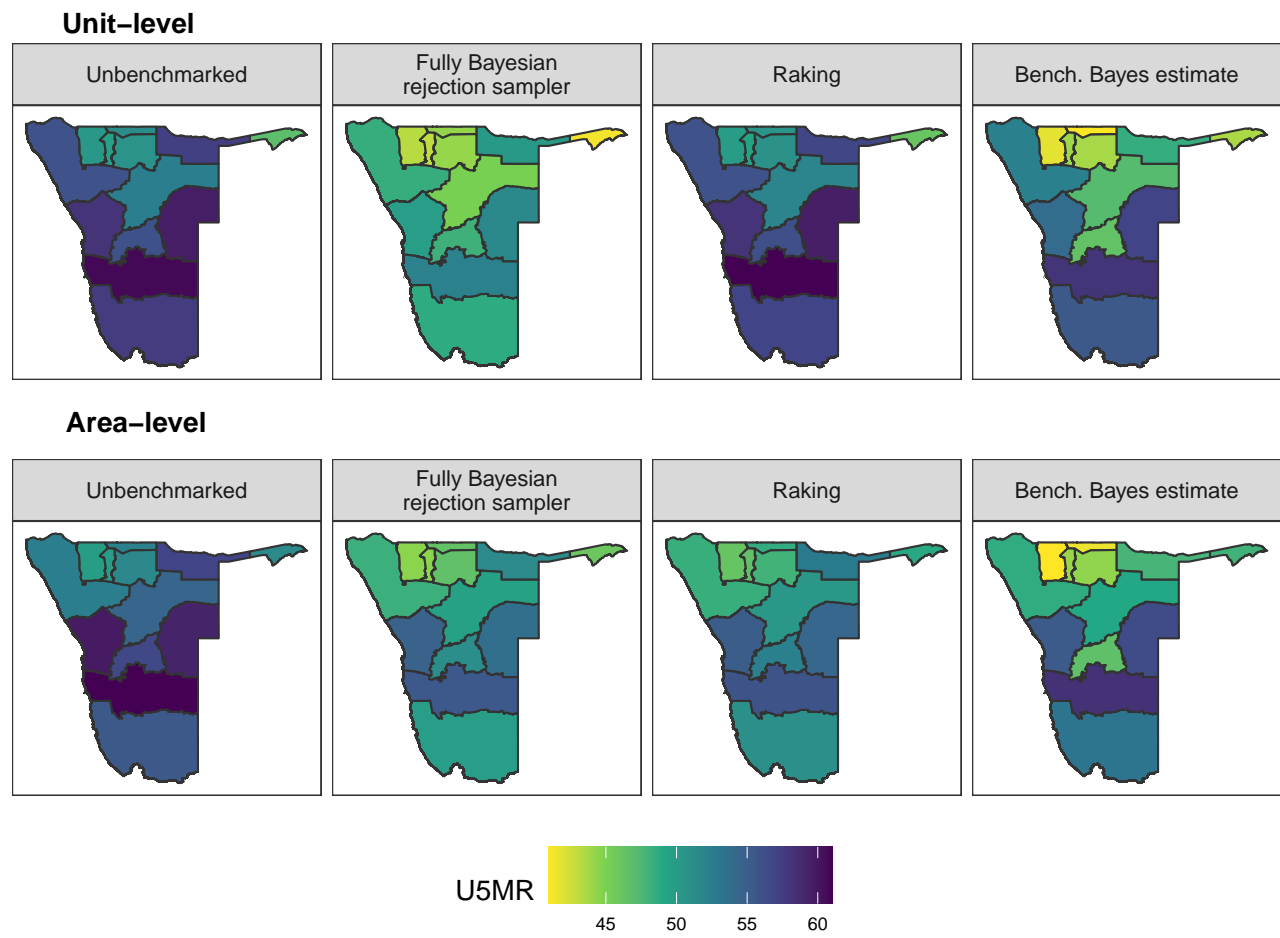


Figure 62: Comparison of median U5MR estimates from benchmarked and unbenchmarked unit- and area-level models for 2014. U5MR is reported as deaths per 1000 live births.

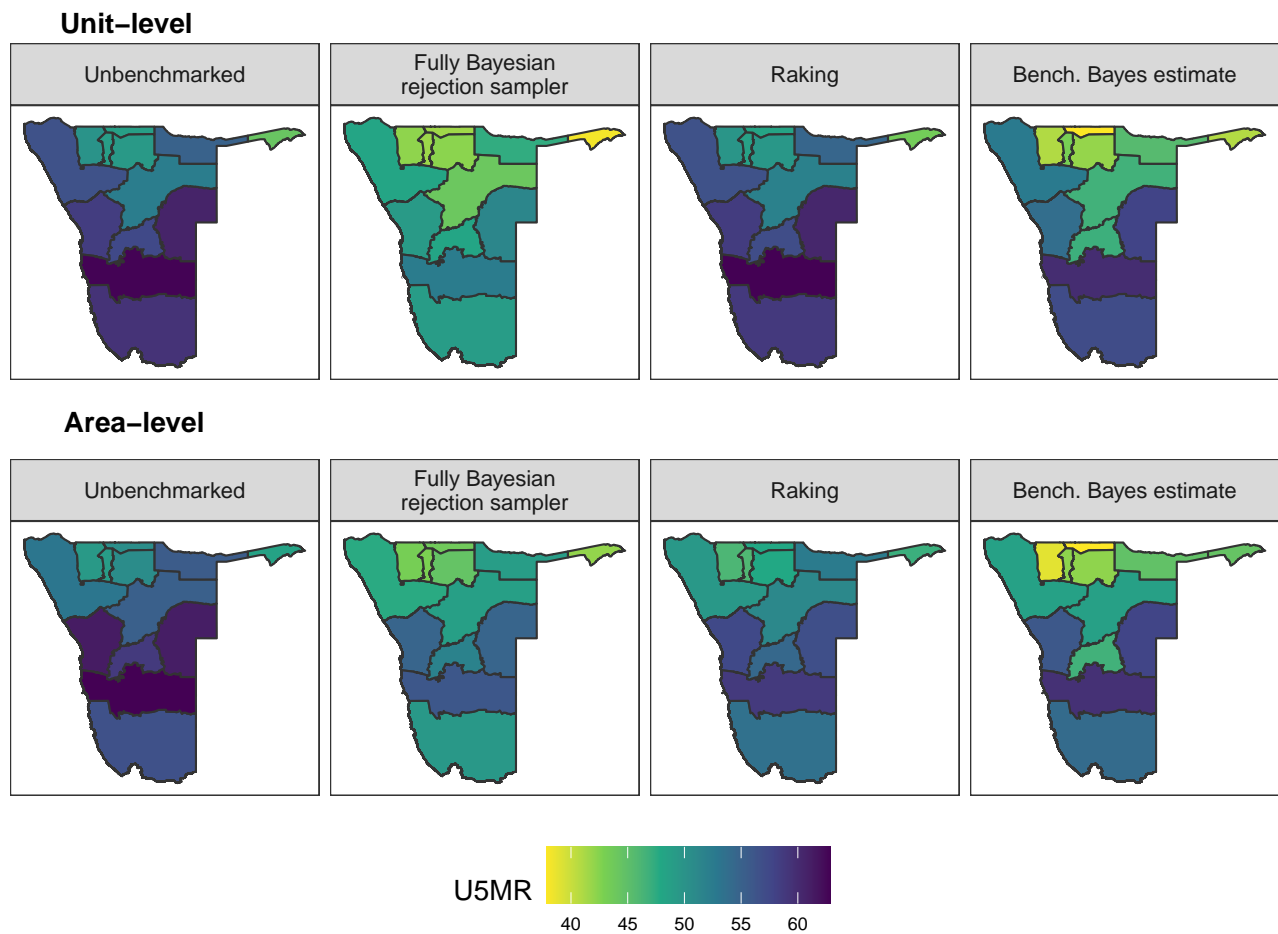


Figure 63: Comparison of median U5MR estimates from benchmarked and unbenchmarked unit- and area-level models for 2015. U5MR is reported as deaths per 1000 live births.

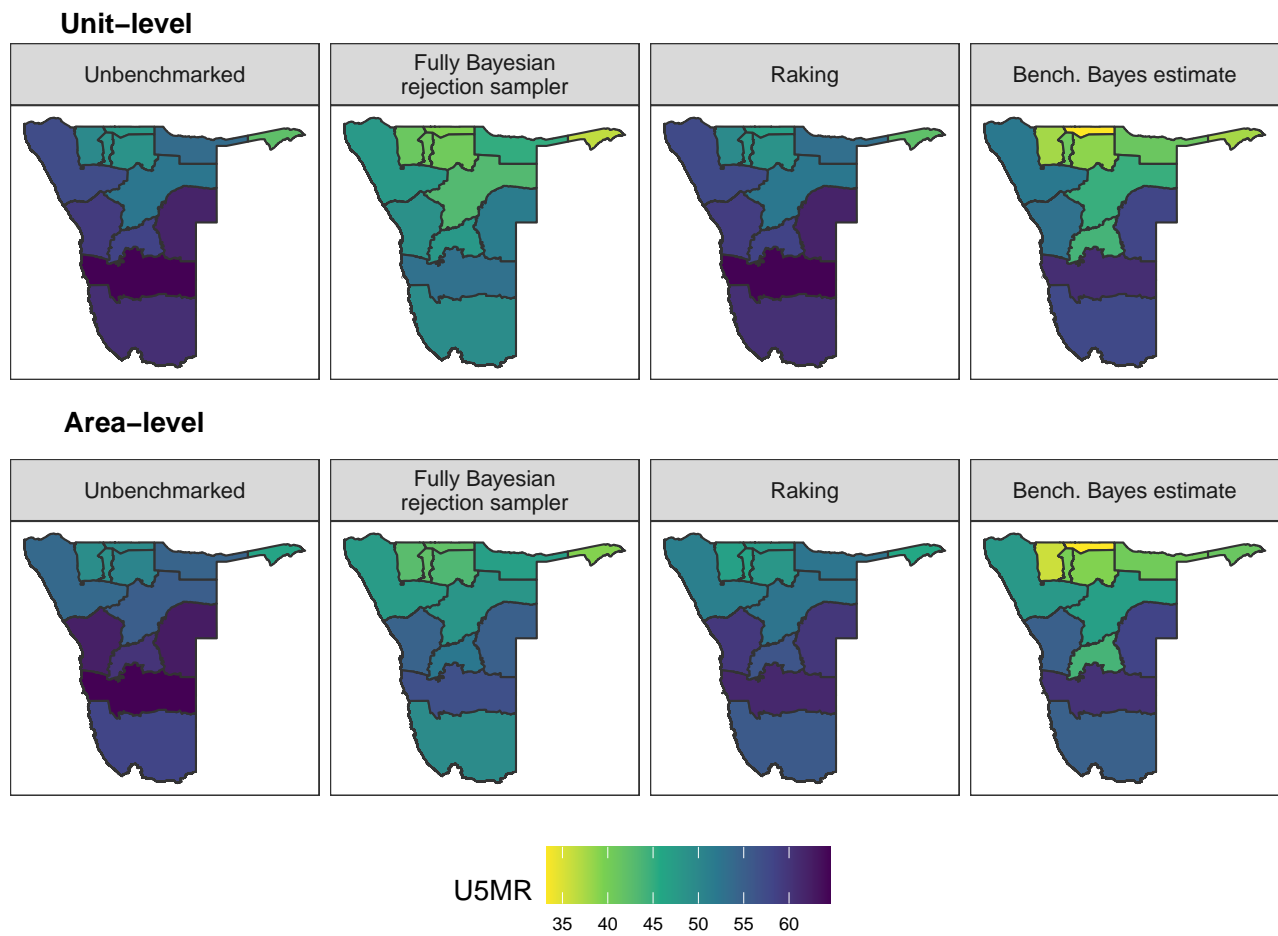


Figure 64: Comparison of median U5MR estimates from benchmarked and unbenchmarked unit- and area-level models for 2016. U5MR is reported as deaths per 1000 live births.

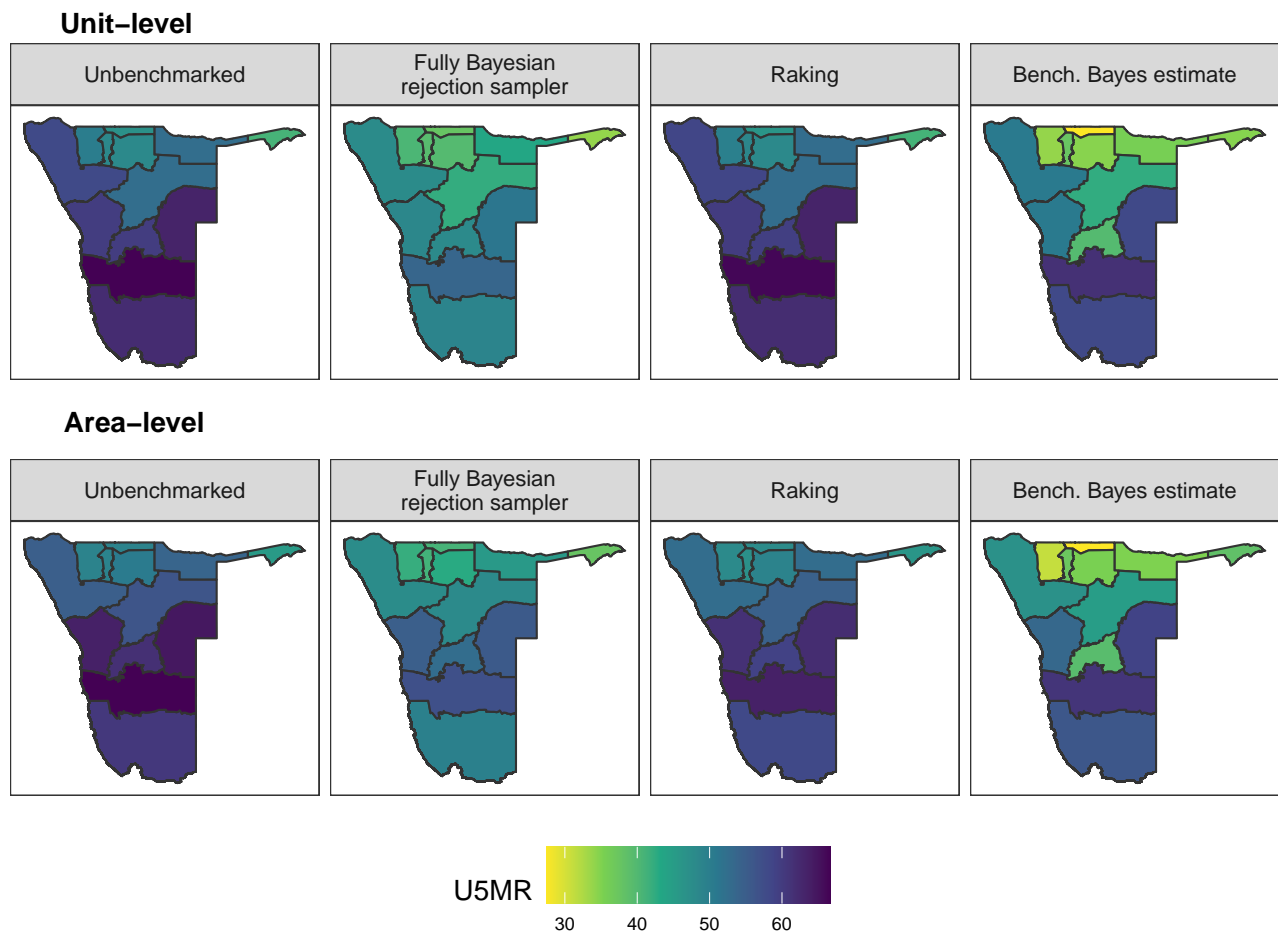


Figure 65: Comparison of median U5MR estimates from benchmarked and unbenchmarked unit- and area-level models for 2017. U5MR is reported as deaths per 1000 live births.

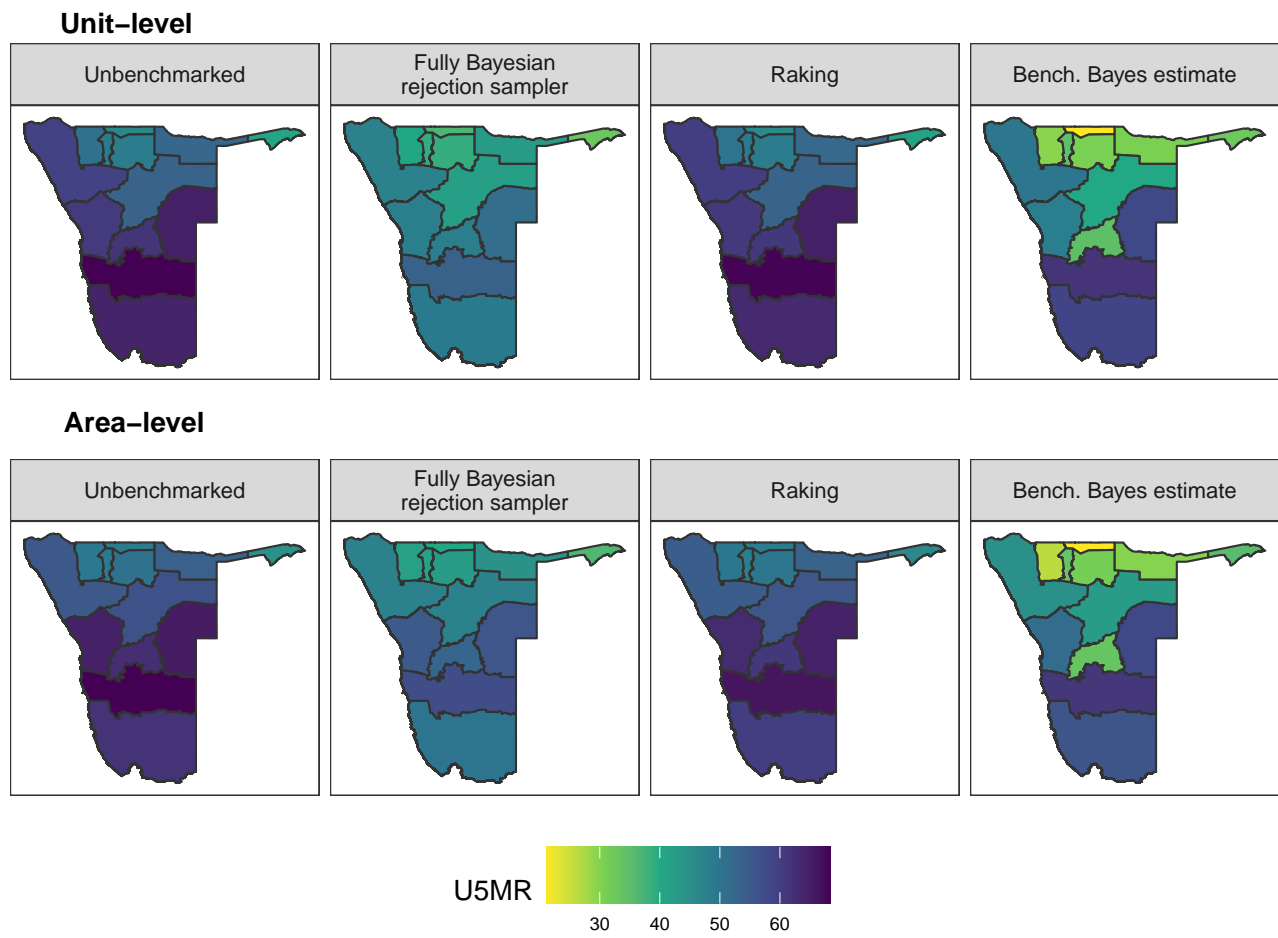


Figure 66: Comparison of median U5MR estimates from benchmarked and unbenchmarked unit- and area-level models for 2018. U5MR is reported as deaths per 1000 live births.

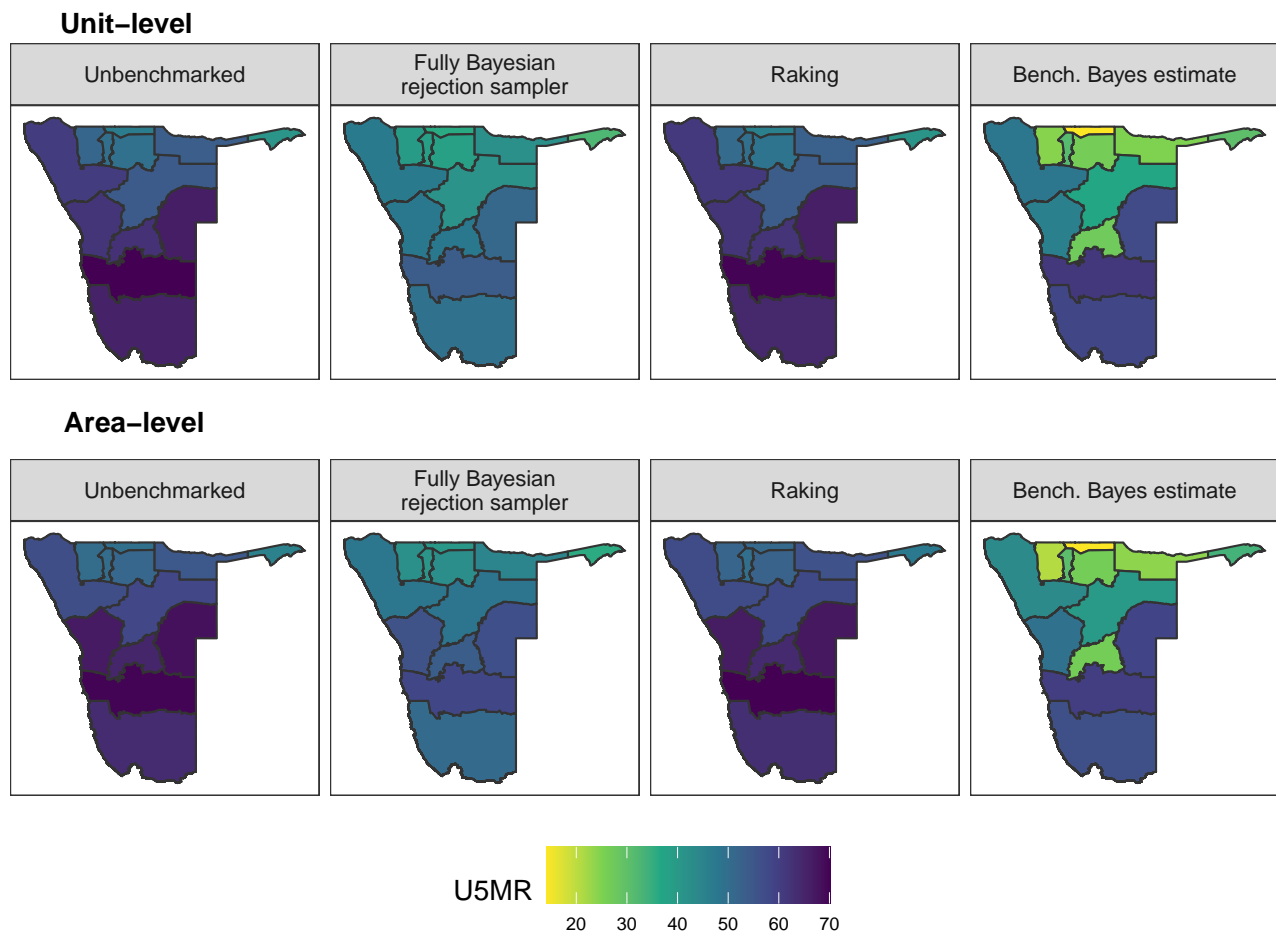


Figure 67: Comparison of median U5MR estimates from benchmarked and unbenchmarkmarked unit- and area-level models for 2019. U5MR is reported as deaths per 1000 live births.

Of note, 10/260 of the 95% credible intervals for subnational estimates constructed from the Bayes estimate approach had lower bounds below zero, using either the unbenchmarkmarked estimates from the unit-level model or the area-level model.

References

Alkema, L., and J. R. New. 2014. “Global estimation of child mortality using a Bayesian B-spline bias-reduction model.” *The Annals of Applied Statistics* 8 (4): 2122–2149. DOI: <https://doi.org/10.1214/14-AOAS768>.

Bachl, F. E., F. Lindgren, D. L. Borchers, and J. B. Illian. 2019. “inlabru: an R package for Bayesian spatial modelling from ecological survey data.” *Methods in Ecology and Evolution* 10 (6): 760–766.

Besag, J., J. York, and A. Mollié. 1991. “Bayesian image restoration, with two applications in spatial statistics.” *Annals of the Institute of Statistical Mathematics* 43 (1): 1–20. DOI: <https://doi.org/10.1007/BF00116466>.

Database of Global Administrative Areas (GADM). 2019. *Global Administrative Areas [Shapefiles]*. Available at: <https://www.gadm.org>. Downloaded January 2020.

Fay, R. E., and R. A. Herriot. 1979. “Estimates of income for small places: an application of James-Stein procedures to census data.” *Journal of the American Statistical Association* 74 (366a): 269–277. DOI: <https://doi.org/10.2307/2286322>.

Inter-agency Group for Child Mortality Estimation. 2020. *Levels and Trends in Child Mortality: Estimates*. Available at <https://childmortality.org>. United Nations Children’s Fund.

Knorr-Held, L. 2000. “Bayesian modelling of inseparable space-time variation in disease risk.” *Statistics in medicine* 19 (17-18): 2555–2567.

Li, Z., Y. Hsiao, J. Godwin, B. D. Martin, J. Wakefield, S. J. Clark, with support from the United Nations Inter-agency Group for Child Mortality Estimation, and its technical advisory group. 2019. “Changes in the spatial distribution of the under-five mortality rate: Small-area analysis of 122 DHS surveys in 262 subregions of 35 countries in Africa.” *PloS One* 14 (1): e0210645.

Li, Z. R., B. D. Martin, T. Q. Dong, G.-A. Fuglstad, J. Paige, A. Riebler, S. Clark, and J. Wakefield. 2020. “Space-Time Smoothing of Demographic and Health Indicators using the R Package SUMMER.” *arXiv:2007.05117*.

Lindgren, F., and H. Rue. 2008. “On the second-order random walk model for irregular locations.” *Scandinavian journal of statistics* 35 (4): 691–700.

Mercer, L. D., J. Wakefield, A. Pantazis, A. M. Lutambi, H. Masanja, and S. Clark. 2015. “Space-time smoothing of complex survey data: small area estimation for child mortality.” *The Annals of Applied Statistics* 9 (4): 1889. DOI: <https://doi.org/10.1214/15-AOAS872>.

Riebler, A., S. H. Sørbye, D. Simpson, and H. Rue. 2016. “An intuitive Bayesian spatial model for disease mapping that accounts for scaling.” *Statistical Methods in Medical Research* 25 (4): 1145–1165. DOI: <https://doi.org/10.1177/0962280216660421>.

Rue, H., S. Martino, and N. Chopin. 2009. “Approximate Bayesian inference for latent Gaussian models by using integrated nested Laplace approximations.” *Journal of the Royal Statistical Society: Series B (statistical methodology)* 71 (2): 319–392. DOI: <https://doi.org/10.1111/j.1467-9868.2008.00700.x>.

Stevens, F. R., A. E. Gaughan, C. Linard, and A. J. Tatem. 2015. “Disaggregating census data for population mapping using random forests with remotely-sensed and ancillary data.” *PLoS One* 10 (2): e0107042.

Tatem, A. J. 2017. “WorldPop, open data for spatial demography.” *Scientific data* 4 (1): 1–4.

Wakefield, J., G.-A. Fuglstad, A. Riebler, J. Godwin, K. Wilson, and S. J. Clark. 2019. “Estimating under-five mortality in space and time in a developing world context.” *Statistical Methods in Medical Research* 28 (9): 2614–2634. DOI: <https://doi.org/10.1177/0962280218767988>.

Walker, N., K. Hill, and F. Zhao. 2012. “Child mortality estimation: methods used to adjust for bias due to AIDS in estimating trends in under-five mortality.”

Zhang, J. L., and J. Bryant. 2020. “Fully Bayesian Benchmarking of Small Area Estimation Models.” *Journal of Official Statistics* 36 (1): 197–223. DOI: <https://doi.org/10.2478/jos-2020-0010>.